Carina Dertnig, BSc

Development of a Novel Synthesis Route for the Preparation of a Sacubitril Precursor in Continuous Flow

MASTER'S THESIS

to achieve the university degree of

Master of Science

Master's degree programme: Chemistry

submitted to

Graz University of Technology

Supervisor

Assoc.Prof. Dipl.-Ing. Dr.techn. Heidrun Gruber-Wölfler

Advisor

Katharina Hiebler, MSc

Institute of Process and Particle Engineering
Graz University of Technology

Graz, October 2019

AFFIDAVIT

I declare that I have authored this thesis independently, that I have not used other than the declared sources/resources, and that I have explicitly indicated all material which has been quoted either literally or by content from the sources used. The text document uploaded to TUGRAZonline is identical to the present master‘s thesis.

Date	Signature

Abstract

Sacubitril and valsartan are the two active pharmaceutical ingredients in a combination drug considered superior in the treatment of hypertension and heart failure. The aim of this master's thesis was the development of a synthesis route to an advanced precursor of sacubitril wherein multiple steps can be conducted as continuous flow process.

The identified pathway yields a late-stage sacubitril precursor, which differs from sacubitril only in a double bond, in six reaction steps. The last three steps, which are a Suzuki-Miyaura cross-coupling reaction, a Boc deprotection and an *N*-acylation, are promising to be achievable in a multistep continuous setup.

For the Suzuki coupling, a heterogeneous palladium catalyst is used, which enables the application of a packed-bed reactor in continuous flow. In batch experiments, the use of the palladium catalyst $Ce_{0.20}Sn_{0.79}Pd_{0.01}O_{2-\delta}$ and the solvent mixture iPrOH:H_2O = 7:3 (v:v) were identified to be optimal for the targeted transformation. With these parameters, the key Suzuki coupling reaction was successfully performed in continuous flow with a yield of 83% at a flow rate of 0.1 mL/min and 80% at 0.2 mL/min, respectively.

Kurzfassung

Die zwei pharmazeutischen Wirkstoffe Sacubitril und Valsartan werden in Kombination in einem Medikament verwendet, welches als überragend in der Behandlung von Bluthochdruck und Herzinsuffizienz gilt. Das Ziel dieser Masterarbeit war die Entwicklung eines Synthesewegs zu einer fortgeschrittenen Sacubitril-Vorstufe, wovon mehrere Schritte in einem kontinuierlichen Flow-Prozess durchgeführt werden können.

Der resultierende Syntheseweg führt in sechs Reaktionsschritten zu einer Vorstufe von Sacubitril, die sich von Sacubitril nur durch eine Doppelbindung unterscheidet. Die Durchführung der letzten drei Schritte, einer Suzuki-Miyaura Kreuzkupplungs-Reaktion, einer Boc-Entschützung und einer *N*-Acylierung, ist nach bisherigen Erkenntnissen als mehrstufiger kontinuierlicher Flow-Prozess möglich.

Für die Suzuki-Kupplung wird ein heterogener Palladium-Katalysator verwendet, der die Anwendung eines Festbett-Reaktors für die kontinuierliche Durchführung der Synthese ermöglicht. In Batch-Experimenten stellten sich diesbezüglich der Palladium-Katalysator $Ce_{0.20}Sn_{0.79}Pd_{0.01}O_{2-\delta}$ sowie das Lösungsmittel-Gemisch iPrOH:H_2O = 7:3 (v:v) als optimal heraus. Mit diesen Parametern wurde die Suzuki-Kupplung erfolgreich in einem kontinuierlichen Flow-Prozess mit einer Ausbeute von 83 % bei einer Durchflussrate von 0,1 mL/min sowie 80 % bei 0,2 mL/min durchgeführt.

Danksagung

Ich möchte diese Gelegenheit nutzen, um all jenen zu danken, die mich während meiner Masterarbeit, meines Studiums oder schon mein ganzes Leben lang unterstützt haben.

Zunächst vielen Dank, Heidi, dass du mir die Möglichkeit gegeben hast, meine Masterarbeit in deiner Arbeitsgruppe zu schreiben, wodurch ich unglaublich viel dazugelernt habe. Deine freundliche, entgegenkommende und vertrauensvolle Art gibst du an die gesamte Arbeitsgruppe weiter und schaffst somit eine Arbeitsatmosphäre, in der man sich gerne einbringt.

Danke an die CoSy Bros für ein Team, in der Hilfsbereitschaft, Unterstützung und auch Spaß an der Tagesordnung stehen. Unsere gemeinsamen Kaffee- und Kuchenpausen und unsere Meme-Wall haben es oft geschafft, mich von frustrierenden Phasen in der Forschung abzulenken und mich weiterhin zu motivieren.

Mein besonderer Dank gilt der besten Masterarbeits-Betreuerin, die man sich wünschen kann. Obwohl ich deine erste Masterstudentin war, hast du für mich von Beginn and den perfekten Ausgleich zwischen Unterstützung und Selbständigkeit geschaffen. Du hast mir alles genau erklärt und ich konnte immer mit Fragen zu dir kommen, zugleich aber hast du mich selbständig arbeiten und ausprobieren lassen. Danke, Kathi, dass du stets so herzlich, hilfsbereit, geduldig und verständnisvoll bist.

Vielen Dank an meine Freunde und Freundinnen, die mich teils schon seit meiner Kindheit, teils seit dem Studium begleiten. Neben gemeinsamen Lernsessions kamen mit euch auch die Ablenkung vom Studienalltag und der Spaß nie zu kurz.

Abschließend gebührt noch ein riesiges Dankeschön meiner wunderbaren Familie. Sandra, auch wenn wir meistens nicht einer Meinung sind, stehen wir immer zueinander und überstehen Höhen und Tiefen gemeinsam. Ich könnte mir ein Leben ohne eine so tolle Schwester nicht vorstellen. Danke an Mama und Papa, dass ihr mich mein ganzes Leben lang unterstützt habt, auch wenn ihr selbst dadurch manchmal zurückstecken musstet. Ohne euch wäre es mir nicht möglich gewesen, überhaupt an diesen Punkt zu gelangen, an dem ich jetzt stehe. Danke, dass ihr mich meinen eigenen Weg gehen lässt und bei all meinen Entscheidungen stets hinter mir steht. Danke, dass ihr immer für mich da seid und die besten Eltern seid.

Contents

1 Introduction and Research Objective

Sacubitril and valsartan are the two active pharmaceutical ingredients in the combination preparation Entresto® (Figure 1.1). This drug is regarded as superior in the treatment of hypertension and heart failure.[1–4] In 2009, hypertension was stated as the main reason of mortality worldwide by the World Health Organisation[5] and its prevalence was predicted to increase significantly.[6] Among others, hypertension is a main cause of heart failure.[7] For these reasons it is assumed that the demand of Entresto® will increase strongly in the next years, which stimulates research in this field. An example is the ONE-FLOW[8] project, whereof this master's thesis is part.

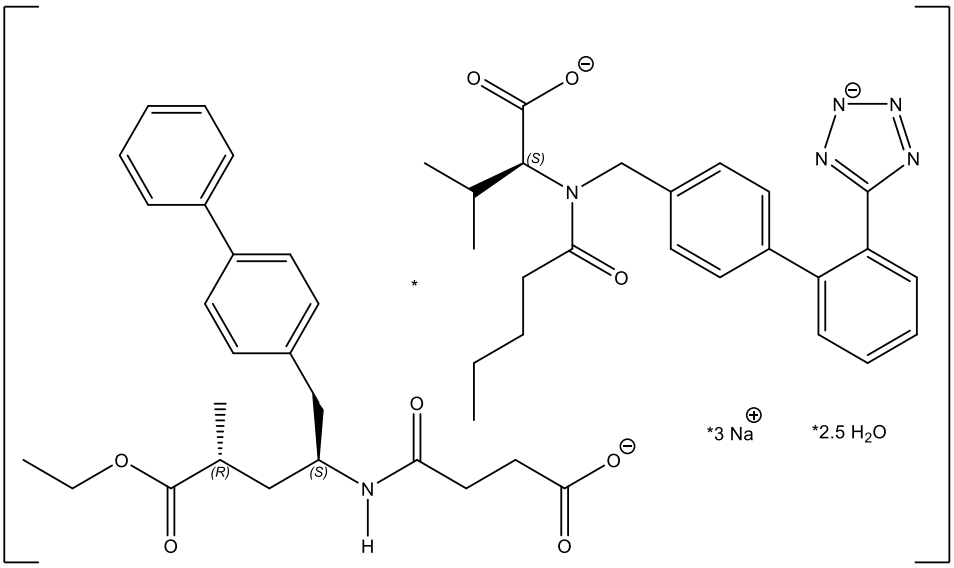

Figure 1.1: Chemical structures of sacubitril and valsartan in the combination drug Entresto®[9]

According to Lee *et al.*, especially for pharmaceuticals which require a production expansion, continuous manufacturing is an asset.[10] At the moment, the pharmaceutical industry largely focuses on batch synthesis despite the benefits of producing in continuous flow.[11,12] These advantages include increased safety, higher efficiency, less ecological impact, the possibility of reaction telescoping and a consistent quality.[10,11,13,14] However, in contrast to other industries, the pharmaceutical industry needs several years for a step-by-step scale-up of the production, as drugs have to undergo different phases of clinical trials. With the proceeding of the trial stages, a higher amount of the pharmaceutical is needed. Because of this tedious process until the final production scale

and because of the strict regulations for pharmaceuticals, the industry is often not willing to invest time and money to redesign existing processes.[10,11,15] However, for new substances as well as for pharmaceuticals which will require an extended production in the future, this does not apply.[10]

Especially for pharmaceuticals, the quality is a crucial factor favoring continuous production. Due to the nature of continuous manufacturing in addition with the consistent process variables, variations of the product are limited. Also, the permanent monitoring of the process stream by different analysis techniques allows a fast reaction in case of out-of-specification production and less material has to be rejected compared to batch manufacturing.[10,11,13,14] A popular case of insufficient quality is the valsartan affair, which came to light in 2018. Several medications containing valsartan were contaminated with *N*-nitrosodimethylamine, which is classed as presumably carcinogenic.[16,17]

Up to now, both active pharmaceutical ingredients of Entresto®, valsartan[18,19] and sacubitril,[20–24] are produced in batch. For valsartan, Hiebler *et al.* have recently published the synthesis of a late-stage precursor in three reaction steps in a multistep continuous setup.[19] Regarding sacubitril, only one[25] published synthesis route to a precursor was implementing flow chemistry. reactions.[20–24,26,27] However, the continuous steps were intermitted by purification or batch reactions and therefore do not allow reaction telescoping.[25]

The aim of this master's thesis was the development of a new synthesis route to an advanced sacubitril precursor. Several steps of this reaction cascade should be realizable as multistep continuous flow process. A key step in the attempted synthesis route to the late-stage sacubitril precursor is a Suzuki-Miyaura coupling. This reaction type is one of the three most important C-C coupling reactions and was awarded the Nobel Prize in 2010 together with the Heck reaction and the Negishi coupling.[28] All of them rely on palladium catalysts[28], which are usually of homogeneous nature.[29] However, for the application in continuous flow, heterogeneous catalysts are advantageous due to their easy separability.[11,30] In a catalytic packed-bed reactor, the reaction mixture flows through a column filled with the heterogeneous catalyst allowing reaction and separation at once.[11,31,32] Two examples for such heterogeneous palladium catalysts are $Pd(OAc)_2$-BOX-MPSG[33] and $Ce_{0.99-x}Sn_xPd_{0.01}O_{2-\delta}$,[34–36] which were both tested within the framework of this master's thesis.

2 Theoretical Background

2.1 Entresto®

Hypertension is the status of increased blood pressure levels with the European definition of ≥140 mmHg for systolic blood pressure or ≥90 mmHg for diastolic blood pressure.[37] In 2009, the World Health Organization stated hypertension as the main reason for global mortality by causing 13% of the worldwide deaths.[5] The number of adults suffering from hypertension is growing. In 2005, Kearney *et al.* predicted an increase from 972 million in 2000 to 1.56 billion in 2025.[6]

Patients being diagnosed with hypertension are in the high-risk group to suffer from heart failure.[7] Heart failure describes the condition in which the heart is not able to pump sufficient blood into the body anymore.[38]

There are several different treatments of heart failure depending on the kind and stage of the illness.[39] Approved in 2015,[1] the drug Entresto® (Novartis) is considered superior to prior medications for the treatment of hypertension and chronic heart failure.[1–4] It is a combination drug (Figure 1.1) composed of the two active pharmaceutical ingredients valsartan (Figure 2.1) and sacubitril (Figure 2.2),[9] which act as angiotensin II receptor antagonist and neprilysin inhibitor, respectively.[40]

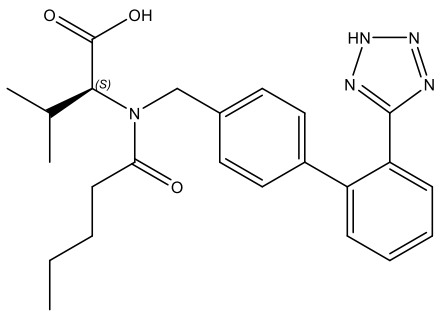

Figure 2.1: Valsartan

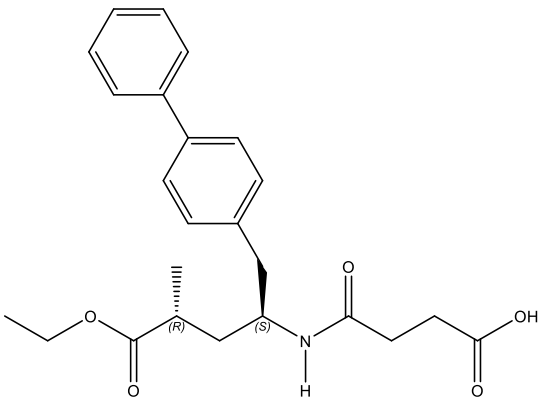

Figure 2.2: Sacubitril

2.1.1 ONE-FLOW Project

As already mentioned before, this master's thesis is part of the ONE-FLOW project. The overall aim of ONE-FLOW is the development of a digital flow cascade machinery, wherein the reaction steps are not aligned after each other but all happen in one reactor. This is attempted by the biomimetic approach of compartmentalization inside the reactor, using methods like Pickering emulsions and switchable fluid structuring. Moreover, ONE-FLOW wants to increase the sustainability by using only environmentally friendly solvents. The research of ONE-FLOW focuses on the production of drugs which will be highly required in 2020, including Entresto®.[8]

So far, both valsartan[18,19] and sacubitril[20–24] are produced in batch manufacturing. However, the benefits of continuous processing (see 2.2.2) as well as the rising number of patients suffering from hypertension[6] speak in favor of developing a continuous flow process for the synthesis of the respective active pharmaceutical ingredients.

2.1.2 Valsartan Synthesis

Several research groups worked on the optimization of the original valsartan synthesis procedure patented by Ciba-Geigy in 1991.[18] Mainly, the improvements were considering more efficient pathways or less toxic reagents compared to the original synthesis while still focusing on batch manufacturing.[19] However, also attempts towards a continuous valsartan synthesis were made. Pandarus *et al.*[41] and Nagaki *et al.*[42] developed synthesis routes to valsartan precursors in continuous flow. A multistep cascade for the continuous synthesis of a more advanced valsartan precursor was recently published by Hiebler *et al*. The key step of this approach is a Suzuki-Miyaura cross-coupling reaction catalyzed by the heterogeneous Pd catalyst $Ce_{0.20}Sn_{0.79}Pd_{0.01}O_{2-\delta}$.[19]

2.1.3 Sacubitril Synthesis

The first sacubitril synthesis was published by Ksander *et al.* in 1995. The linear reaction route started from the amino acid derivative *N*-Boc-D-tyrosine-methylester and yielded sacubitril over nine steps including a Wittig reaction, a stereoselective hydrogenation and an *N*-acylation (Scheme 2.1).[43] Several alternative procedures were published over time, however, almost all of them were exclusively consisting of batch reactions.[20–24,26,27] The only publication so far, employing steps in continuous flow to yield a sacubitril precursor, is the work of Lau *et al.* In a machine-assisted approach, they synthesized a sacubitril precursor starting from 4-iodobiphenyl over 7 reaction steps (Scheme 2.1). However,

their reactions in continuous flow were intermitted by batch steps or purification and thus did not allow reaction telescoping.[25]

A new approach for the continuous synthesis of a late-stage sacubitril precursor has been developed within this master's thesis, which starts from Boc-4-bromo-D-phenylalanine (Scheme 2.1). One of its assets are the three consecutive steps which are promising to be implementable in continuous flow and therefore allow a multistep cascade without intermediate work-up. Furthermore, these steps are promising to be realizable with a comparatively simple setup. The first step of the continuous system was performed successfully employing a packed-bed reactor and for the two subsequent steps, coil reactor units should be applicable.

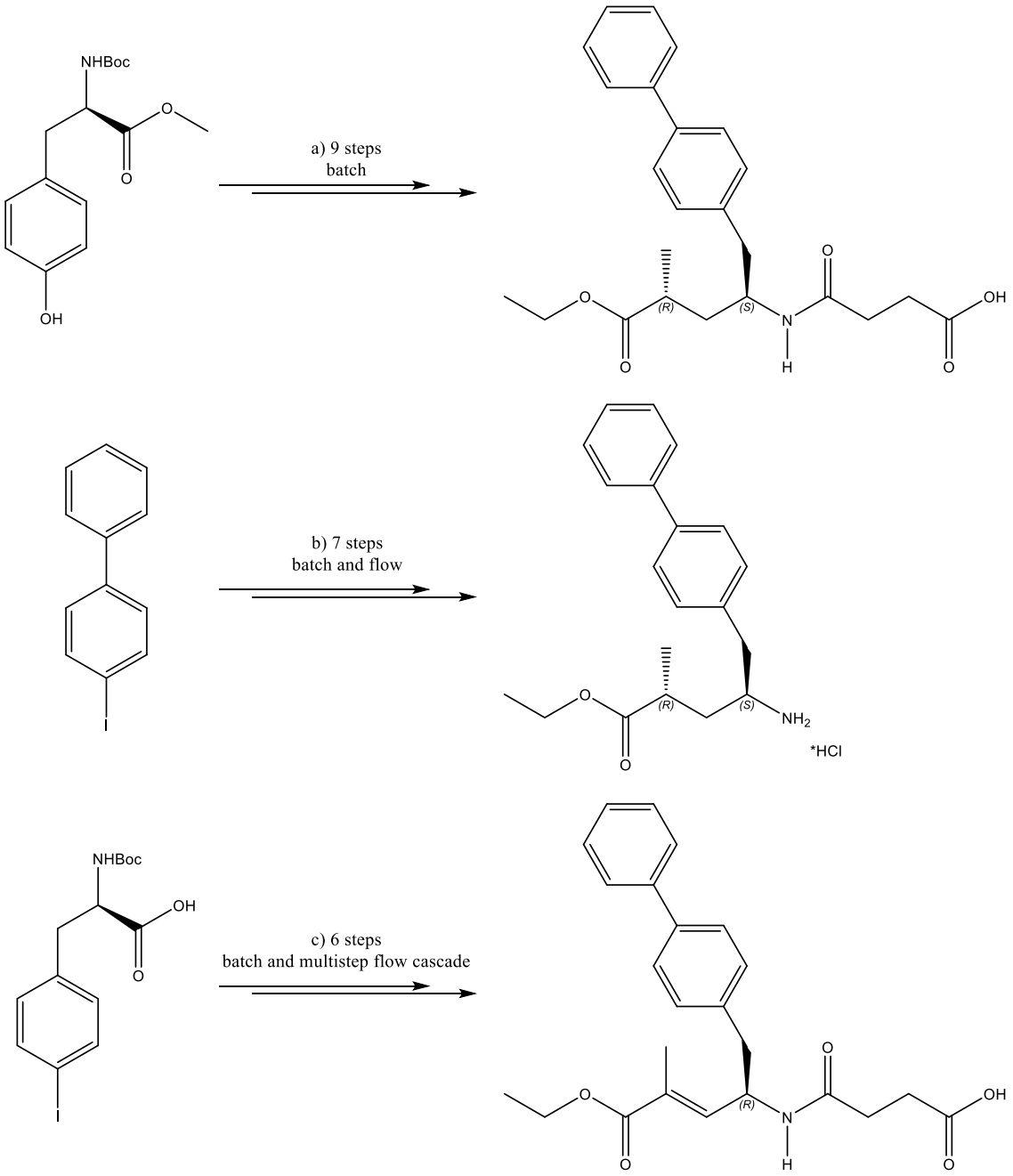

Scheme 2.1: Reaction procedures to sacubitril (precursors) developed a) by Ksander *et al.*,[43] b) by Lau *et al.*,[25] c) in this master's thesis

In the following section, the characteristics of continuous flow synthesis in general as well as its benefits and challenges will be explained in more detail.

2.2 Continuous Flow Synthesis

2.2.1 Chemical Processes and Reactor Types

Chemical processes can be classified as batch or continuous, which are described in the following together with their related reactor types. However, it has to be noted that some processes cannot be considered solely batch or continuous and are thus defined as semi-batch or semi-continuous.[31,44]

2.2.1.1 Batch Processes

In a batch process, all components are initially put into the system. During the reaction, no components are added or removed from the vessel and the mixture is only discharged after the process (Figure 2.3).[31,44]

Batch processes are performed in batch reactors (BRs), which are closed systems. The composition changes over time but is spatially uniform throughout the whole reactor (Figure 2.4). To maintain these conditions, sufficient stirring is required.[32,45]

2.2.1.2 Continuous Processes

In a continuous process, the charging of the reaction mixture and the discharging of the product mixture are performed continuously throughout the whole process (Figure 2.3).[31,44]

The two ideal cases for continuous reactors are continuous stirred tank reactors (CSTRs) and plug flow reactors (PFRs), which differ in their mixing behavior. Like in the batch reactor, the mixture in the CSTR is stirred rapidly to receive a spatially uniform composition throughout the reactor (Figure 2.4). Therefore, the composition in the outlet is the same as in the reaction mixture and the composition over time is constant as well.[32,45] In the PFR, no diffusion or mixing in the direction of the flow takes place and only lateral mixing is present.[32,45] As a result, the composition is uniform over time but not over space (Figure 2.4).

The PFR and CSTR show the two ideal flow patterns of continuous processes. In practice, however, partial mixing properties between these ideals always occur due to channeling, turbulence or stagnation of fluid.[31,45]

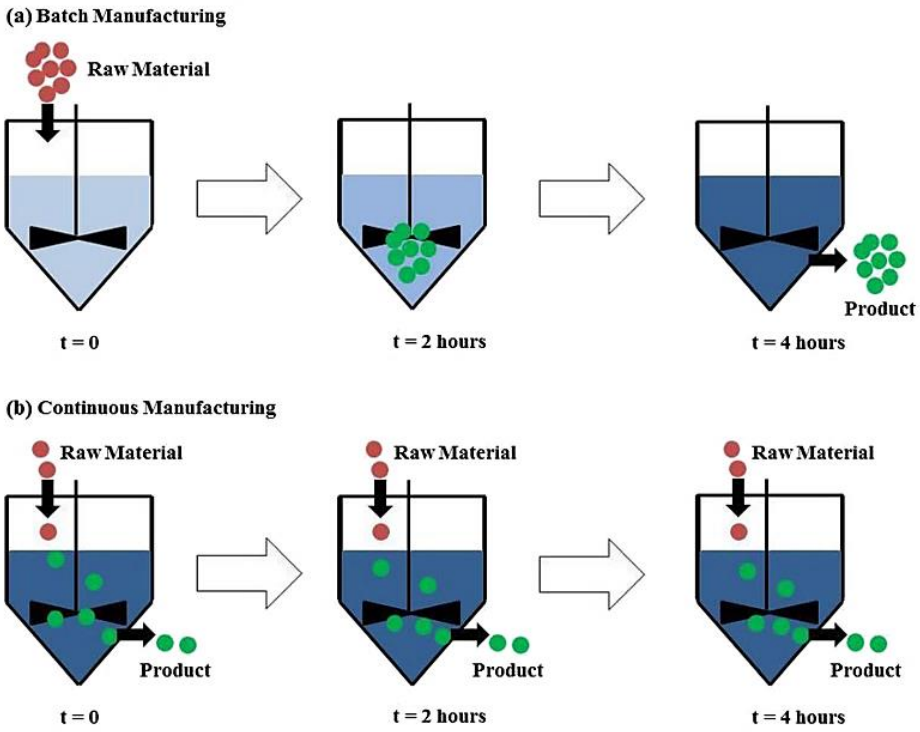

Figure 2.3: Batch processes vs. continuous processes[10]

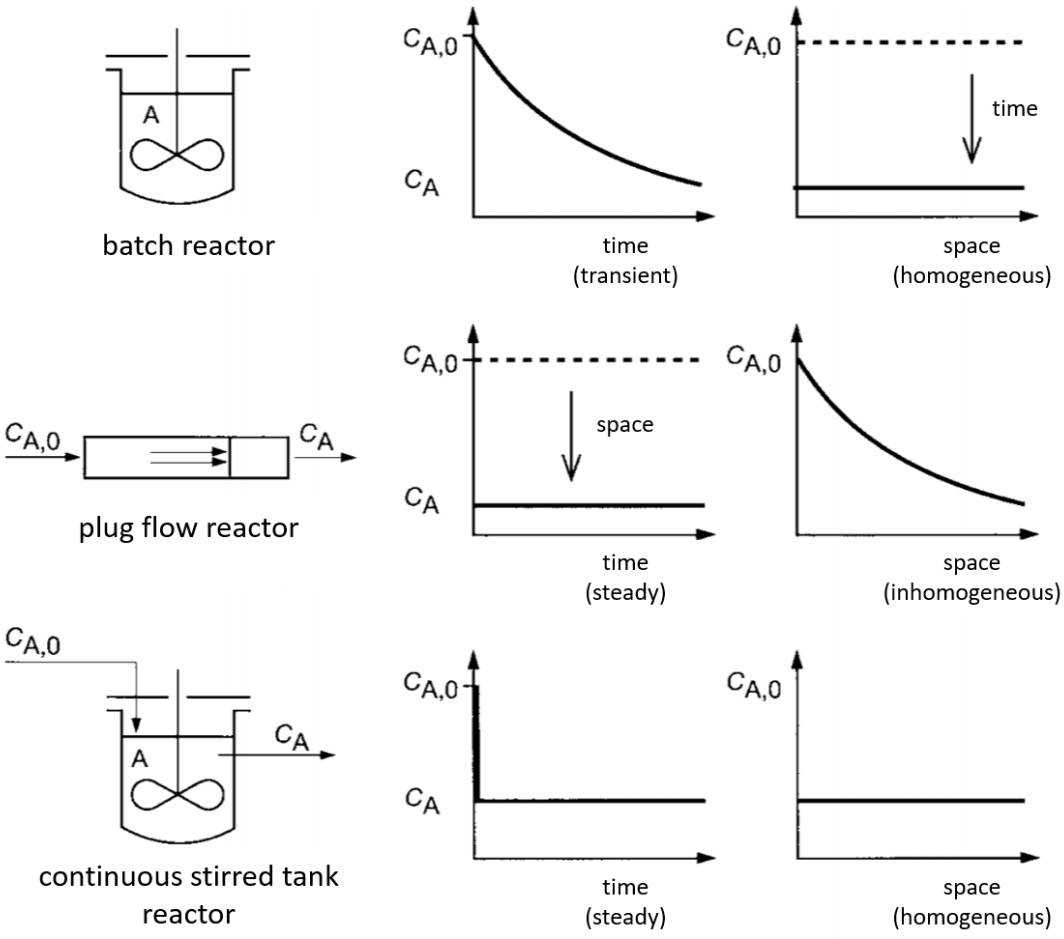

Figure 2.4: Ideal reactor types and their concentration profiles over time and space[30]

Compared to batch manufacturing, continuous flow chemistry offers a lot of benefits, which is discussed in more detail in the following section.

2.2.2 Benefits of Continuous Synthesis

Numerous reviews deal with the advantages of continuous synthesis over batch processes. Also, research and development as well as industries increasingly focus on continuous manufacturing.[10,11,13,14] Herein, some of the benefits of continuous flow are summarized.

2.2.2.1 Safety

The safety of continuous flow reactions is superior to batch chemistry in two aspects. On the one hand, the potentially dangerous or hazardous substances are enclosed in an automated system and the operator is not exposed to it. On the other hand, highly exothermic batch reactions require cautious work over a long period of time and cryogenic conditions. As flow reactors have a much higher surface-to-volume ratio, cooling can be performed faster and easier.[10,11,13,14]

2.2.2.2 Efficiency

The enhanced heat transfer does not only account for a more efficient cooling but also heating of the reaction mixture, which saves energy and time. The reaction efficiency itself is improved as well, as a reaction can often be accelerated by a simple temperature increase. In batch synthesis, the reaction temperature is often limited to the boiling point of the used compounds and solvents. In flow chemistry, however, the reaction setup can be pressurized easily and consequently reactions can be performed at much higher temperatures. Moreover, a very important factor accounting for the efficiency of continuous reactors is that they do not require the start-and-stop procedure necessary for batch reactors, which means the repeating units of loading, heating, reaction, cooling, unloading and cleaning. The remarkable efficiency of continuous reactors is reflected by their high output per time and volume.[10,11,13,14]

2.2.2.3 Ecological Impact

Reactions in continuous flow are often more sustainable than in batch in several aspects. As already mentioned, they are more energy efficient and less chemicals are exposed to the environment during the process. Additionally, there is the possibility for the recycling of reagents and energy formed during the reactions. Due to higher concentrations, simplified work-up and others, [10,11,13,14] less waste is generated and also the use of organic

solvents can be minimized. Ley *et al.* have stated that their flow laboratory requires almost ten times less solvent than their conventional laboratory.[14]

2.2.2.4 Reaction Telescoping

In flow chemistry, consecutive reaction steps can be performed directly after each other with no or simplified intermediate work-up. Such a reaction telescoping reduces the use of chemicals and eliminates hold time between individual reaction steps. Furthermore, intermediates can be directly used for the next step without exposing them to the environment. This is especially important for substances which are hazardous, sensitive or unstable.[10,11,13,14]

2.2.2.5 Quality

Continuously manufactured products feature a consistent product quality in contrast to the varying lots of batch manufacturing. The main reason is the continuity of the production itself, as it avoids separate lots. Additionally, the low variations are due to the better control of heating and mixing as well as the consistency of all process variables over time.

Regarding quality control, continuous reactions can be monitored constantly during the entire process by employing e.g. UV, IR, MS, HPLC or NMR analysis. This allows a permanent control of the product and, in case of a faulty process, less material has to be rejected than in batch production. Furthermore, in research and development, the continuous monitoring can be coupled with automated altering of the process parameters to find the optimal reaction conditions. It also enables easier and more comprehensive data collection.[10,11,13,14]

Four different types of reaction monitoring in continuous manufacturing have to be distinguished. At-line and off-line measurements require manual sample taking and transfer to the analysis instrument. At-line analyzers are located close to the manufacturing, whereas off-line measurements are conducted further away (e.g. in a central analysis facility) and thus do not deliver real-time results. In contrast, both in-line and on-line analysis are automated processes with the measurement instrument directly connected to the reactor. In in-line analysis, the probe is located in the reaction stream, whereas in on-line, a split-stream is analyzed and later recombined with the main stream.[46,47] The mentioned advantages are mainly attributed to the automated, direct control systems.[10,11,13,14,46,47]

2.2.3 Challenges and the Situation in the Pharmaceutical Industry

Certainly, continuous flow chemistry does not only entail advantages but also challenges. For example, if a synthesis needs a long reaction time to yield the right product, a flow reactor is not ideal.[11] Also, the handling of solids in flow is difficult and precipitation of compounds causes problems because of reactor blockage.[11,14] Assets of the batch reactor are the low costs and the flexibility for changes in the product. Thus, if only small amounts of product are needed, the production is usually performed in a batch reactor.[30]

Although many industries, like the polymer, petrochemical and bulk chemical industries, have already implemented continuous processes, the pharmaceutical industry is largely using batch manufacturing.[11,12] This difference is due to the development procedure in the pharmaceutical industry. It takes several years from the start of the development at a milligram scale over a step-by-step scale-up to the production in tons.[11,15] The reason for this are the required clinical trial stages, which each need a higher quantity of the pharmaceutical.[15] For economical and time reasons, the already existing and successful manufacturing might not be re-designed as a continuous process. However, continuous manufacturing can efficiently be implemented for either new substances or for already produced drugs which require an extended production because of high market demand.[10] Jiménez-González *et al.* have identified continuous processing as the most important research field of pharmaceutical industry regarding sustainable manufacturing.[12] Roberge *et al.* have studied numerous syntheses in pharmaceutical industry and have found that for 50% thereof, continuous production would be a benefit.[48] Especially if drug shortages occur due to a manufacturing failure or a pandemic, continuous manufacturing allows fast reaction and altering of the production according to needs.[10] Whereas batch scale-up often requires different reaction conditions for bigger reactors, flow scale-up can easily be achieved by increasing the operation time of a reactor or running multiple reactors simultaneously.[11]

After discussing the benefits of continuous flow chemistry, two specific devices employed in the flow experiments of this master's thesis are explained in the following, namely the catalytic packed-bed reactor and the plug & play reactor.

2.2.4 Catalytic Packed-Bed Reactor

Not only homogeneous but also heterogeneous reactions can be performed both in batch and continuously. To enable and promote reactions between two or more different

phases, the interface between these has to be as large as possible. Therefore, usually one of the components is handled as continuous phase, wherein the other phases are dispersed. There are numerous different reactor types for multiphase reactions in continuous flow, depending on the aggregation state of the phases and the involvement of a catalyst.[30,31]

The most common multiphase reactor in industry is the catalytic packed-bed reactor (Figure 2.5). It consists of a column packed with the solid catalyst. The gas or liquid flows continuously through the space between the stationary catalyst particles.[31,32]

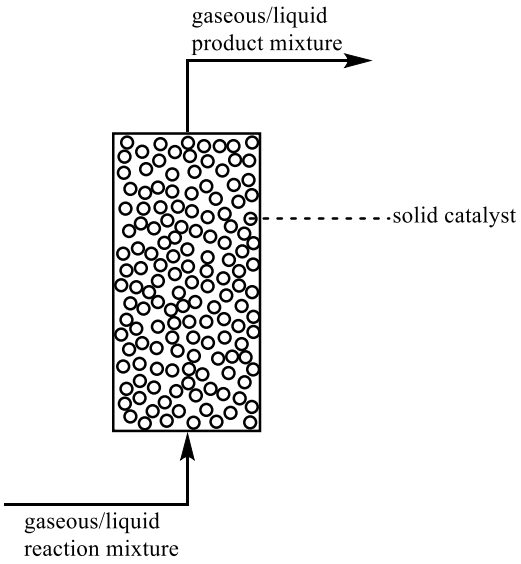

Figure 2.5: Catalytic packed-bed reactor[31]

In addition to the several advantages of continuous flow in general, some benefits pertain specifically to heterogeneously catalyzed reactions, comparing catalytic packed-bed reactors with batch reactors. First of all, the reaction and catalyst separation are performed in the same step, which renders a tedious catalyst recovery unnecessary. Furthermore, the comparably short exposure of the catalyst to the environment leads to a longer catalyst lifetime. Due to higher catalyst concentrations, a larger interfacial area as well as facile catalyst recycling, the efficiency of the catalyst is increased as well.[11]

2.2.5 Plug & Play Reactor

The so-called plug & play reactor (Figure 2.6) is a flexible setup embedding HPLC columns filled with catalyst particles. Hence, the columns work as catalytic packed-bed reactors

and these reaction segments are exchangeable depending on the needs of the process. The device offers modules for heating, cooling or mixing and can be used for liquid-solid, gas-solid as well as gas-liquid-solid reactions.[49,50] Its successful application in Suzuki-Miyaura cross-coupling reactions with a heterogeneous Pd catalyst has already been proven by Lichtenegger *et al.*[50] and Hiebler *et al.*[19] This catalyst type and reaction class corresponds to the application of the plug & play reactor in the course of this master's thesis.

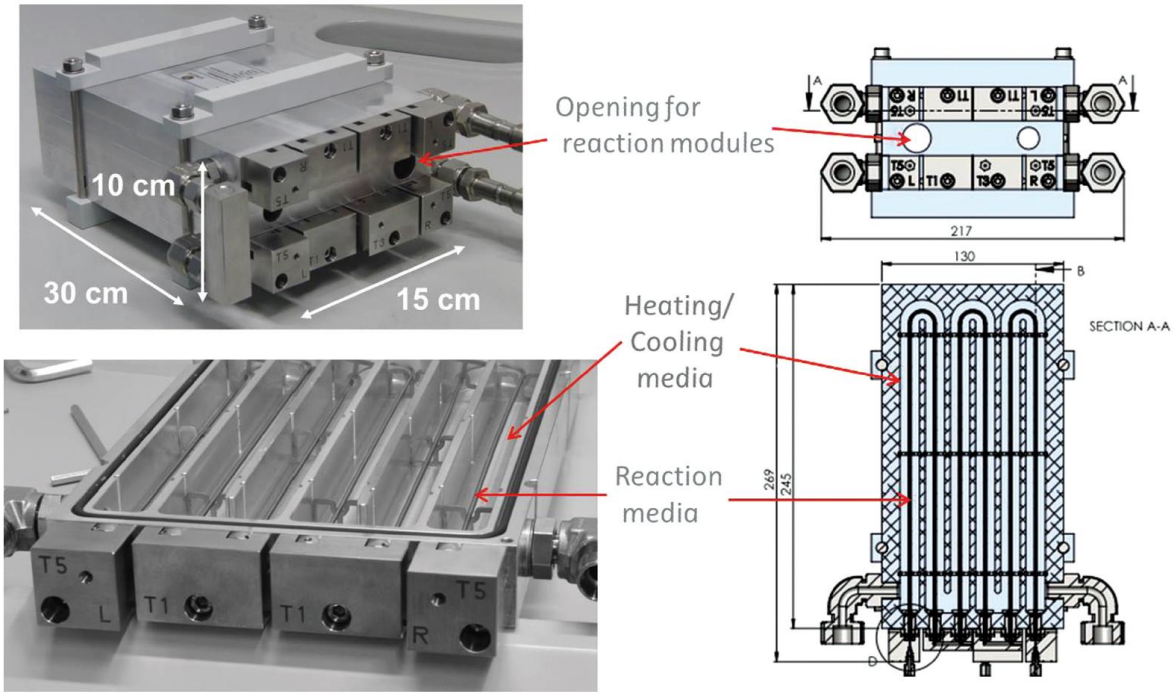

Figure 2.6: Pictures and schematic illustration of the plug & play reactor[49]

The topic of catalysis is explained extensively in the following chapter.

2.3 Catalysis

2.3.1 Fundamentals

2.3.1.1 Definition

Catalysts are compounds which accelerate chemical reactions by lowering their activation energy, but do not change the reaction equilibrium. In theory, the catalyst itself is not consumed during the reaction.[51,52]

2.3.1.2 The Catalytic Cycle

The catalytic cycle, depicted in Scheme 2.2, starts with the bonding of at least one of the reactants with the catalyst. In the next step, product formation takes place. Finally, the product is released from the catalyst.[51–53]

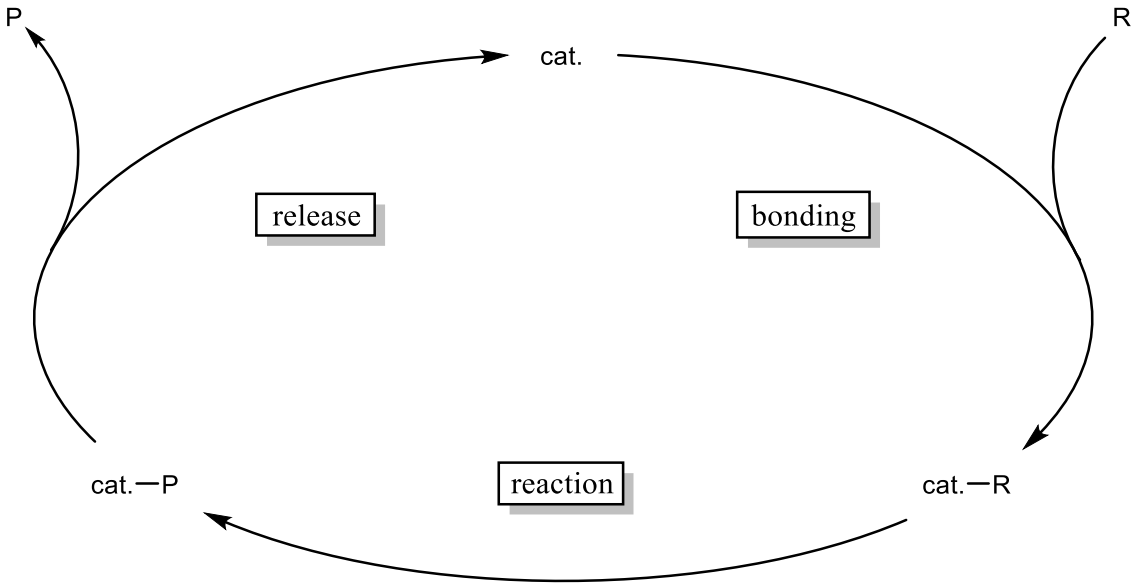

Scheme 2.2: General catalytic cycle[52]

The catalytic cycle illustrates why an ideal catalyst is not consumed during this process. After taking part in the reaction, it regains its original form, which differentiates it from reactants.[51,54] In practice, however, the catalyst can be subjected to changes and its activity can be decreased, which is explained in 2.3.1.5.[51]

2.3.1.3 Activation Energy

As shown in Figure 2.7, a chemical reaction has to undergo a transition state Z_1 with a relatively high potential energy E_{pot} while converting the educts A_G to the product P_G. The

difference in potential energy between the reactants and the transition state is defined as the activation energy $E_{a,0}$. The catalyst accelerates the reaction by lowering this activation energy.[53]

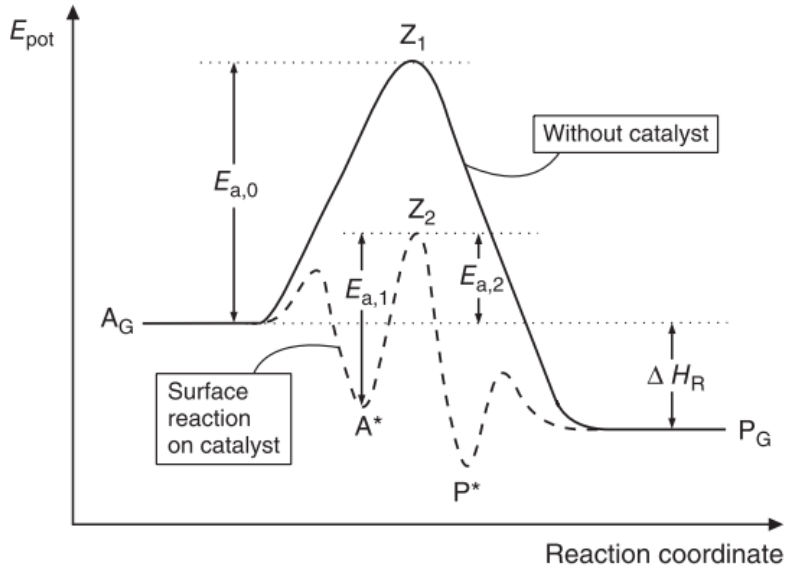

Figure 2.7: Comparison of a catalyzed and an uncatalyzed reaction in a potential energy diagram[51]

Every catalyzed or uncatalyzed reaction can consist of multiple elementary steps.[54] In Figure 2.7, a catalyzed reaction with three transition states is depicted. The three steps can be first the binding of one educt to the catalyst, second the reaction of the educts with each other and third the cleavage of the product from the catalyst.[51,52] The activation energy is the difference between the potential energies of the energetically highest transition state Z_2 and the educts.[51] As can be seen, the catalyzed reaction has a much lower activation energy ($E_{a,1}$ = true activation energy; $E_{a,2}$ = apparent activation energy) than the uncatalyzed one. However, the catalyst does not alter the potential energy of the educts or the product and hence the equilibrium constant does not change. Consequently, the reaction enthalpy and the Gibbs free energy are not influenced.[51,52] This means that a catalyst only affects the kinetics but never the thermodynamics of a reaction. A catalyst is not able to get a thermodynamically unfavored reaction to work.[52]

It has to be noted that the activation energy is lowered for both the forward and the reverse reaction. Furthermore, the binding strength between catalyst and educts or products is an important factor for the performance of a catalyst. If the bond between

catalyst and educts is too weak, the catalyst cannot really affect the conversion of the educts. In contrast, a tight bonding of the catalyst to the product prevents its release from the catalyst.[52]

Apart from accelerating a chemical transformation, catalysts can also influence the selectivity and specificity of a reaction.[55]

2.3.1.4 Selectivity and Specificity

Another important advantage of catalysts is their potential to increase the selectivity of a reaction. The selectivity *S* is defined as the rate of desired product formed per converted reactant. Equation 2.1 describes the selectivity of a model reaction shown in Scheme 2.3.[54]

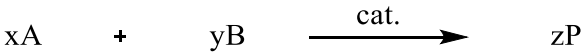

Scheme 2.3: Model reaction for selectivity calculation[54]

$$S_P = \frac{n_{P,t}}{n_{A,0} - n_{A,t}} \frac{x}{z} = \frac{Y}{X}$$

Equation 2.1: Selectivity; t = time after reaction, x and z = stoichiometric coefficients, Y = yield, X = conversion[54,56]

A catalyst can increase the selectivity by favoring the formation of the desired product over a side product. For example, it can decrease the activation energy for one specific step of a reaction sequence. By accelerating this step, the selectivity of the desired product can be increased. Different catalysts may have different influences on the selectivity which means favoring other products.[54]

Whereas the selectivity describes the preference of one of the possible reactions over the others, the specificity expresses the favoring of a certain reaction depending on the structure of the educt.[55]

For example, if a prochiral compound can be converted into two different enantiomers, an enantioselective catalyst prefers the formation of one of them. However, if, for example, a catalyst is able to convert the (*E*)-educt into the *trans*-product and the (*Z*)-educt into the *cis*-product, it is a stereospecific reaction. Specific reactions are always selective, but not vice versa.[55]

Although in theory regaining its original form after the reaction, a catalyst can be subjected to changes leading to a decrease of activity or even deactivation, as explained in the following section.[54,56]

2.3.1.5 Catalyst Deactivation

Although the ideal catalyst is not consumed during the reaction, various factors can lead to catalyst deactivation in practice.[56] The most common causes are catalyst sintering and catalyst poisoning due to impurities.[54]

If a competing molecule binds to the catalyst, the binding of the substrate is prevented. This can either be caused by binding of the competitive substrate to the same active site or by influencing the catalyst's active site by binding to another position. The catalytic activity is then decreased or lost completely. Catalyst inhibition means that this process is reversible, catalyst poisoning describes the irreversible process.[56]

Sintering occurs at high temperatures and, depending on the catalyst, it can already happen at around 200 °C. Sintering decreases the surface area of the catalyst and as a result the amount of accessible active sites.[56]

Various further reasons can have a negative influence on the catalytic activity. For example, temperature or pH changes can destroy the ligands. Also, dimerization or oligomerization of a catalyst can occur.[56] Leaching is another possible cause of decreasing catalyst activity and is an issue for immobilized catalysts.[11,51]

The topic of catalyst immobilization together with the different characteristics of homogeneous and heterogeneous catalysts will be dealt with in the next session.

2.3.2 Classification of Catalysts

Many different types of categorizing catalysts are conventional. Two of the main classes are homogeneous and heterogeneous catalysts.[52,56]

2.3.2.1 Homogeneous Catalysis

In homogeneous catalysis, the catalyst is present in the same aggregation state as the reactants, which usually is a liquid but can also be a gas.[52,56] Homogeneous catalysts have better accessible active sites and a higher activity than heterogeneous ones because of their high degree of dispersion.[51] Due to the higher probability of collisions, in general milder reaction conditions can be applied and less catalyst is needed. Homogeneous catalysts show a better selectivity but a lower thermal stability.[51] However, the most

significant disadvantage is the difficult separation and recovery of the catalyst from the mixture after the reaction.[56]

2.3.2.2 Heterogeneous Catalysis

In heterogeneous catalysis, the catalyst is present in a different phase than the reactants. Mostly, the catalyst is solid, whereas the reaction mixture is gaseous or liquid.[51,56] Due to the heterogeneity, only the surface of the catalyst can take part in the reaction, which in general results in a lower activity per catalyst mass. Thus, heterogeneous catalysts are usually required in higher concentrations. Also, the selectivity is lower compared to homogeneous catalysts. On the contrary, they have a higher thermal stability and, most importantly, are easily separable from the reaction mixture.[51] Therefore, they are highly preferred for industrial purposes and frequently applied for catalytic reactions on a large scale.[52]

2.3.2.3 Immobilization

The conversion of homogeneous catalysts into an insoluble form is called immobilization. It is used to combine the advantages of homogeneous and heterogeneous catalysis. The immobilized catalyst should show high activity and selectivity as well as feature an easy catalyst separation and recycling. A disadvantage of immobilized catalysts is the decrease in activity compared to homogeneous ones as the active sites are less accessible.[51] Additionally, leaching of the catalyst into the reaction mixture is a big problem.[11,51]

Four different immobilization methods are commonly used. Both adsorption and covalent binding to an insoluble support are frequently employed techniques. Also, immobilization via electrostatic interaction between the catalyst and a suitable porous solid, like zeolites or silicates, is possible. In all of these methods, the support has to interact with the catalyst and thereby modifies it. In encapsulation, however, no interaction takes place. The support is either assembled around the catalyst or the catalyst is assembled in the porous support.[51,57]

The heterogeneous Pd catalysts used for the Suzuki coupling reactions in the course of this master's thesis will be described in 2.5, after giving an overview about the respective reaction type.

2.4 Suzuki-Miyaura Cross-Coupling Reaction

2.4.1 Definition

Cross-coupling reactions comprise the carbon-carbon bond formation between an organic halide or triflate and an organometallic compound, following the general scheme depicted in Scheme 2.4. In order to obtain a decent yield, the utilization of a transition metal catalyst is necessary. Most commonly, Pd catalysts are used.[58,59]

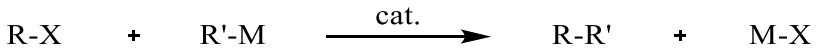

Scheme 2.4: General cross-coupling reaction; R and R' = usually aryl or alkenyl, M = metal, X = halide or triflate[59]

Depending on the organometallic species, different types of cross-coupling reactions are defined. Examples are the Suzuki coupling with boronic acid derivatives, the Stille coupling with organotin compounds, the Kumada coupling with lithium or magnesium alkyls and the Negishi coupling with zinc organyles.[58,59]

The first successful coupling reactions of alk-1-enylboranes with aryl halides were published by Miyaura and Suzuki in 1979. The reactions were performed using a base and the catalyst $Pd(PPh_3)_4$.[60] Later, the generalized reaction type, namely the Pd catalyzed coupling of an organic halide or triflate with an organoboron compound (Scheme 2.5), was referred to as Suzuki-Miyaura coupling or Suzuki coupling.[61]

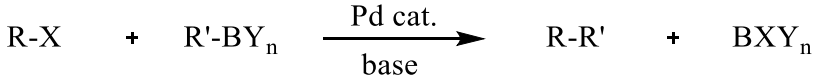

Scheme 2.5: General Suzuki-Miyaura cross-coupling reaction; R and R' = usually aryl or alkenyl, X = halide or triflate, Y_n = usually $(OH)_2$[62]

Most commonly, the Suzuki coupling is performed as C_{sp2}-C_{sp2} bond formation, as mainly aryls or alkenyls are used as organic residues.[62] However, it has been shown that also Suzuki couplings with C_{sp3}-B and C_{sp}-B bonds are possible.[61] The reactivity of the organic halide is associated with the strength of the C-X bond and follows the order X = I > Br ≥ OTf ≫ Cl with I as the most reactive species.[63] Therefore, iodine and bromine

compounds are most widely used.[62] As organoboron species, boronic acids are the most widespread[62] because of their commercial availability.[58,62] For catalyst, base and solvent there are a lot of different options and finding the best conditions for a specific reaction has to be performed empirically by screenings.[63] A common base for Suzuki-Miyaura couplings is sodium carbonate,[63] but also various others can be used, including carbonate, fluoride, phosphate or hydroxide bases.[62] Examples for suitable solvents are dimethyl ether, THF, dioxane and alcohols, whereby often water is added to improve the reaction.[63] As catalyst, the originally used $Pd(PPh_3)_4$[60] is still employed most frequently.[64] However, also numerous other palladium and even non-palladium transition metal catalysts, e.g. nickel catalysts, have been successfully used for Suzuki coupling reactions.[29,35,64–67]

2.4.2 Catalytic Cycle

The general catalytic cycle of a Suzuki-Miyaura coupling is depicted in Scheme 2.6. The three main steps are firstly oxidative addition, secondly transmetalation and thirdly reductive elimination.[58,63] Either the oxidative addition or the transmetalation can be the rate determining step.[63] The actual catalytic species is a coordinatively unsaturated 14-electron Pd(0) complex. It is generated from the applied Pd(0) or Pd(II) pre-catalyst either via ligand dissociation or reduction, accordingly.[58] With the oxidative addition, the Pd(0) is converted into Pd(II). After the reductive elimination, the active catalytic Pd(0) species is regenerated.[63]

It is known that a base accelerates the Suzuki-Miyaura coupling in the transmetalation step, but the exact mechanism is still not completely elucidated. There are two proposed pathways for the effect of the base. Path A describes the formation of a borate from the boronic acid and the base. The electron-rich borate then takes part in the transmetalation reaction. In path B, the transmetalation proceeds over an (oxo)palladium(II) intermediate. It is assumed that the dominating pathway depends on the particular reaction.[62,68]

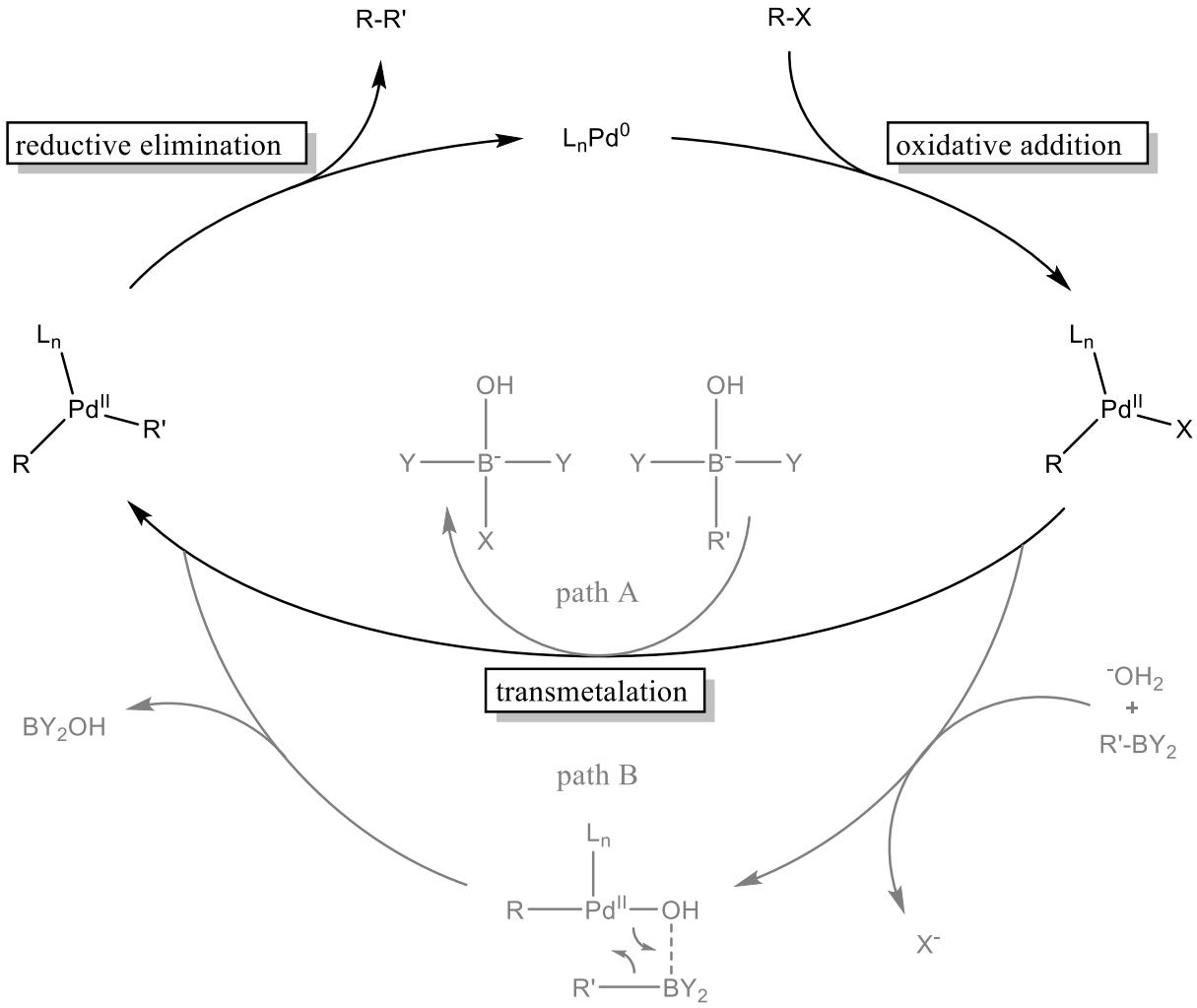

Scheme 2.6: Catalytic cycle of a Suzuki-Miyaura cross-coupling[62]

2.4.3 Importance in Organic Synthesis

The Suzuki coupling was awarded the Nobel Prize in 2010 together with the Heck reaction and the Negishi coupling. They are the three main C-C coupling reactions, all involving palladium catalysts.[28] Nowadays, the Suzuki coupling is the most performed cross-coupling reaction in research as well as in industry[62] and especially for the synthesis of biaryls it is the most important reaction.[28] Biaryls are very abundant substructures in bioactive molecules, which renders Suzuki couplings highly significant in pharmaceutical industry.[65] Also in natural products, new electronic materials and agrochemicals, biaryls are frequent motifs.[28]

The advantages of the Suzuki reaction mainly derive from the benefits of the boronic acid derivatives used.[62] They are usually air, moisture[28,58,62] and temperature stable[62] and thus do not have to be produced *in situ*.[63] Furthermore, they are often commercially

available,[58,62,64,65] typically non-toxic,[28,62,63,69] comparatively environmentally friendly[64] and the boron side-products can be removed easily.[58,64,69] In addition, Suzuki couplings tolerate a huge variety of functional groups[28,58,62,65,69] and allow mild reaction conditions.[64,65,69]

As already mentioned in 2.4.1, for Suzuki-Miyaura cross-coupling reactions, a plethora of different homo- and heterogeneous transition metal catalysts can be utilized. In the following, the use of heterogeneous Pd catalysts will be discussed in more detail.

2.5 Heterogeneous Pd Catalysts in Suzuki Coupling Reactions

The classically used Pd catalysts for Suzuki reactions, like $Pd(PPh_3)_4$, are of homogeneous nature.[29] As already described in 2.4.3 and 2.3.2 respectively, the Suzuki coupling is a highly important reaction for various industries and heterogeneous catalysis is the preferred system for industrial applications, especially for synthesis in continuous flow. Thus, various heterogeneous and immobilized homogeneous Pd catalysts have been developed and applied for Suzuki-Miyaura reactions.[29,33,35,36,50,70] Examples are Pd on polymer beads,[70] Pd on modified silica,[29,70] Pd on carbon[29] and Pd substituted Ce-Sn oxides.[35,36,50] The two types of heterogeneous Pd catalysts employed in this master's thesis, $Pd(OAc)_2$-BOX-MPSG and $Ce_{0.99-x}Sn_xPd_{0.01}O_{2-\delta}$, are immobilized by covalent bonding to modified silica gel and by incorporation into a crystal lattice, respectively.

However, as for immobilized catalysts in general, a big drawback of many of these Pd catalysts is leaching, which does not only lower the catalyst activity and reusability but also contaminates the product. The leaching of heterogeneous Pd catalysts is a result of their proposed (quasi)homogeneous catalytic mechanism. In this mechanism, the Pd(II) species is released from the original heterogeneous catalyst and dissolved. It is assumed that the dissolved Pd(II) species is the actually catalytically active species. After the catalytic cycle, which means after the reductive elimination step, the dissolved species is captured again by the support. This readsorption process is working sufficiently effective in batch reactions but is more difficult in continuous flow, as the leached palladium can migrate out of the reactor with the reaction stream, before a recapture is possible.[71]

Nevertheless, if the leaching is low and a stable catalytic activity and reusability are given, heterogeneous Pd catalysts can be effectively used in continuous Suzuki-Miyaura cross-coupling reactions.[36,50] If the Pd levels in the product are below the regulatory limits of

5 ppm in oral pharmaceuticals,[72] even applications in the pharmaceutical industry are possible.[34]

In the following, the heterogeneous Pd catalysts $Pd(OAc)_2$-BOX-MPSG and $Ce_{0.99-x}Sn_xPd_{0.01}O_{2-\delta}$ are described including their benefits, which were the reason for their utilization in the performed Suzuki coupling reactions.

2.5.1 $Pd(OAc)_2$-BOX-MPSG

$Pd(OAc)_2$-BOX-MPSG is a heterogeneous Pd catalyst consisting of $Pd(OAc)_2$ with a bis(oxazoline) (=BOX) ligand which is bound to a 3-mercaptopropyl-functionalized silica gel (MPSG) (Figure 2.8). The preparation of this catalyst consists of two steps, firstly the immobilization of the BOX ligand on MPSG particles and secondly the metalation of the resulting BOX-MPSG with $Pd(OAc)_2$ to yield the final complex. It was proven to show a high stability and reusability in the tested heterogeneous Suzuki coupling reactions of phenylboronic acid with aryl halides. Therein, it can be used for at least ten times and almost no Pd leaching takes place.[33]

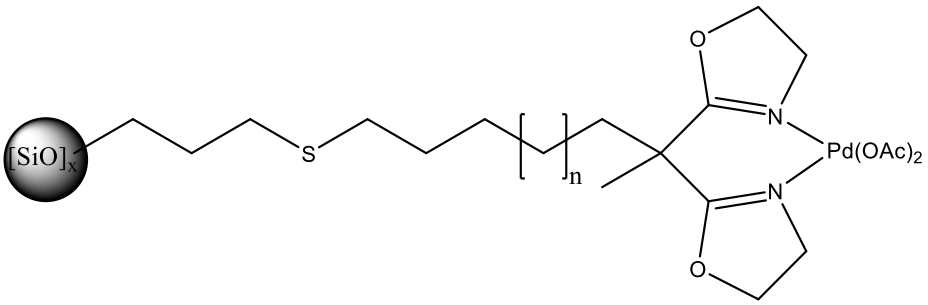

Figure 2.8: $Pd(OAc)_2$-BOX-MPSG catalyst[33]

2.5.2 $Ce_{0.99-x}Sn_xPd_{0.01}O_{2-\delta}$

Further potent heterogeneous Pd catalysts are the palladium substituted Ce-Sn oxides $Ce_{0.99-x}Sn_xPd_{0.01}O_{2-\delta}$ (x = 0 – 0.99; δ represents the vacancies in the oxide crystal lattice). Especially the catalysts with x = 0.20, 0.79 and 0.99 show a high activity in Suzuki couplings and good recyclability.[35] Also, the compliance with the limit of 5 ppm for Pd in oral pharmaceuticals has been considered in batch and flow. The results obtained were promising that the application of these catalysts for the synthesis of advanced chemical intermediates meets this regulation.[34–36,72]

Another benefit of this catalyst type is its easy preparation via a modification[35] of the solution combustion synthesis described by Baidya *et al.*[73] The solution combustion technique is a type of self-propagating high-temperature synthesis.[74] For this specific catalyst, the reactants together with glycine as fuel are pestled, mixed with water and put into a furnace at 350 °C. After 1 h, it is again pestled and put back into the oven (see 5.4.1). Thus, the preparation is a straightforward and fast method, which can be performed with standard laboratory equipment.[36]

The catalyst $Ce_{0.20}Sn_{0.79}Pd_{0.01}O_{2-\delta}$ was applied in a recently published multistep flow synthesis of an advanced valsartan precursor by Hiebler *et al.* It was used for a Suzuki cross-coupling reaction performed in a packed-bed reactor, like it was aimed and achieved for sacubitril in this master's thesis.[19]

3 Results and Discussion

The aim of this master's thesis was the development of a new synthesis route to a late-stage sacubitril precursor, whereof multiple steps can be performed in continuous flow. Therefore, preliminary experiments were first performed in batch. After finding an appropriate synthetic route, the Suzuki coupling as key step was optimized in batch in terms of different reaction parameters (catalyst type, catalyst concentration, solvent). Finally, first experiments in continuous flow were performed to demonstrate the applicability of the Suzuki coupling in a continuous process.

If not stated otherwise, for the Suzuki coupling reactions mentioned throughout this chapter, the same conditions were applied. These were based on previous work[35] with the used catalysts as well as preliminary experiments. The conditions are a reaction temperature of 75 °C, iPrOH:H_2O = 7:3 (v:v) as solvent, 25 mM substrate, 1.5 eq. phenylboronic acid, 1.5 eq. K_2CO_3 and 1 mol% $Ce_{0.20}Sn_{0.79}Pd_{0.01}O_{2-\delta}$ (catalyst **I**). For a better readability, these parameters are not mentioned again for each reaction.

3.1 Development of a Synthesis Route in Batch

Experiments were first performed in batch in order to find a successful synthesis route to sacubitril precursor **7**, which can later be performed and optimized in continuous flow. In this chapter, the research process from the initial approach to the final reaction pathway yielding late-stage sacubitril precursor **7** is described. For a better understanding, the finally elaborated synthesis route is anticipated in Scheme 3.1. Herein, aryl iodide **4a** is synthesized over three steps in batch, followed by a Suzuki coupling, *tert*-butyloxycarbonyl (Boc) deprotection and *N*-acylation in continuous flow.

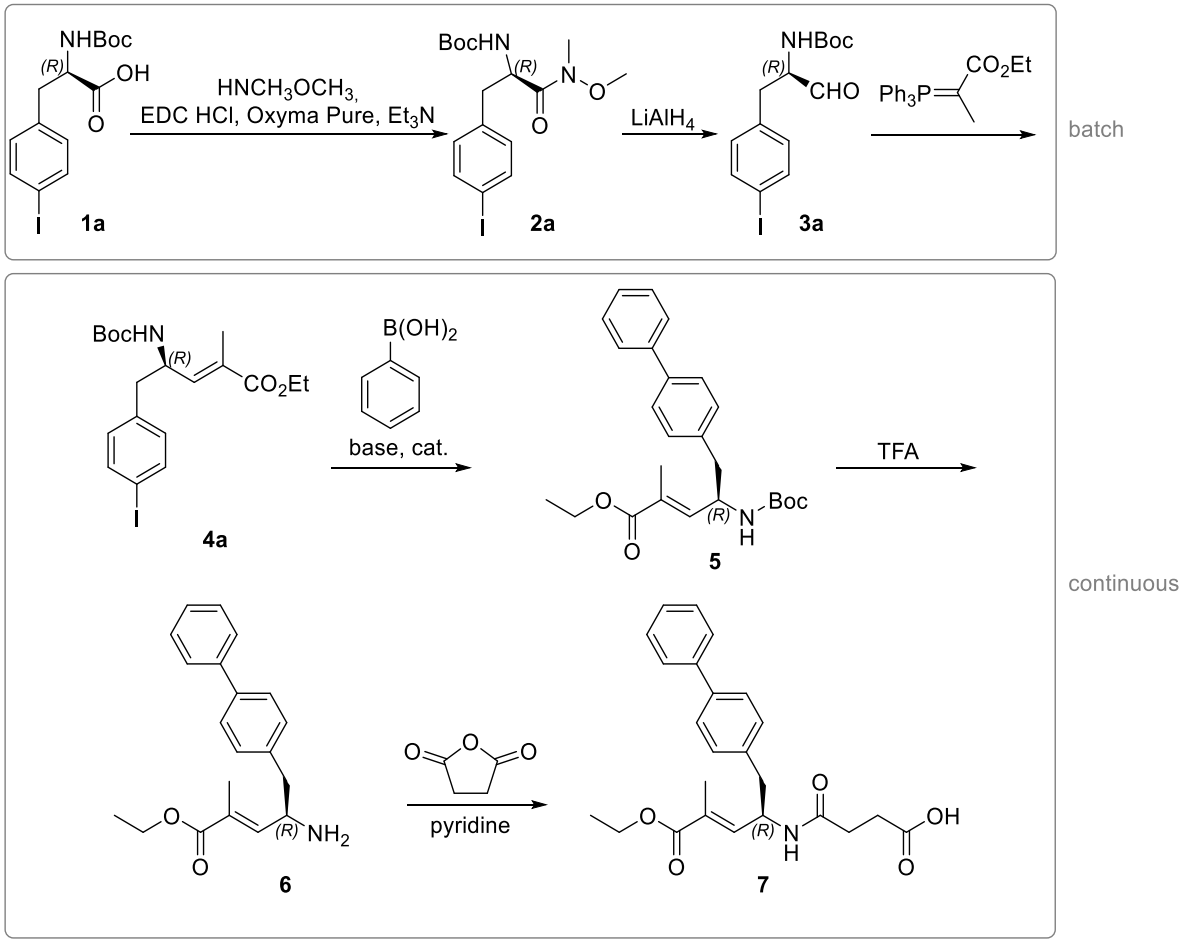

Scheme 3.1: Final synthesis route to sacubitril precursor **7**

3.1.1 Initial Approach

The initial approach for the synthesis of the late-stage sacubitril precursor **7** is shown in Scheme 3.2. This approach consists of six reaction steps, starting from commercially available Boc-4-bromo-D-phenylalanine **1b**. The substrate is converted into Weinreb amide **2b**, which is then reduced to the according aldehyde **3b**. Subsequently, aryl bromide **4b** is obtained via a Wittig reaction. An *N*-acylation with succinic anhydride, a Suzuki-Miyaura cross-coupling reaction and a deprotection step should finally yield precursor **7**. The first three steps need to be performed in batch, whereas the last three steps were intended to be achieved and optimized in continuous flow.

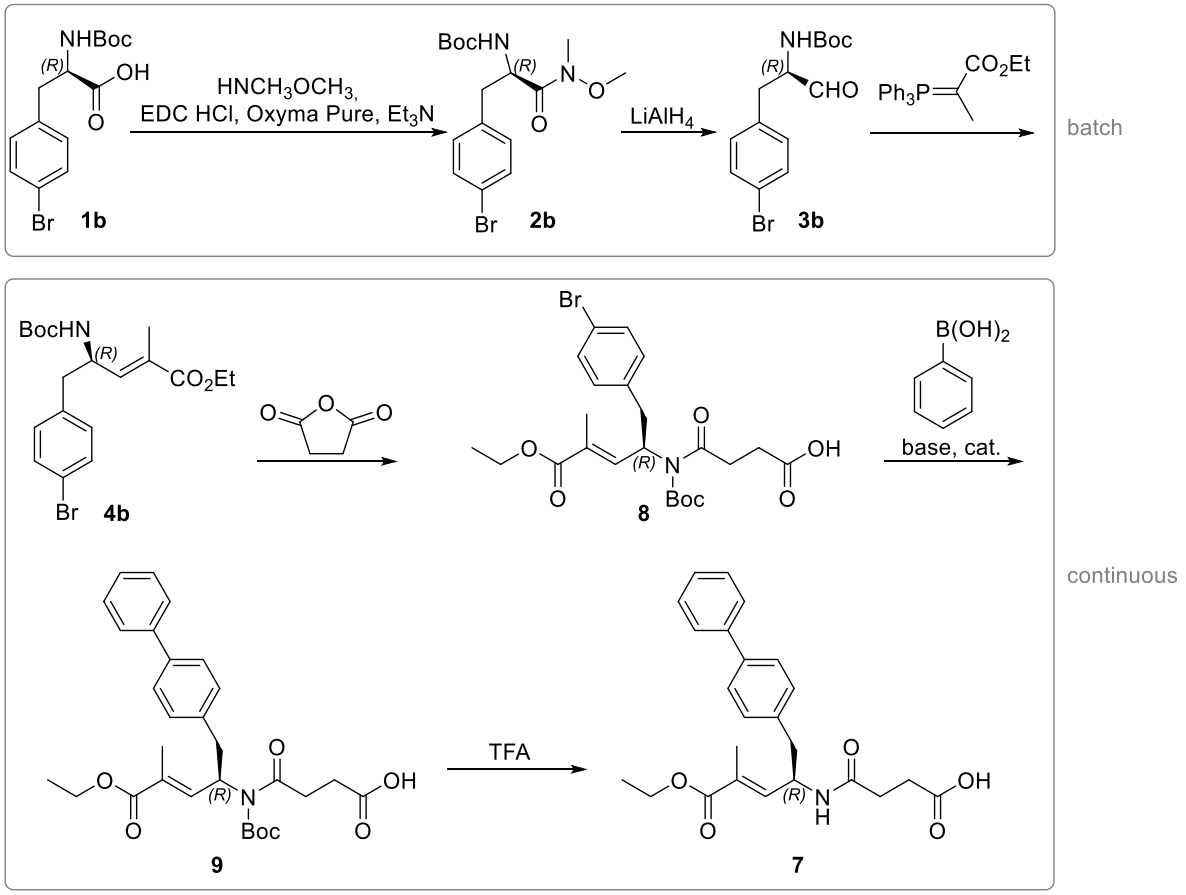

Scheme 3.2: Initial approach for the synthesis of sacubitril precursor **7**

3.1.1.1 Successful Synthesis of Aryl Bromide 4b

The three-step synthesis of **4b** in batch was successfully performed as planned (Scheme 3.3).

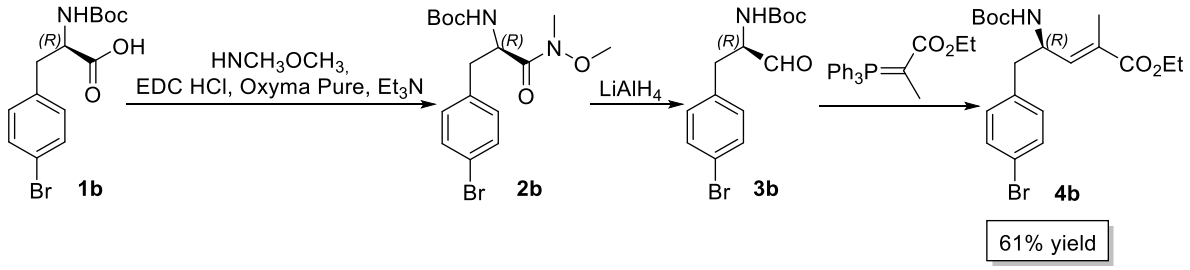

Scheme 3.3: Synthesis of **4b**

The procedure was based on a similar synthesis reported by Ksander *et al.*[43] and gave a decent overall yield of 61%. All products **2b**, **3b** and **4b** were isolated and identified by

^{1}H and ^{13}C NMR. However, isolation of the intermediate products was found to be redundant and, in view of an easier and faster overall synthesis, purification of **4b** was consequently performed only after the three-step batch process.

The first and third step were straightforward overnight reactions at room temperature. The reduction of **2b** with $LiAlH_4$ (2 eq.) was completed within only 30 min and was tested at two temperatures (0 °C[43] and -40 °C[75]). As the reaction worked well at both temperatures, 0 °C was chosen for further synthesis for simplicity reasons.

3.1.1.2 Unsuccessful Acylation of Aryl Bromide 4b

The initially intended fourth reaction step, which was the acylation of the Wittig product **4b** with succinic anhydride, was not successful (Scheme 3.4). The performed experiments were based on similar procedures for *N*-acylation reactions found in literature. The reaction of **4b** with an excess of succinic anhydride (1.2 eq.) in THF at room temperature was tested with only the substrates,[76,77] the addition of triethylamine (Et_3N)[78] (1 eq.) and the addition of both Et_3N (1 eq.) and 4-dimethylaminopyridine (4-DMAP) (0.2 eq.). The latter was also performed at 60 °C.[79] In further experiments, NaH was allowed to react with substrate **4b** before an addition of succinic anhydride. These trials were carried out at room temperature in THF with a 1:5:10 ratio[80] of **4b**:succinic anhydride:NaH and in dimethylformamide (DMF) with an according ratio of 1:2:2.[81]

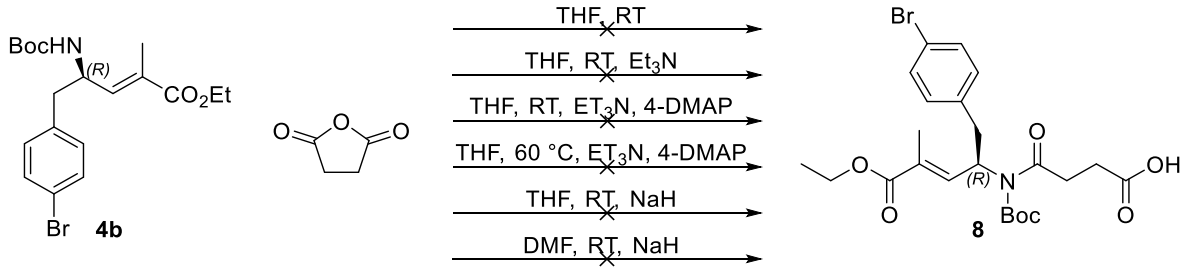

Scheme 3.4: Unsuccessful acylation of **4b**

The uncatalyzed reaction between the two substrates is presumably prevented by the weak nucleophilicity of the amide substrate. The addition of different bases was tested in order to convert the amide into the conjugated base, which is a strong nucleophile and could possibly attack the anhydride. However, neither Et_3N alone, its combination with the catalyst 4-DMAP nor NaH led to the desired effect. The only experiment that gave an

observable conversion was the one with the very strong base NaH in DMF. Still, HPLC analysis showed a mixture of mainly educt with a lot of different compounds. Even if product **8** was among these, the yield would have been very low and the isolation very tedious. Hence, this approach was not studied further.

3.1.2 Alternative Attempts

As the intended acylation of **4b** was not possible, other approaches to yield the desired sacubitril precursor **7** were tested. In this chapter, the main research steps before finding the final solution are described.

3.1.2.1 Preponement of the Suzuki Coupling

The first alternative approach was changing the order of the last three reaction steps, namely *N*-acylation, Suzuki coupling and deprotection. However, previous experiments with the $Ce_{0.99-x}Sn_xPd_{0.01}O_{2-\delta}$ catalysts used for the Suzuki coupling suggested an interference of NH groups with the catalyst. Thus, neither performing the deprotection first in order to enable the acylation reaction nor performing the Suzuki coupling with **4b** seemed reasonable. Hence, it was intended to initially protect the remaining NH group of **4b** before performing the Suzuki coupling, followed by the deprotection and the subsequent acylation reaction (Scheme 3.5).

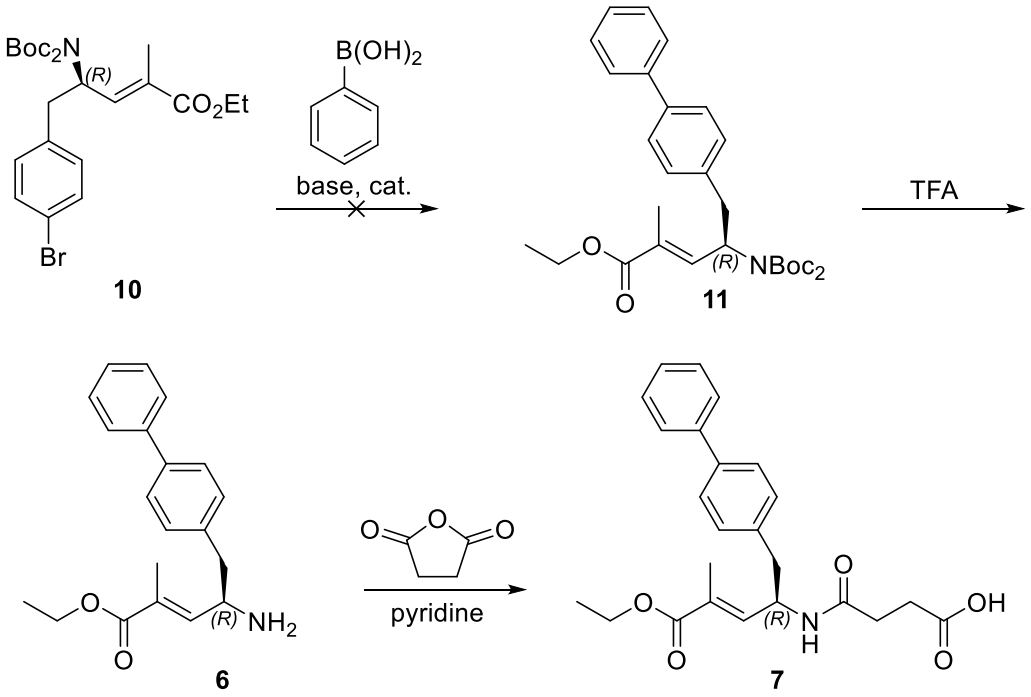

Scheme 3.5: Preponement of the Suzuki coupling

In order to obtain the double protected Wittig product **10**, Boc protections of **1b**, **3b** and **4b** were tried (Scheme 3.6). According to Basel and Hassner, depending on the substrate, different reaction conditions influence the Boc protection. These include the equivalents of Boc_2O, the presence of 4-DMAP and Et_3N as well as their ratio.[82] Therefore, the experiments were carried out with different equivalents of Boc_2O in combination with 4-DMAP, Et_3N or both under argon in MeCN at room temperature. However, only **4b** could successfully be protected, which was verified by ^1H and ^{13}C NMR. In this 24 h reaction with a yield of 91%, 4 eq. Boc_2O and 0.2 eq. 4-DMAP were used.

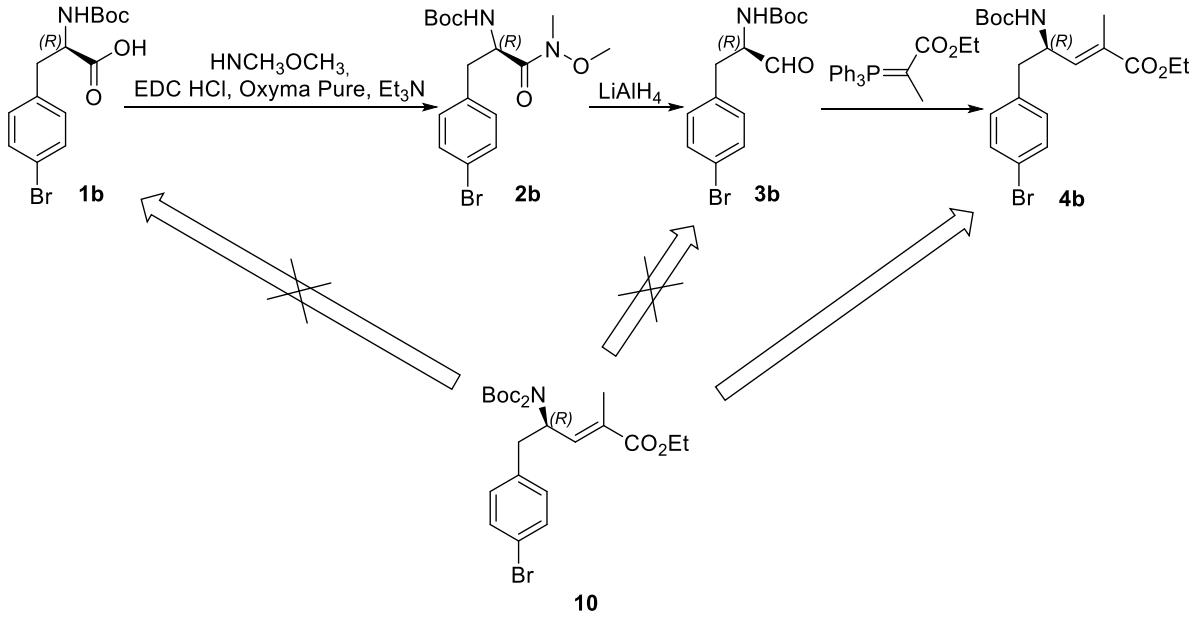

Scheme 3.6: Synthesis of the double protected Wittig product **10**

The succeeding Suzuki coupling of **10** gave a poor conversion of 45% after a reaction time of 2 h (Figure 3.1, see 3.1.3.3). As the Suzuki coupling did not seem to work with any of the intermediate products, other approaches were tried based on literature research.

3.1.2.2 Methylester Approach

The next approach, shown in Scheme 3.7, started with an esterification of the carboxyl group of the original substrate **1b**. According to Tang *et al.*, an esterification with MeOH and $SOCl_2$ is simultaneously deprotecting the Boc group and should therefore yield methylester **12**.[83] The reaction route should then be continued with a protection with two Boc groups and a Suzuki coupling to yield biphenyl **14**.

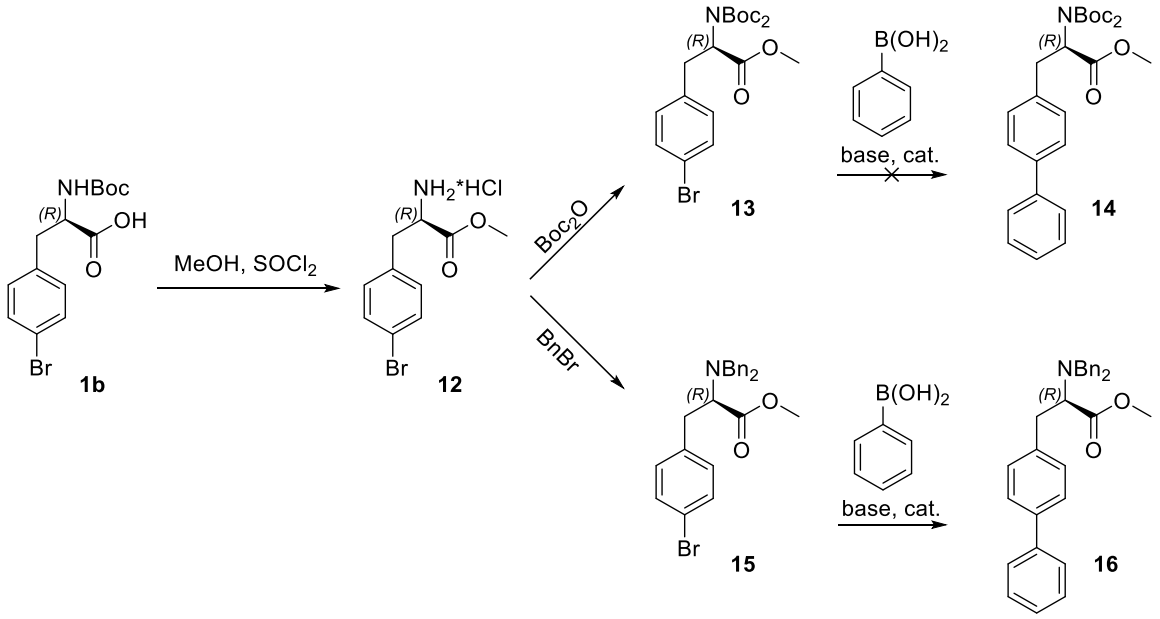

Scheme 3.7: Methylester approach

Based on similar literature procedures,[84,85] the esterification to **12** was performed by a dropwise addition of thionyl chloride (5 eq.) to a solution of substrate **1b** in MeOH at 0 °C followed by stirring at room temperature. The crude product was directly used in the Boc protection with Boc_2O (4 eq.), 4-DMAP (0.2 eq.) and Et_3N (1 eq.) under argon in MeCN at room temperature. Again, different conditions for the Boc protection were compared,[82] but the described procedure was the most efficient one, although it only gave 19% yield over two steps.

The following Suzuki coupling of isolated compound **13** showed only around 19% conversion after 2 h (Figure 3.1, see 3.1.3.3). Two possible sources of catalyst deactivation were considered. As found out by Liu *et al.*,[86] elemental sulfur could be generated during the esterification reaction and act as a catalyst poison. Another possibility would be a complexation of the catalytic palladium by the two neighboring Boc carbonyl groups.

Thus, the same reaction pathway was performed with benzyl (Bn) instead of Boc as protecting groups (Scheme 3.7). The protection of **12** with BnBr (3 eq.) and $NaHCO_3$ (5 eq.) in MeCN at reflux was based on similar literature procedures[87–89] and gave **15** in a modest yield of 27% over two reaction steps. In contrast to compound **13**, compound **15** could successfully be converted in the Suzuki coupling with around 94% conversion after a reaction time of 2 h (Figure 3.1, see 3.1.3.3). This was the Suzuki coupling with the highest conversion so far and led to the assumption that the interference with the catalyst

had been caused by the two Boc groups. It could also be possible that in the Bn pathway, less sulfur was remaining due to the aqueous washes in the workup of compound **15**. However, it is rather unlikely that these washes are the cause of such a huge difference in reactivity.[86]

Still, the methylester approach seemed not efficient enough for the overall synthesis of sacubitril precursor **7**. On the one hand, the Bn protection gave only a low yield and would demand a more cumbersome deprotection than the originally intended Boc protecting group.[90] On the other hand, the Suzuki coupling had indeed the highest conversion so far, but according to previous studies with the used catalyst, a faster reaction is needed for continuous flow applications. Furthermore, the separation of the Suzuki product from the educt and an obtained side product by column chromatography would be tedious due to their similar polarity.

3.1.2.3 Benzyl Protecting Groups Approach

Another alternative reaction pathway (Scheme 3.8) started from a similar starting material as **1b** but without a protecting group. In a similar procedure found in literature,[91] compound **17** would first be protected and esterified by three Bn groups, then reduced with $LiAlH_4$ and afterwards converted into the according aldehyde **20** by a Swern oxidation. This synthesis route would yield aldehyde **20** in three steps instead of the two-step initial approach, differing from **3b** only in the protecting groups.

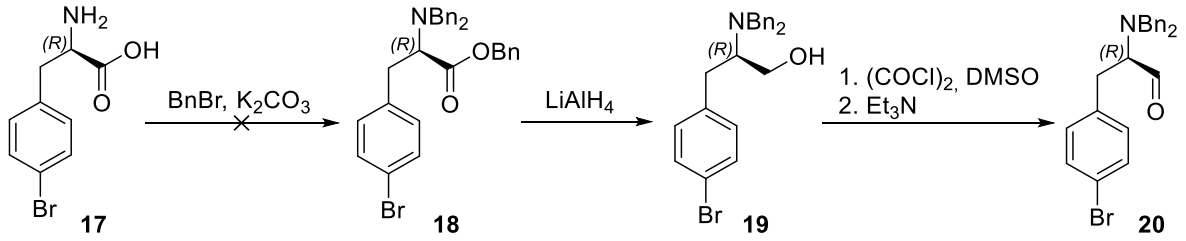

Scheme 3.8: Benzyl protecting groups approach[91]

The substitution of the Boc groups with Bn groups was intended in order to enable an efficient Suzuki coupling as described in 3.1.2.2. The approach would still have the disadvantage of a necessary Bn deprotection instead of the easier Boc deprotection.[90] Nevertheless, if a high yield and an efficient Suzuki coupling were achieved, the overall reaction route would be applicable.

However, already the first reaction step failed and product **18** was not formed according to ^{1}H and ^{13}C NMR analysis.

3.1.2.4 Erlenmeyer-Plöchl Approach

A different idea was the conversion of bromobenzaldehyde **21** into dicarbonyl **23** via an Erlenmeyer-Plöchl synthesis (Scheme 3.9). The obtained dicarbonyl **23** could then be used as Suzuki coupling substrate. Later, the nitrogen could be introduced enzymatically.[92]

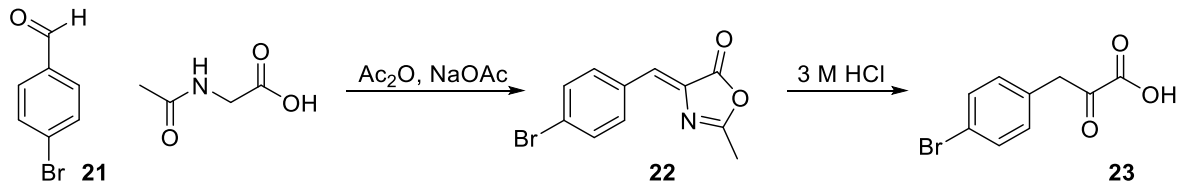

Scheme 3.9: Erlenmeyer-Plöchl approach[92]

The isolated product **23**, which was synthesized according to Ahmed *et al.*,[92] could not be analyzed by NMR due to its insolubility in $CDCl_3$. The Suzuki coupling experiments were performed with **23** as well as **21** as substrates. A quantitative comparison of the reaction with **23** is not possible, as the HPLC peaks could not be separated sufficiently. However, qualitatively it can be said that almost no conversion was obtained.

On the contrary, substrate **21** was already fully converted after 15 min (Figure 3.1, see 3.1.3.3). Thus, starting with the Suzuki coupling of **21**, then performing the Erlenmeyer-Plöchl synthesis and later introducing the nitrogen enzymatically would be an appropriate option for the synthesis of **7**. Still, due to missing NMR data, it was not clear if the Erlenmeyer-Plöchl reaction is yielding the intended product. Additionally, as a multistep continuous process is attempted, a different option would be preferable.

3.1.3 Final Synthesis Route

3.1.3.1 Preliminary Tests

In order to review the interference of NH groups with the catalyst, a Suzuki coupling experiment with **1b** as educt was performed. Against expectations, **1b** was one of the most reactive substrates so far with around 82% conversion after 2 h (Figure 3.1, see 3.1.3.3).

However, further improvement of the conversion was targeted before implementing the Suzuki coupling in continuous flow.

As this experiment showed that the NH group does not necessarily interfere with the catalyst, also **4b** was evaluated as Suzuki substrate. However, after a reaction time of 2 h, a conversion of only 44% was achieved (Figure 3.1, see 3.1.3.3).

Up to this point, due to economic reasons, all reactions had been performed with cheaper aryl bromides, even though aryl iodides are usually more reactive Suzuki coupling substrates.[63] In order to evaluate the different reactivity of the iodine and bromine compounds in the attempted Suzuki coupling reaction, an experiment was performed with the according iodo-substituted substrate **1a**. It showed superior results to **1b** with 82% conversion after 15 min and a full conversion after 90 min (Figure 3.1, see 3.1.3.3). As this result showed a significant difference between aryl iodide and bromide reactivity, the Suzuki coupling of iodo-substituted sacubitril precursor **4a** with phenylboronic acid was targeted.

3.1.3.2 Synthesis of Aryl Iodide 4a

The first three reaction steps in batch were performed similarly to the original approach but with the according iodo-substituted substrate **1a** (Scheme 3.10). The three-step synthesis of **4a** went smoothly with an overall yield of 55% and without intermediate purification steps. The isolated product **4a** was analyzed and identified by ^{1}H and ^{13}C NMR before testing it in the Suzuki coupling reaction with phenylboronic acid.

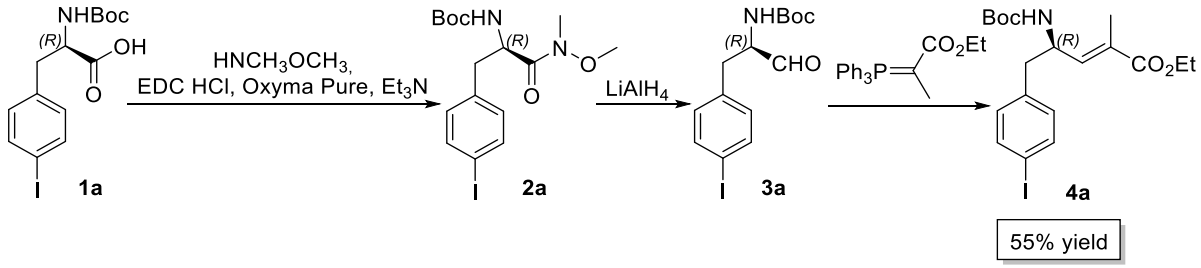

Scheme 3.10: Synthesis of **4a**

3.1.3.3 Suzuki Coupling of Aryl Iodide 4a

The Suzuki coupling of iodo-substituted sacubitril precursor **4a** (Scheme 3.11) gave much better results than the bromo-substituted derivative **4b** (Figure 3.1). With full conversion

already after 15 min, it was one of the most efficient Suzuki couplings tested. Only substrate **21** was converted with a comparable reaction rate. The Suzuki coupling of both substrates is considered to be realizable in continuous flow, but the Suzuki coupling of **4a** allows the implementation in the targeted multistep continuous process.

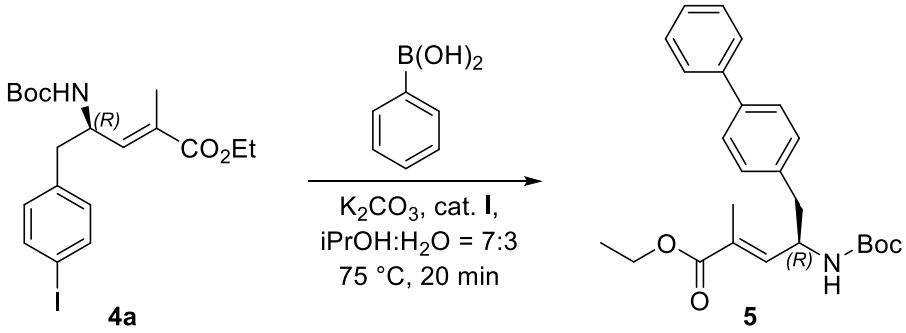

Scheme 3.11: Suzuki coupling of **4a**; cat. **I** = $Ce_{0.20}Sn_{0.79}Pd_{0.01}O_{2-\delta}$

The performance of the different tested substrates in the Suzuki coupling reaction with phenylboronic acid employing $Ce_{0.20}Sn_{0.79}Pd_{0.01}O_{2-\delta}$ as catalyst are summarized in Figure 3.1.

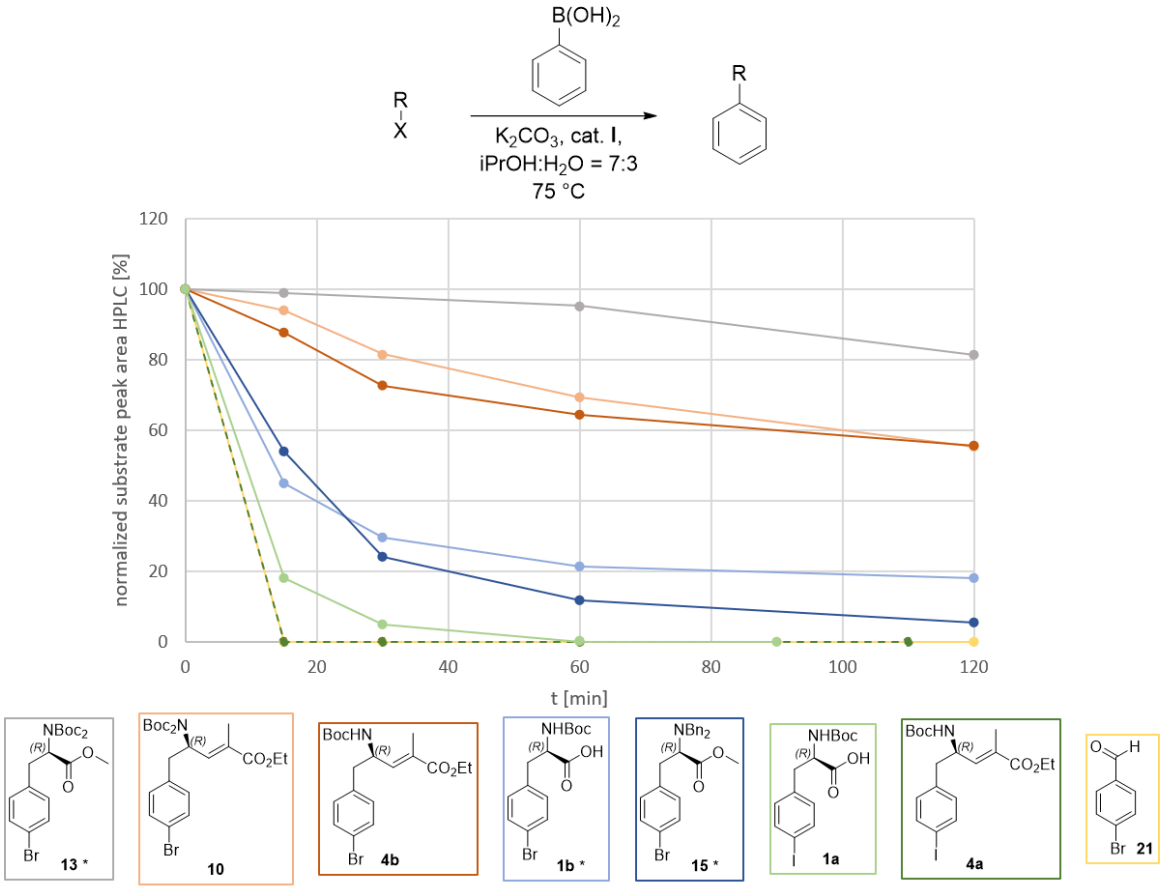

Figure 3.1: Peak areas of iodo and bromo substrates obtained with HPLC vs. reaction time for Suzuki-Miyaura couplings with substrates **13**, **10**, **4b**, **1b**, **15**, **1a**, **4a** and **21**; reactions were carried out with 1 mol% catalyst $Ce_{0.20}Sn_{0.79}Pd_{0.01}O_{2-\delta}$, 25 mM substrate, 1.5 eq. phenylboronic acid, 1.5 eq. K_2CO_3, iPrOH:H_2O = 7:3 (v:v), 75 °C; *no internal standard used

The optimization of the reaction conditions is described further in 3.2. After isolation of biphenyl compound **5**, the Boc deprotection as well as the *N*-acylation were tested in batch to yield the targeted sacubitril precursor **7**.

3.1.3.4 Deprotection and Acylation

As acidic conditions are required for Boc deprotection,[90] trifluoroacetic acid (TFA) in dichloromethane (DCM) was used for the deprotection of Suzuki product **5**. The reaction was straightforward and after stirring at room temperature for 2.5 h, full conversion was obtained. The quantitatively yielded crude product was already pure according to HPLC analysis and therefore directly used in the next reaction step (Scheme 3.12).

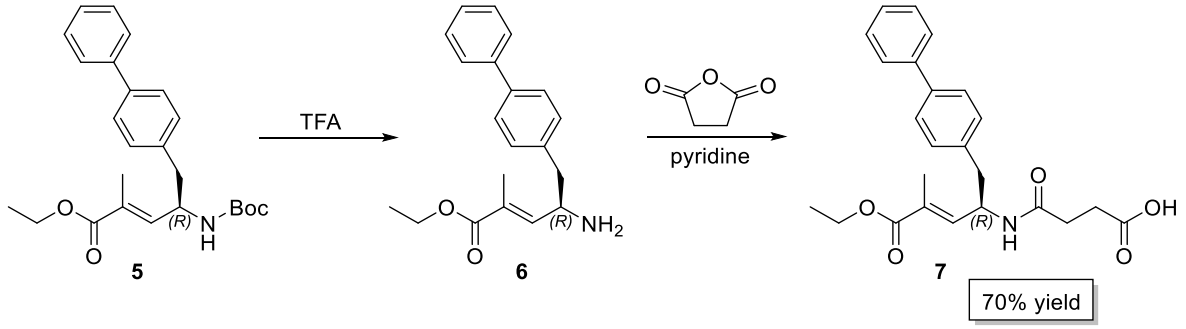

Scheme 3.12: Deprotection and acylation to sacubitril precursor **7**

The last reaction step, the acylation of **6** with succinic anhydride, was performed based on a similar synthesis by Ksander *et al.*[43] with succinic anhydride (1.5 eq.), DCM and pyridine. After an overnight reaction at room temperature, the desired product **7** was isolated with an overall yield of 70% over both reaction steps. The successful acylation reaction confirmed the assumption that the previous acylation attempt of **4b** had not been possible due to the unreactivity of the amide substrate.

Summarizing, the last two reaction steps in batch went smoothly and a synthesis route to sacubitril precursor **7** transferable to a multistep continuous setup was identified (Scheme 3.1). In the following, further experiments were performed to optimize the reaction conditions for the Suzuki coupling and verify its applicability in continuous flow.

3.2 Optimization of the Suzuki Coupling Conditions in Batch

As commonly known, various reaction parameters can have significant effects on the outcome of a Suzuki-Miyaura cross-coupling reaction.[63] Therefore, the reaction of **4a** to **5** as key step of the reaction pathway was optimized regarding catalyst type, catalyst amount and reaction solvent. If not stated otherwise, the conditions applied for these experiments were a temperature of 75 °C, iPrOH:H_2O = 7:3 (v:v) as solvent, 25 mM substrate, 1.5 eq. phenylboronic acid, 1.5 eq. K_2CO_3, 1 mol% catalyst **I** and anisole as internal standard (ISt). Samples were taken after certain time points and analyzed by HPLC.

3.2.1 Comparison of Catalysts

A comparison of the catalysts had already been performed in preliminary experiments before the identification of the final reaction pathway. Among our self-prepared, heterogeneous palladium catalysts $Ce_{0.20}Sn_{0.79}Pd_{0.01}O_{2-\delta}$ (cat. **I**), $Ce_{0.79}Sn_{0.20}Pd_{0.01}O_{2-\delta}$

(cat. **II**), $Sn_{0.99}Pd_{0.01}O_{2-\delta}$ (cat. **III**) and $Pd(OAc)_2$-BOX-MPSG (cat. **IV**), cat. **I** was identified as the most effective one for the Suzuki coupling of advanced chemical intermediates.

Exemplarily, the results for substrate **10** are given in Figure 3.2 and Figure 3.3. Here, it has to be noted that different reaction conditions were applied with cat. **IV** (2 mol% cat., toluene as solvent, no internal standard). Despite the higher catalyst concentration and one of the highest conversions, it showed the worst results in terms of product formation. Out of the three Pd substituted Ce-Sn oxides, cat. **I** proved to be the most suitable one with the highest conversion as well as product formation.

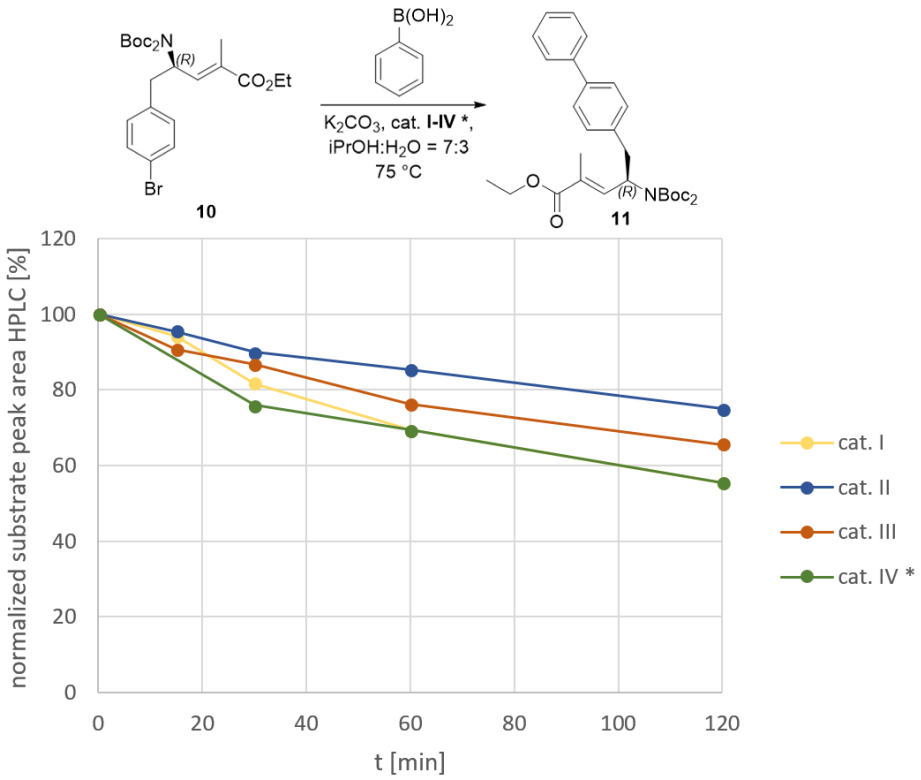

Figure 3.2: Comparison of catalysts by HPLC substrate area% for Suzuki coupling of substrate **10**; reaction conditions: 25 mM substrate, 1.5 eq. phenylboronic acid, 1.5 eq. K_2CO_3, iPrOH:H_2O = 7:3 (v:v), 75 °C, 1 mol% cat. $Ce_{0.99-x}Sn_xPd_{0.01}O_{2-\delta}$ (for cat. **I/II/III** x = 0.79/0.20/0.99); *2 mol% cat. $Pd(OAc)_2$-BOX-MPSG, toluene, no ISt

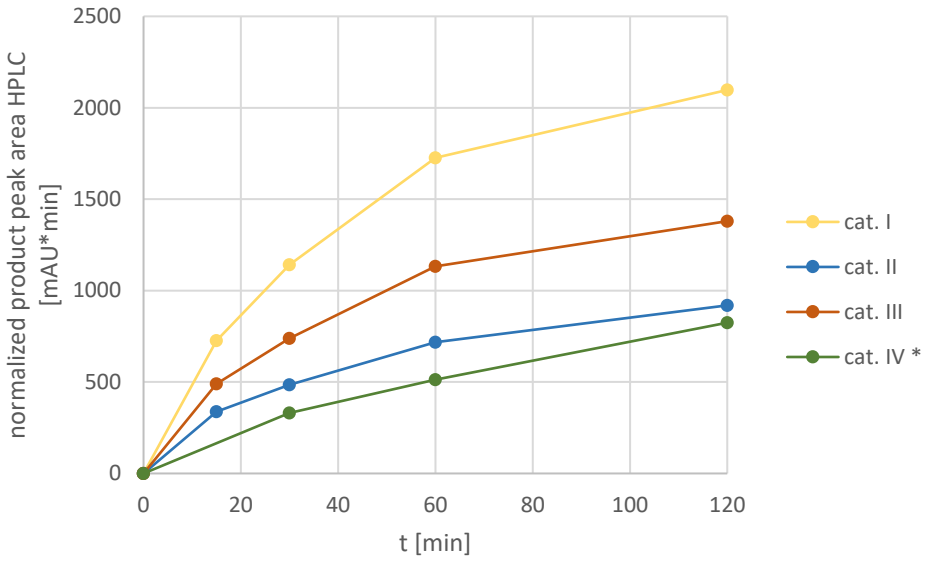

Figure 3.3: Comparison of catalysts by HPLC peak area of product **11** at 237 nm for Suzuki coupling of substrate **10**; reaction conditions: 25 mM substrate, 1.5 eq. phenylboronic acid, 1.5 eq. K_2CO_3, iPrOH:H_2O = 7:3 (v:v), 75 °C, 1 mol% cat. $Ce_{0.99-x}Sn_xPd_{0.01}O_{2-\delta}$ (for cat. **I/II/III** x = 0.79/0.20/0.99); *2 mol% cat. $Pd(OAc)_2$-BOX-MPSG, toluene, no ISt

3.2.2 Comparison of Catalyst Concentrations

For the analysis of the ultimate Suzuki coupling reaction from **4a** to **5**, calibrations of anisole, substrate **4a** and product **5** were necessary. The calibrations of anisole and product **5** went smoothly and are described in 7.1.2. However, an accurate substrate calibration was not possible due to an impurity overlapping with the substrate peak in the HPLC chromatogram. As a result, the conversion was not determined and the yield values are approximations. Therefore, results stating more than 100% yield are occurring in the comparison of solvents and catalyst concentrations. Still, the data analysis is sufficient to determine trends.

In Figure 3.4, the usage of 0.25 mol% and 1 mol% catalyst is compared. Both show similar results with approximately quantitative yield already after a reaction time of 15 min.

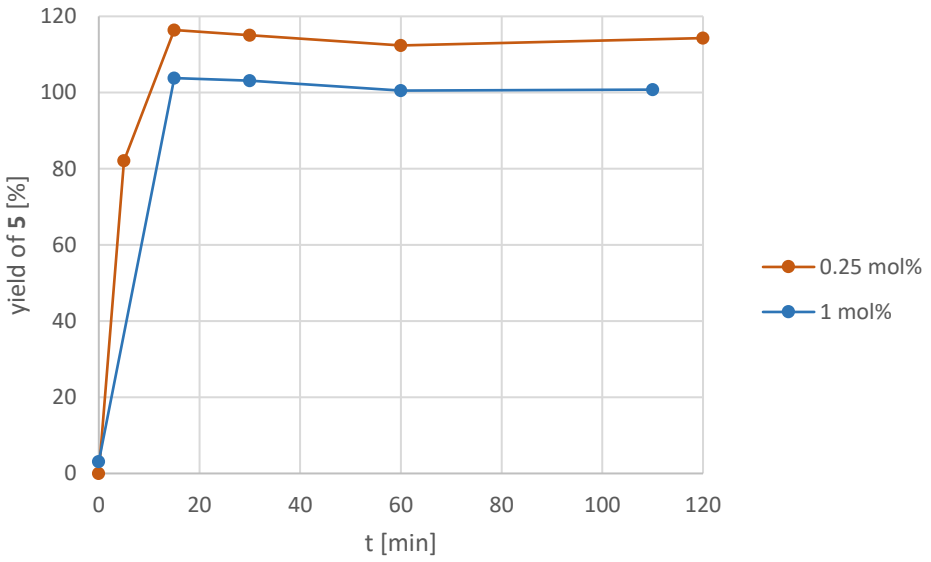

Figure 3.4: Comparison of catalyst concentrations by yield of **5** for Suzuki coupling of substrate **4a** with 0.25 mol% and 1 mol% cat. $Ce_{0.20}Sn_{0.79}Pd_{0.01}O_{2-\delta}$;
reaction conditions: 25 mM substrate, 1.5 eq. phenylboronic acid, 1.5 eq. K_2CO_3, iPrOH:H_2O = 7:3 (v:v), 75 °C

3.2.3 Comparison of Solvents

As reaction solvent, mixtures of iPrOH, EtOH and MeOH with H_2O in a ratio of ROH:H_2O = 7:3 (v:v) were tested. For these experiments, a concentration of 0.25 mol% catalyst **I** was used. As can be seen in Figure 3.5, the iPrOH and EtOH mixtures gave a much better yield than aqueous MeOH. Again, the values of the yield are approximations, as described in 3.2.2.

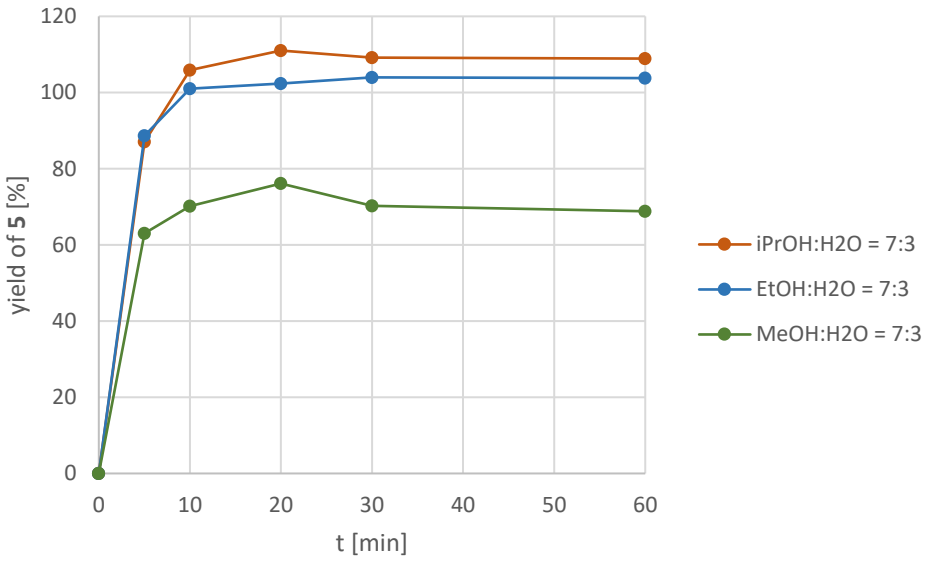

Figure 3.5: Comparison of reaction solvents by yield of **5** for Suzuki coupling of substrate **4a**; reaction conditions: 25 mM substrate, 1.5 eq. phenylboronic acid, 1.5 eq. K_2CO_3, 75 °C, 0.25 mol% cat. $Ce_{0.20}Sn_{0.79}Pd_{0.01}O_{2-\delta}$

An additional comparison of the same solvents was performed in the Crystalline (Technobis) in order to monitor the solubility of educt and product during the reaction. All three reaction mixtures were completely dissolved throughout the whole reaction (75 °C used for iPrOH and EtOH, 65 °C for MeOH). Precipitation started only during the cooling down process after the reaction, at first in aqueous (aq.) MeOH, later in aq. EtOH and only after hours in aq. iPrOH.

Summarizing, the solvent mixtures with iPrOH and EtOH gave comparable yields, but iPrOH showed the best solubility for the considered reaction. Due to the results of the optimization experiments, iPrOH:H_2O = 7:3 (v:v) and cat. **I** were applied for the synthesis of **5** in continuous flow.

3.3 Implementation of the Suzuki Coupling in Continuous Flow

After identifying a feasible reaction route to sacubitril precursor **7** in batch, the translation of the key step of the reaction cascade into continuous flow was targeted. Therefore, the Suzuki coupling of iodo-substituted sacubitril precursor **4a** with phenylboronic acid was tested in continuous flow employing different flow rates of 0.1 mL/min and 0.2 mL/min. The optimal reaction conditions determined in 3.2 were applied and an HPLC column (L x I.D. = 120 x 8 mm) filled with cat. **I** (5 g) was used as packed-bed reactor. Like in the batch reactions, 25 mM substrate, 1.5 eq. phenylboronic acid, 1.5 eq. K_2CO_3 and a reaction

temperature of 75 °C were used. Samples were taken in regular time intervals and analyzed by HPLC, using anisole as internal standard.

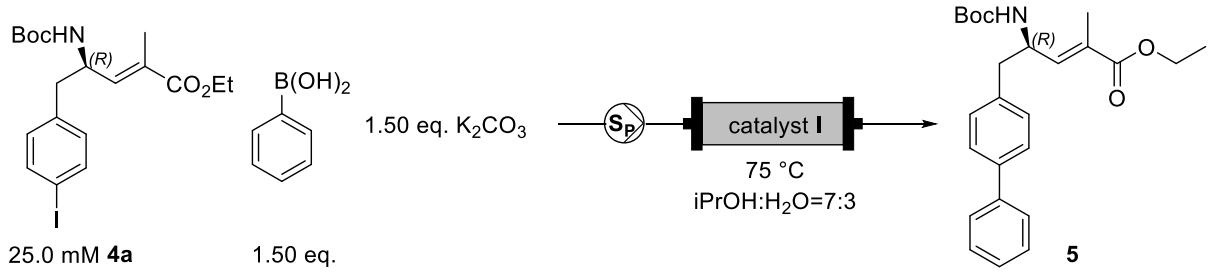

Scheme 3.13: Implementation of the Suzuki coupling to **5** in continuous flow; S_P = syringe pump, catalyst **I** = $Ce_{0.20}Sn_{0.79}Pd_{0.01}O_{2-\delta}$

As shown in Figure 3.6, by using the continuous setup, target compound **5** was obtained in good yields of 80% at 0.2 mL/min and 83% at 0.1 mL/min. After an initial equilibration phase, the system started to stabilize. However, based on the shape of the curves, it can be assumed that a steady state was not yet reached during the applied run time.

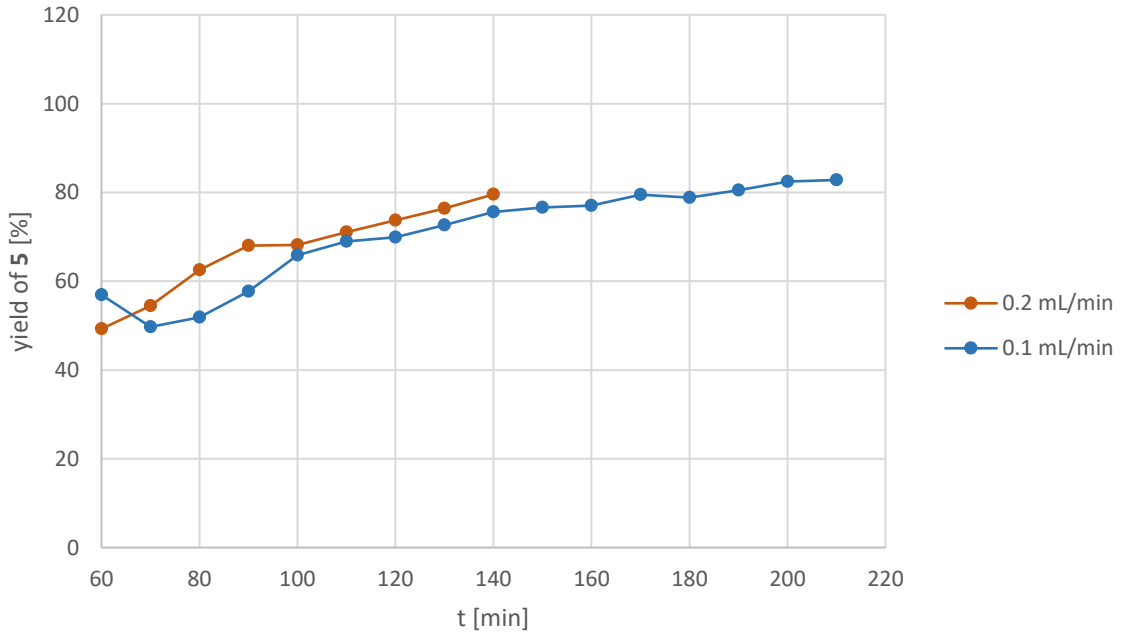

Figure 3.6: Yield for Suzuki coupling of **4a** to **5** in continuous flow at 0.1 mL/min and 0.2 mL/min with cat. $Ce_{0.20}Sn_{0.79}Pd_{0.01}O_{2-\delta}$;
reaction conditions: 25 mM substrate, 1.5 eq. phenylboronic acid, 1.5 eq. K_2CO_3, iPrOH:H_2O = 7:3 (v:v), 75 °C

As already described in 3.2.2, a calibration of **4a** was not possible, which is why the conversion could not be analyzed. Still, it could be shown that the Suzuki coupling can be implemented in continuous flow with a good yield at both tested flow rates and further optimization is planned to be performed in future experiments. Also, next steps include the performance of the Boc deprotection and the acylation with succinic anhydride in continuous flow. Finally, the examination of the multistep process in continuous flow for the synthesis of sacubitril precursor **7** is targeted.

4 Conclusion and Outlook

The aim of this master's thesis was the identification of a suitable synthesis route to an advanced precursor of the active pharmaceutical ingredient sacubitril. Multiple steps of this reaction cascade should be implementable as continuous flow process. By testing different approaches in batch experiments, a reaction pathway to yield late-stage sacubitril precursor **7** was found. The finally realized synthesis route consists of six reaction steps starting from commercially available Boc-4-iodo-D-phenylalanine **1a**. This compound is converted into the according Weinreb amide **2a**, followed by a reduction with $LiAlH_4$ and a Wittig reaction. These first three steps have to be performed as batch reactions. The succeeding three steps, which are a Suzuki coupling, a Boc deprotection and an *N*-acylation, should then be realized in a multistep continuous flow process. The performed reactions already gave good yields, which could probably be even improved by testing varying reaction conditions in future experiments.

The Suzuki coupling as key step of the reaction route was optimized in batch experiments in terms of catalyst type, catalyst concentration and solvent. The results revealed iPrOH:H_2O = 7:3 (v:v) and EtOH:H_2O = 7:3 (v:v) as similarly efficient and catalyst **I** $Ce_{0.20}Sn_{0.79}Pd_{0.01}O_{2-\delta}$ as the most suitable one regarding conversion as well as product formation. The tested catalyst concentrations of 0.25 mol% and 1 mol% gave similar results as well. For the synthesis in continuous flow, it was decided to use catalyst **I** and, due to solubility reasons, the iPrOH mixture as solvent.

The first step of the continuous flow process, the Suzuki coupling, was proved to work in continuous flow by using a packed-bed reactor filled with the heterogeneous palladium catalyst. Two flow rates, namely 0.1 mL/min and 0.2 mL/min, were compared and showed similar results with 83% and 80% yield, respectively. In future experiments, the deprotection and the acylation step will be performed in continuous flow in order to prove their applicability in an integrated setup. Afterwards, a multistep continuous process of the three reaction steps can be developed and optimized. Also, the analysis of Pd leaching of the used catalyst will be of interest.

A further future research topic is the extension of the synthesis route to the total synthesis of sacubitril. Precursor **7** differs from sacubitril only in a double bond (Scheme 4.1). The reduction to a single bond could be performed by a hydrogenation reaction of **7** or at an earlier stage. Hereby, a correct introduction of the chiral center has to be considered.

Catalysts for homogeneous[93] as well as heterogeneous[94] asymmetric hydrogenation methods are reported in literature.

Summarizing, compound **7** as an advanced precursor of the active pharmaceutical ingredient sacubitril can be synthesized via a six-step reaction pathway. The usage of a heterogeneous palladium catalyst allows the performance of the Suzuki coupling in continuous flow by using a packed-bed reactor. This reaction step and the two following should be performed in continuous flow, which brings along several advantages. Among these are a higher efficiency, less ecological impact, a better quality assurance and easier scale-up to allow a fast reaction on needs.[10,11,13,14]

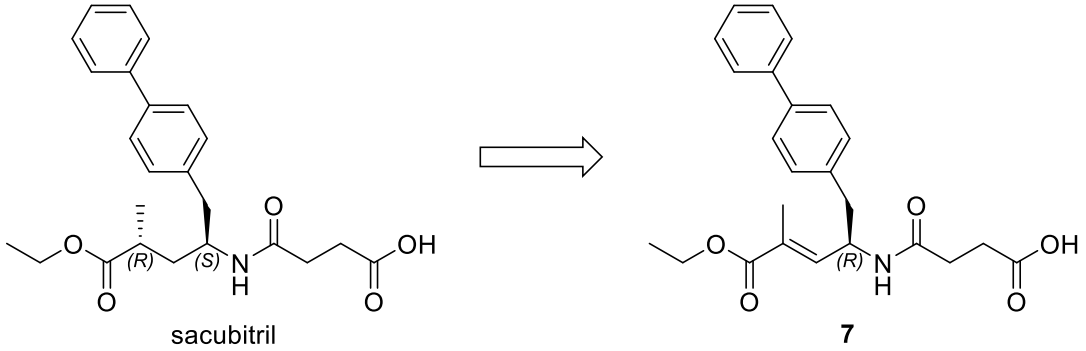

Scheme 4.1: Comparison of sacubitril with precursor **7**

5 Experimental Part

5.1 General Information

All chemicals and solvents were used as received from commercial suppliers unless stated otherwise. The H_3PO_4 buffer mentioned in the experimental procedures is H_2O:H_3PO_4 = 300:1 (v:v). If a reaction was performed under inert atmosphere, it is indicated in the experimental procedure and standard Schlenk technique with argon gas was applied. For analytical thin layer chromatography, pre-coated aluminum plates (Merck, silica gel 60, F_{254}) were used and visualization was performed with UV light (254 nm), potassium permanganate stain or ninhydrin stain. Purifications by column chromatography were conducted with MN silica gel 60 (70 – 230 mesh).

For HPLC analyses, an Agilent 1100 series HPLC system with the following equipment was used: online degasser, quaternary pump, autosampler, thermostated column compartment, ThermoFischer Scientific Accucore™ C18 reversed phase column (50 x 4.6 mm; 2.6 µm), UV-visible diode array detector. The methods used for HPLC measurements are stated in 7.1.1. The resulting calibration curves and related procedures are illustrated in 7.1.2.

NMR spectra were measured on a Bruker Avance III 300 MHz spectrometer (^{1}H: 300 MHz, ^{13}C: 75 MHz). The according NMR spectra are depicted in 7.2. The chemical shifts δ and coupling constants J are listed in this chapter. For reporting the multiplicities, the following abbreviations were used: s (singlet), d (doublet), t (triplet), q (quartet), m (multiplet), bs (broad singlet), dd (doublet of doublets), dt (doublet of triplets).

5.2 Synthesis Route in Batch

5.2.1 Synthesis of *tert*-butyl-(*R*)-(3-(4-iodophenyl)-1-(methoxy(methyl)amino)-1-oxopropan-2-yl)carbamate **2a** and *tert*-butyl-(*R*)-(3-(4-bromophenyl)-1-(methoxy(methyl)amino)-1-oxopropan-2-yl)carbamate **2b**

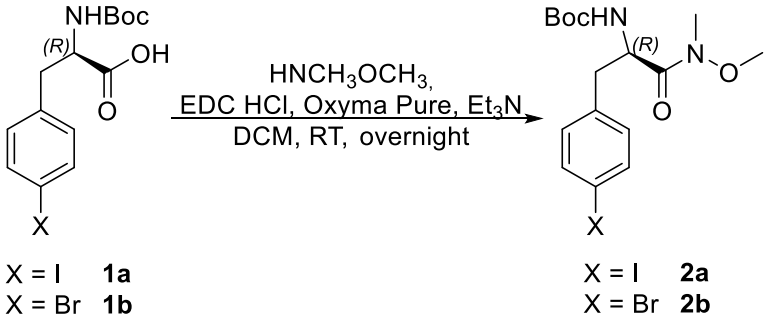

Scheme 5.1: Synthesis of *tert*-butyl-(*R*)-(3-(4-iodophenyl)-1-(methoxy(methyl)amino)-1-oxopropan-2-yl)carbamate **2a** and *tert*-butyl-(*R*)-(3-(4-bromophenyl)-1-(methoxy(methyl)amino)-1-oxopropan-2-yl)carbamate **2b**

Synthesis of 2a: The reaction was performed under Ar. Based on a similar synthesis procedure described in literature[43], Boc-4-iodo-D-phenylalanine **1a** (2.92 g, 7.48 mmol, 1.15 eq.), *O*,*N*-dimethylhydroxylamine hydrochloride (0.634 g, 6.50 mmol, 1.00 eq.), 1-ethyl-3-(3-dimethylaminopropyl)carbodiimide hydrochloride (EDC HCl) (2.85 g, 14.9 mmol, 2.29 eq.), ethyl(hydroxyimino)cyanoacetate (Oxyma Pure) (1.60 g, 11.3 mmol, 1.73 eq.) and triethylamine (1.24 mL, 8.91 mmol, 1.37 eq.) were dissolved in dichloromethane (25 mL) in a 50 mL two-necked round-bottom flask. The orange, clear reaction solution was stirred overnight at room temperature. The solvent was carefully evaporated from the dark brown reaction mixture and the residue was taken up in ethyl acetate (EtOAc) (50 mL). The organic phase was washed with saturated (sat.) aq. $NaHCO_3$ (2 x 30 mL), 1 M HCl (2 x 30 mL), sat. aq. NaCl (1 x 30 mL) successively and dried over Na_2SO_4. The solvent was removed under reduced pressure to yield crude **2a** as an orange-brown, viscous oil (3.00 g), which was directly used in the next step without further purification. TLC (silica gel, PE:EtOAc = 7:3): R_f = 0.5.

Synthesis of 2b: The reaction was performed according to the synthesis of compound **2a** but using Boc-4-bromo-D-phenylalanine **1b** as starting material. Product **2b** was obtained as an orange-brown, viscous oil and was used in the next step without further purification.

For NMR-measurements, chromatographic purification was performed as filtration over silica gel with EtOAc as eluent, which gave **2b** as orange-brown, viscous oil with 91% yield. TLC (silica gel, PE:EtOAc = 7:3): R_f = 0.5.

^{1}H NMR (300 MHz, $CDCl_3$): δ_H [ppm] = 7.39 (d, J = 8.1 Hz, 2H, -C*H*CBr), 7.03 (d, J = 8.0 Hz, 2H, -C*H*CHCBr-), 5.33 – 5.04 (m, 1H, -N*H*-), 5.04 – 4.76 (m, 1H, -NHC*H*-), 3.68 (s, 3H, -OCH_3), 3.16 (s, 3H, -NCH_3), 3.00 (dd, J_1 = 13.4 Hz, J_2 = 5.8 Hz, 1H, -CH_2-), 2.82 (dd, J_1 = 12.9 Hz, J_2 = 6.8 Hz, 1H, -CH_2-), 1.38 (s, 9H, -C(CH_3)$_3$). **^{13}C NMR (76 MHz, $CDCl_3$):** δ_C [ppm] = 172.0 (-*C*OO-), 155.2 (-*C*ONCH$_3$-), 135.7 (-*C*$_{ar}$CH$_2$-), 131.5 (2C, -*C*HCHCBr-), 131.3 (2C, -*C*HCBr-), 120.9 (-*C*Br-), 79.9 (-*C*(CH$_3$)$_3$), 61.7 (-O*C*H$_3$), 51.4 (-*C*HNH-), 38.4 (-*C*H$_2$-), 32.2 (-N*C*H$_3$), 28.4 (3C, -C(*C*H$_3$)$_3$). The ^{1}H NMR data were in accordance with literature values.[95,96] Additional peaks of residual EtOAc were visible.[97] No literature data for ^{13}C NMR were available.

5.2.2 Synthesis of *tert*-butyl (*R*)-(1-(4-iodophenyl)-3-oxopropan-2-yl)carbamate 3a and *tert*-butyl (*R*)-(1-(4-bromophenyl)-3-oxopropan-2-yl)carbamate 3b

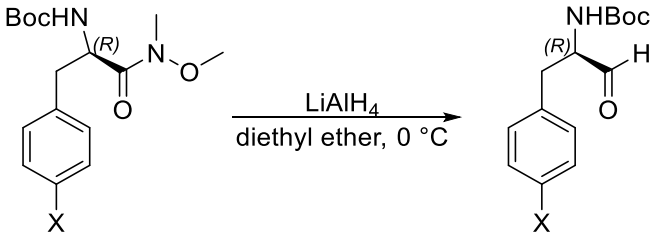

Scheme 5.2: Synthesis of *tert*-butyl (*R*)-(1-(4-iodophenyl)-3-oxopropan-2-yl)carbamate **3a** and *tert*-butyl (*R*)-(1-(4-bromophenyl)-3-oxopropan-2-yl)carbamate **3b**

Synthesis of 3a: The reaction was performed under Ar. Based on a similar reaction procedure performed by Ksander *et al.*[43], crude **2a** (6.50 mmol, 1.00 eq.) was dissolved in dry diethyl ether (110 mL) in a 500 mL three-necked round-bottom flask and cooled to 0 °C in an ice bath. $LiAlH_4$ (1.0 M in diethyl ether, 13.0 mL, 13.0 mmol, 2.00 eq.) was added dropwise and the yellow reaction mixture was kept stirring for 30 min at 0 °C. To quench the reaction, cold 5% (m/v) aq. $KHSO_4$ (44.3 mL, 16.3 mmol, 2.50 eq.) was added dropwise, giving a white precipitate, and the reaction mixture was warmed to room

temperature. The reaction mixture was washed with cold 1 M HCl (2 x 40 mL) and sat. aq. NaCl (2 x 40 mL, 1 x 20 mL) successively and the organic phase was dried over Na_2SO_4. The solvent was removed under reduced pressure to yield crude **3b** as a yellow solid, which was used in the next step without further purification.

Synthesis of 3b: The reaction was performed according to the synthesis of **3a** but using **2b** as educt. Starting from purified **2b**, product **3b** was obtained already in pure form, as shown by NMR analysis, as a white solid with 80% yield. Starting from crude **2b**, crude **3b** was obtained as a yellow solid and was used in the next step without further purification. For NMR-measurements, crude **3b** was purified by column chromatography (silica gel, PE:EtOAc = 8:2) giving a white solid with 53% yield over two steps starting from **1b**. TLC (silica gel, PE:EtOAc = 8:2): R_f = 0.5.

^{1}H NMR (300 MHz, $CDCl_3$): δ_H [ppm] = 9.61 (s, 1H, -C*H*O), 7.43 (d, *J*=8.2 Hz, 2H, -C*H*CBr-), 7.04 (d, *J*=8.2 Hz, 2H, -C*H*CHCBr-), 5.04 (bs, 1H, -N*H*-), 4.50 – 4.29 (m, 1H, -NHC*H*-), 3.26 – 2.91 (m, 2H, -CH_2-), 1.43 (s, 9H, -C(CH_3)$_3$). **^{13}C NMR (76 MHz, $CDCl_3$):** δ_C [ppm] = 199.0 (-*C*HO-), 155.4 (-*C*OO-), 135.0 (-$C_{ar}CH_2$-), 132.0 (2C, -*C*HCHCBr-), 131.2 (2C, -*C*HCBr-), 121.2 (-*C*Br-), 80.5 (-*C*(CH$_3$)$_3$-), 60.7 (-NH*C*H-), 34.9 (-*C*H$_2$-), 28.4 (3C, -C(*C*H$_3$)$_3$). The ^{1}H NMR data were in accordance with literature values.[95,96] Additional peaks of residual EtOAc and silicon grease were visible.[97] For ^{13}C NMR, no literature data were available.

5.2.3 Synthesis of ethyl-(*R*,*E*)-4-((*tert*-butoxycarbonyl)amino)-5-(4-iodophenyl)-2-methylpent-2-enoate 4a and ethyl-(*R*,*E*)-4-((*tert*-butoxycarbonyl)amino)-5-(4-bromophenyl)-2-methylpent-2-enoate 4b

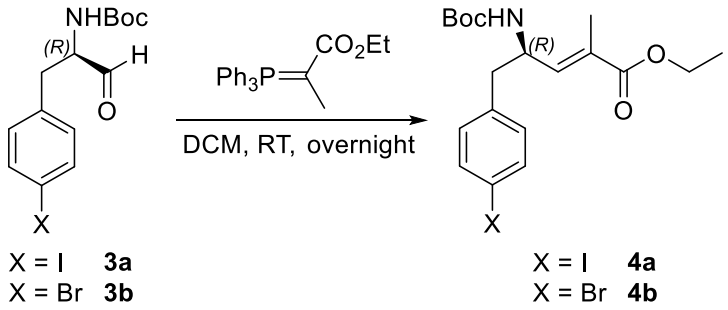

Scheme 5.3: Synthesis of ethyl-(*R*,*E*)-4-((*tert*-butoxycarbonyl)amino)-5-(4-iodophenyl)-2-methylpent-2-enoate **4a** and ethyl-(*R*,*E*)-4-((*tert*-butoxycarbonyl)amino)-5-(4-bromophenyl)-2-methylpent-2-enoate **4b**

Synthesis of 4a: The reaction was performed under Ar. Referring to a similar synthesis procedure described by Ksander *et al.*[43], crude **3a** (6.50 mmol, 1.00 eq.) and (carbethoxyethylidene)triphenylphosphorane (4.71 g, 13.0 mmol, 2.00 eq.) were dissolved in dichloromethane (110 mL) in a 250 mL two-necked round-bottom flask. The yellow, clear reaction mixture was stirred at room temperature overnight. The solvent was removed under reduced pressure, giving a yellow oil. Purification of the crude product by column chromatography (silica gel, toluene:EtOAc = 95:5) gave **4a** (1.64 g, 3.58 mmol) as a white solid with 55% yield over three steps starting from **1a**. TLC (silica gel, toluene:EtOAc = 95:5): R_f = 0.3.

^{1}H NMR (300 MHz, $CDCl_3$): δ_H [ppm] = 7.60 (d, *J* = 8.1 Hz, 2H, -C*H*Cl-), 6.92 (d, *J* = 8.1 Hz, 2H, -C*H*CHCl-), 6.47 (d, *J* = 7.8 Hz, 1H, -C*H*=C-), 4.76 – 4.40 (m, 2H, -C*H*N*H*-), 4.18 (q, *J* = 7.1 Hz, 2H, -CH_2CH$_3$-), 2.86 (dd, J_1 = 12.6 Hz, J_2 = 4.5 Hz, 1H, -C$_{ar}$CH_2-), 2.72 (dd, J_1 = 13.4 Hz, J_2 = 6.7 Hz, 1H, -C$_{ar}$CH_2-), 1.70 (s, 3H, -CH=C(CH_3)-), 1.40 (s, 9H, -C(CH_3)$_3$), 1.28 (t, *J* = 7.1 Hz, 3H, -CH$_2$CH_3). **^{13}C NMR (76 MHz, $CDCl_3$):** δ_C [ppm] = 167.8 (-C*C*OO-), 155.0 (-N*C*OO-), 139.7 (-*C*H=C-), 137.6 (2C, -*C*HCl-), 136.6 (-*C*$_{ar}$CH$_2$-), 131.7 (2C, -*C*HCHI-), 130.0 (-CH=*C*-), 92.2 (-*C*I-), 80.0 (-*C*(CH$_3$)$_3$-), 60.9 (-*C*H$_2$CH$_3$), 50.1 (-*C*HNH-), 40.9 (-C$_{ar}$*C*H$_2$-), 28.5 (3C, -C(*C*H$_3$)$_3$), 14.4 (-CH$_2$*C*H$_3$), 12.9 (-CH=C(*C*H$_3$)-). No NMR data of **4a** were available in literature. However, the ^{1}H and ^{13}C NMR values were in accordance with the corresponding literature data of a similar compound, where the –I is replaced by a -H.[98]

Synthesis of 4b: The reaction was performed according to the synthesis of **4a** but using **3b** as starting material. Crude **4b** was obtained as a yellow oil. Purification by column chromatography (silica gel, PE:EtOAc = 90:10) gave **4b** as a white solid (0.639 g, 1.55 mmol) with 61% yield over three steps starting from **1b**. Starting from pure **3b**, a yield of 80% could be determined for the single step. TLC (silica gel, PE:EtOAc = 90:10): R_f = 0.3.

^{1}H NMR (300 MHz, $CDCl_3$): δ_H [ppm] = 7.40 (d, *J* = 8.2 Hz, 2H, -C*H*CBr-), 7.04 (d, *J* = 8.1 Hz, 2H, -C*H*CHCBr-), 6.48 (d, *J* = 8.6 Hz, 1H, -C*H*=C-), 4.78 – 4.35 (m, 2H, -C*H*N*H*-), 4.18 (q, *J* = 7.0 Hz, 2H, -CH_2CH$_3$-), 2.88 (dd, J_1 = 12.6 Hz, J_2 = 4.9 Hz, 1H, -C$_{ar}$CH_2-), 2.73 (dd, J_1 = 13.3 Hz, J_2 = 6.9 Hz, 1H, -C$_{ar}$CH_2-), 1.70 (s, 3H, -CH=C(CH_3)-), 1.38 (s, 9H, -C(CH_3)$_3$), 1.28 (t, *J* = 7.1 Hz, 3H, -CH$_2$CH_3). **^{13}C NMR (76 MHz, $CDCl_3$):** δ_C [ppm] = 167.8 (-C*C*OO-), 155.0 (-N*C*OO-), 139.7 (-*C*H=C-), 135.9 (-*C*$_{ar}$CH$_2$-), 131.7 (2C, -*C*HCHCBr-), 131.4

(2C, -*C*HCBr-), 130.0 (-CH=*C*-), 120.8 (-*C*Br-), 80.0 (-*C*(CH_3)$_3$-), 61.0 (-*C*$H_2$$CH_3$), 50.2 (-*C*HNH-), 40.8 (-C_{ar}*C*H_2-), 28.5 (3C, -C(*C*H_3)$_3$), 14.4 (-CH_2*C*H_3), 12.9 (-CH=C(*C*H_3)-). No NMR data of **4b** were available in literature. However, the ^{1}H and ^{13}C NMR values were in accordance with the corresponding literature data of a similar compound, where the –Br is replaced by a –H.[98]

5.2.4 Synthesis of ethyl-(*R*,*E*)-5-([1,1'-biphenyl]-4-yl)-4-((*tert*-butoxycarbonyl)amino)-2-methylpent-2-enoate 5

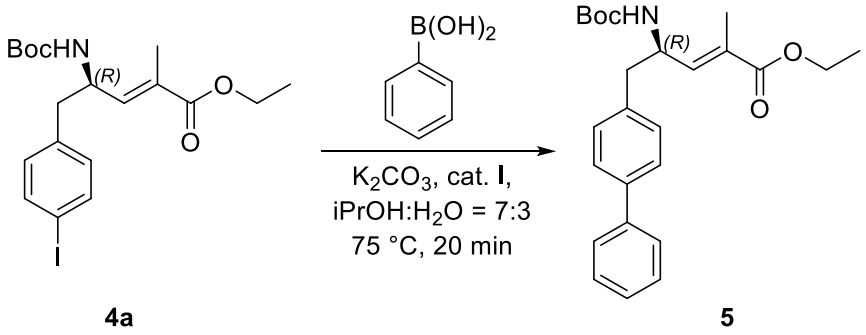

4a **5**

Scheme 5.4: Synthesis of ethyl-(*R*,*E*)-5-([1,1'-biphenyl]-4-yl)-4-((*tert*-butoxycarbonyl)amino)-2-methylpent-2-enoate **5**; cat. **I** = $Ce_{0.20}Sn_{0.79}Pd_{0.01}O_{2-\delta}$

Compound **4a** (300 mg, 653 µmol, 1.00 eq.), phenylboronic acid (120 mg, 984 µmol, 1.51 eq.) and potassium carbonate (135 mg, 980 µmol, 1.50 eq.) were dissolved in iPrOH:H_2O = 7:3 (v:v) (26 mL). The reaction mixture was stirred at 75 °C until all reactants were dissolved and catalyst $Ce_{0.20}Sn_{0.79}Pd_{0.01}O_{2-\delta}$ (cat. **I**) (94.1 mg, 1.00 mol%) was added. After 20 min, HPLC analysis showed completion of the reaction. The solvent was evaporated under reduced pressure, the residue was diluted with EtOAc (25 mL) and washed with H_2O (2 x 15 mL) as well as sat. aq. NaCl (1 x 15 mL). The organic phase was dried over Na_2SO_4 and the solvent was removed under reduced pressure. The crude product, a white solid, was purified by column chromatography (silica gel, PE:EtOAc = 85:15) to give **5** as a white solid. As for column chromatography, combined crude products of several experiments were used, no yield can be given. TLC (silica gel, PE:EtOAc = 85:15): R_f = 0.7.

^{1}H NMR (300 MHz, $CDCl_3$): δ_H [ppm] = 7.62 – 6.99 (m, 9H, all -C*H*$_{ar}$-), 6.48 (d, *J* = 7.9 Hz, 1H, -C*H*=C-), 4.82 – 4.40 (m, 2H, -C*H*N*H*-), 4.23 – 3.93 (m, 2H, -C*H*$_2$$CH_3$, residual EtOAc), 2.88 (dd, J_1 = 12.8 Hz, J_2 = 5.0 Hz, 1H, -C*H*$_2$$C_{ar}$-), 2.76 (dd, J_1 = 13.4 Hz, J_2 = 6.5 Hz,

1H, -CH_2C_{ar}-), 1.67 (s, 3H, -CH=C(CH_3)-), 1.33 (s, 9H, -C(CH_3)$_3$), 1.28 – 1.05 (m, 3H, -CH_2CH_3, residual EtOAc, residual H grease). **^{13}C NMR (76 MHz, $CDCl_3$):** δ_C [ppm] = 167.9 (-*C*OOCH_2CH_3), 155.1 (-*C*OOC$(CH_3)_3$), 140.9 (-CH_2Ph*C*$_{ar}$-), 140.3 (-*C*H=C-), 139.7 (-CH_2(CCHCH*C*)$_{ar}$-), 135.9 (-CH_2*C*$_{ar}$-), 130.1 (2C, -CH_2(C*C*H)$_{ar}$-), 128.9 (2C, -CH_2Ph(CCH*C*H)$_{ar}$-), 127.3 (-CH_2Ph(CCHCH*C*H)$_{ar}$-), 127.3 (2C, -CH_2Ph(C*C*H)$_{ar}$-), 127.1 (2C, -CH_2(CCH*C*H)$_{ar}$-), 79.9 (-*C*$(CH_3)_3$), 60.9 (-*C*H_2CH_3), 50.2 (-*C*HNH-), 41.0 (-*C*H_2C_{ar}-), 28.5 (3C, -C(*C*$H_3)_3$), 14.4 (-CH_2*C*H_3), 12.8 (-CH=C(*C*H_3)-). No NMR data of **5** were available in literature. However, the ^{1}H and ^{13}C NMR data were in accordance with the corresponding literature values of a similar compound bearing a phenyl instead of a biphenyl substituent.[98] Additional peaks of residual EtOAc and grease were visible.[97] The -C_q=CH- signal was not strong enough to be visible in the ^{13}C NMR.

5.2.5 Synthesis of ethyl-(*R*,*E*)-5-([1,1'-biphenyl]-4-yl)-4-amino-2-methylpent-2-enoate 6

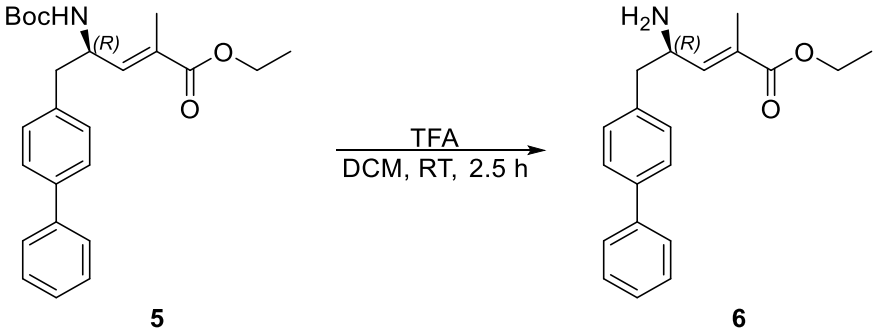

Scheme 5.5: Synthesis of ethyl-(*R*,*E*)-5-([1,1'-biphenyl]-4-yl)-4-amino-2-methylpent-2-enoate **6**

As common, the Boc deprotection was performed under acidic conditions.[90] Compound **5** (100 mg, 0.245 mmol) was dissolved in dichloromethane (1.5 mL) in a 10 mL round-bottom flask. Trifluoroacetic acid (1.50 mL, 19.6 mmol, 80.0 eq.) was added slowly to the reaction mixture, which was kept stirring at room temperature for 2.5 h. A septum with a cannula was put on top of the flask to allow the emerging CO_2 to escape. The solvent was removed under reduced pressure and the residual brown oil was taken up in EtOAc (20 mL) and washed with sat. aq. Na_2CO_3 (2 x 10 mL) as well as sat. aq. NaCl (1 x 10 mL) successively. The organic phase was dried over Na_2SO_4 and the solvent was removed under reduced pressure to give crude **6** (75.8 mg) as a yellow oil. The quantitatively

yielded crude product was already pure according to HPLC analysis and was used in the next step without further purification. TLC (silica gel, PE:EtOAc = 85:15): R_f = 0.

5.2.6 Synthesis of (*R*,*E*)-4-((1-([1,1'-biphenyl]-4-yl)-5-ethoxy-4-methyl-5-oxopent-3-en-2-yl)amino)-4-oxobutanoic acid **7**

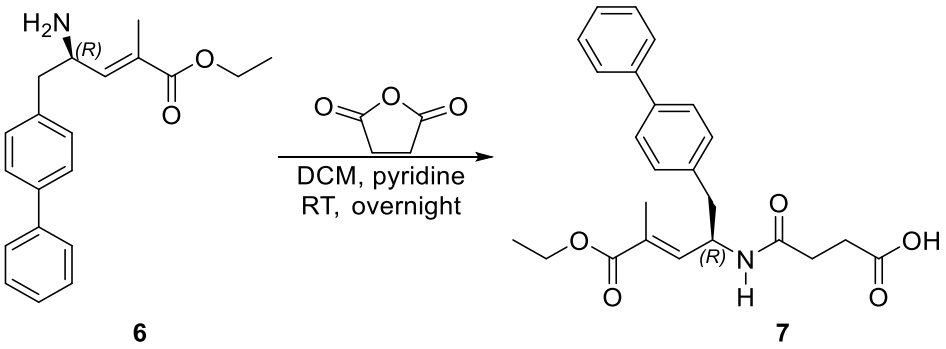

Scheme 5.6: Synthesis of (*R*,*E*)-4-((1-([1,1'-biphenyl]-4-yl)-5-ethoxy-4-methyl-5-oxopent-3-en-2-yl)amino)-4-oxobutanoic acid **7**

Based on a similar synthesis procedure performed by Ksander *et al.*[43], crude **6** (245 µmol) was dissolved in dichloromethane (1.5 mL) and pyridine (1.5 mL) in a 10 mL round-bottom flask. Succinic anhydride (37.2 mg, 372 µmol, 1.52 eq.) was added and the yellow, clear reaction mixture was stirred at room temperature overnight. The solvent was removed by rotary evaporation. The residue was taken up in EtOAc (20 mL), washed with 1 M HCl (3 x 10 mL) and sat. aq. NaCl (1 x 10 mL) successively and the organic phase was dried over Na_2SO_4. The solvent was removed under reduced pressure to give crude **7** as a beige sticky solid. Purification by column chromatography (silica gel, EtOAc + 0.5% acetic acid) gave **7** (70.2 mg, 0.171mmol) as a yellowish oil with 70% yield over two steps starting from **5**. TLC (silica gel, EtOAc + 0.5% acetic acid): R_f = 0.6.

^{1}H NMR (300 MHz, $CDCl_3$): δ_H [ppm] = 9.67 (bs, 1H, -O*H*), 7.85 – 6.91 (m, 9H, -C_{ar}*H*-), 6.50 (d, *J* = 9.2 Hz, 1H, -C*H*=C-), 6.10 (d, *J* = 7.9 Hz, 1H, -N*H*), 4.95 (dt, J_1 = 14.9 Hz, J_2 = 7.4 Hz, 1H, -C*H*NH-), 4.10 (q, *J* = 7.0 Hz, 2H, -CH_2CH$_3$-), 2.90 (dd, J_1 = 13.5 Hz, J_2 = 6.1 Hz, 1H, -C_{ar}CH_2-), 2.78 (dd, J_1 = 13.5 Hz, J_2 = 7.2 Hz, 1H, -C_{ar}CH_2-), 2.67 – 2.45 (m, 2H, -CH_2COOH), 2.36 (t, *J* = 6.2 Hz, 2H, -CH_2CH$_2$COOH), 1.67 (s, 3H, -CH=C(CH_3)-), 1.20 (t, *J* = 7.1 Hz, 3H, -CH$_2$CH_3). **^{13}C NMR (76 MHz, $CDCl_3$):** δ_C [ppm] = 177.0 (-*C*OOH), 171.5 (-*C*ONH-), 168.0 (-*C*OOCH$_2$-), 140.8 (-CH$_2$Ph*C*$_{ar}$-), 139.8 (-CH$_2$(CCHCH*C*)$_{ar}$-), 139.4 (-*C*H=C-), 135.6 (-CH$_2$*C*$_{ar}$-), 130.4 (-CH=*C*-), 130.0 (2C, -CH$_2$(C*C*H)$_{ar}$-), 128.9

(2C, -CH_2Ph(CCH*C*H)$_{ar}$-), 127.4 (-CH_2Ph(CCHCH*C*H)$_{ar}$-), 127.3 (2C, -CH_2Ph(C*C*H)$_{ar}$-), 127.1 (2C, -CH_2(CCH*C*H)$_{ar}$-), 61.1 (-*C*H_2CH_3), 49.1 (-*C*HNH-), 40.3 (-C_{ar}*C*H_2-), 30.9 (-*C*H_2COOH), 29.6 (-*C*H_2CH_2COOH), 14.3 (-CH_2*C*H_3), 12.9 (-CH=C(*C*H_3)-). No NMR data of compound **7** were available in literature. However, the ^{1}H NMR values were comparable with the corresponding literature data of a similar compound, where the -CH=C(CH_3)- group of **7** is replaced by a -CH_2- group.[99] No ^{13}C NMR data of a similar compound were available in literature.

5.3 Suzuki-Miyaura Cross-Coupling Reaction

5.3.1 Optimization of the Reaction Conditions in Batch

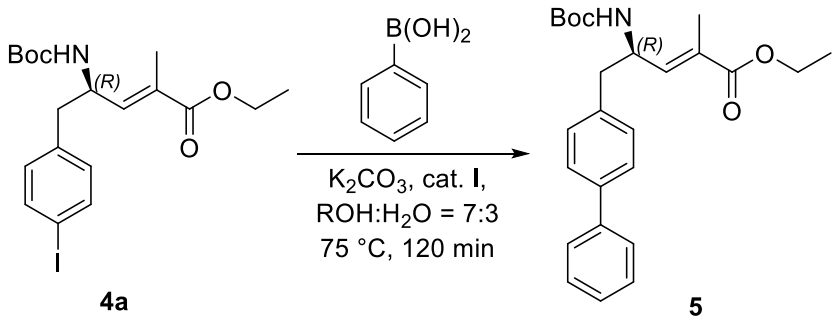

Scheme 5.7: Optimization of the reaction conditions for the Suzuki-Miyaura cross-coupling; cat. **I** = $Ce_{0.20}Sn_{0.79}Pd_{0.01}O_{2-\delta}$

Aryl halide **4a** (75.0 µmol, 1.00 eq.), phenylboronic acid (13.7 mg, 113 µmol, 1.50 eq.), potassium carbonate (15.6 mg, 113 µmol, 1.50 eq.) and anisole (43 µL) as internal standard were dissolved in ROH:H_2O = 7:3 (v:v) (3 mL, ROH = MeOH, EtOH, iPrOH) at 75 °C in an oil bath. Then, Pd catalyst **I** (0.25 – 1.0 mol%) was added and the reaction mixture was kept stirring at 75 °C. Certain time points after the addition of the catalyst (0, 5, 15, 30, 60 and 120 min), an aliquot (40 µL) was withdrawn from the reaction mixture and quenched with MeOH:H_3PO_4 buffer = 75:25 (400 µL). Samples were filtered through cotton wool and analyzed by HPLC (method A for solvent comparison, method B for catalyst concentration comparison).

5.3.2 Synthesis of **5** in Continuous Flow

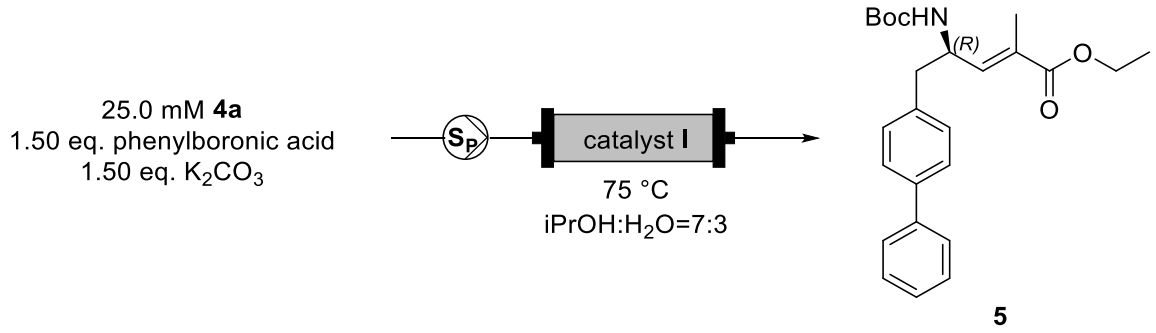

Scheme 5.8: Synthesis of **5** in continuous flow; S_P = syringe pump, catalyst **I** = $Ce_{0.20}Sn_{0.79}Pd_{0.01}O_{2-\delta}$

The Suzuki coupling of **4a** with phenylboronic acid in continuous flow was performed in the plug & play reactor[49,50] using optimized reaction conditions (see 3.2.3). For the flow experiment, a stock solution containing **4a** (25 mM, 1.00 eq.), phenylboronic acid (37.5 mM, 1.50 eq.), potassium carbonate (37.5 mM, 1.50 eq.) and anisole (67 mM, 2.68 eq.) was prepared in iPrOH:H_2O = 7:3 (v:v), dissolved by ultrasonic treatment and filtered through a syringe filter. A preparative HPLC column (L x I.D. = 120 x 8 mm) was filled with Pd catalyst **I** (ca. 5 g) and flushed vertically with iPrOH:H_2O = 7:3 (v:v) for removal of air bubbles. Then, the column was introduced into the plug & play reactor at 75 °C. Between the column and the outlet, a back pressure regulator (IDEX BPR Cartridge 40 psi Gold Coat) was installed. The reagent solution was transferred into a stainless steel syringe and pumped through the reactor setup with a flow rate of 0.1 and 0.2 mL/min, respectively, using a syringe pump (VIT-FIT HP, Lambda Instruments). To analyze the reaction progress, every 10 min an aliquot from the outlet flow (40 µL) was quenched with MeOH:H_3PO_4 buffer = 75:25 (400 µL) and analyzed by HPLC (method A).

5.4 $Ce_{0.20}Sn_{0.79}Pd_{0.01}O_{2-\delta}$ (Catalyst **I**)

5.4.1 Preparation of Catalyst **I**

$Ce_{0.20}Sn_{0.79}Pd_{0.01}O_{2-\delta}$ (catalyst **I**) was synthesized according to a modification[35] of the solution combustion technique described by Baidya *et al.*[73] Ammonium cerium(IV) nitrate (6.37 g), tin(II) oxalate (9.49 g), palladium(II) chloride (0.102 g) and glycine (10.0 g) were

pestled in a mortar to achieve a fine powder. After addition of HPLC grade water (6 mL), the mixture was subjected to ultrasonic radiation for 30 min and placed in the muffle furnace at 350 °C for 1 h for combustion. The obtained voluminous solid was again pestled in a mortar and dried in the muffle furnace at 350 °C overnight. After activity testing, which is described in 5.4.2, the catalyst was used as such for Suzuki-Miyaura cross-coupling reactions.

5.4.2 Activity Testing of Catalyst I

The activity of $Ce_{0.20}Sn_{0.79}Pd_{0.01}O_{2-\delta}$ (catalyst **I**) was tested in a Suzuki-Miyaura cross-coupling reaction described by Lichtenegger *et al.*[35] 4-Bromotoluene (125 mg, 0.731 mmol, 1.00 eq.), phenylboronic acid (128 mg, 1.05 mmol, 1.44 eq.) and potassium carbonate (146 mg, 1.06 mmol, 1.44 eq.) were dissolved in EtOH:H_2O = 7:3 (v:v) (20 mL) at 75 °C. Then, catalyst **I** (6.1 mg, 0.06 mol%) was added and the reaction mixture was kept stirring at 75 °C for 60 min. Certain time points after the addition of the catalyst (0, 15, 30 and 60 min), an aliquot (100 µL) was withdrawn from the reaction solution, quenched with MeOH:H_3PO_4 buffer = 6:4 (1000 µL) and analyzed by HPLC (method C). HPLC analysis proved that the catalyst is active for Suzuki-Miyaura cross-coupling reactions.

6 References

(1) Fala, L. Entresto (Sacubitril/Valsartan): First-in-Class Angiotensin Receptor Neprilysin Inhibitor FDA Approved for Patients with Heart Failure. *Am. Health Drug Benefits* **2015**, *8*.

(2) Nielsen, P. M.; Grimm, D.; Wehland, M.; Simonsen, U.; Krüger, M. The Combination of Valsartan and Sacubitril in the Treatment of Hypertension and Heart Failure - an Update. *Basic Clin. Physiol. Pharmacol.* **2018**, *122*, 9–18.

(3) Khalil, P.; Kabbach, G.; Said, S.; Mukherjee, D. Entresto, a New Panacea for Heart Failure? *Cardiovasc. Hematol. Agents Med. Chem.* **2018**, *16*, 5–11.

(4) Vilela-Martin, J. F. Spotlight on valsartan-sacubitril fixed-dose combination for heart failure: the evidence to date. *Drug. Des. Devel. Ther.* **2016**, *10*, 1627–1639.

(5) World Health Organization. *Global health risks: Mortality and burden of disease attributable to selected major risks*; World Health Organization: Geneva, Switzerland, 2009.

(6) Kearney, P. M.; Whelton, M.; Reynolds, K.; Muntner, P.; Whelton, P. K.; He, J. Global burden of hypertension: analysis of worldwide data. *Lancet* **2005**, *365*, 217–223.

(7) Lloyd-Jones, D.; Adams, R. J.; Brown, T. M.; Carnethon, M.; Dai, S.; Simone, G. de; Ferguson, T. B.; Ford, E.; Furie, K.; Gillespie, C. *et al.* Heart Disease and Stroke Statistics - 2010 Update. *Circulation* **2010**, *121*, e46-e215.

(8) One-Flow. https://one-flow.org/ (accessed October 14, 2019).

(9) McCormack, P. L. Sacubitril/Valsartan: A Review in Chronic Heart Failure with Reduced Ejection Fraction. *Drugs* **2016**, *76*, 387–396.

(10) Lee, S. L.; O'Connor, T. F.; Yang, X.; Cruz, C. N.; Chatterjee, S.; Madurawe, R. D.; Moore, C. M. V.; Yu, L. X.; Woodcock, J. Modernizing Pharmaceutical Manufacturing: from Batch to Continuous Production. *J. Pharm. Innov.* **2015**, *10*, 191–199.

(11) Newman, S. G.; Jensen, K. F. The role of flow in green chemistry and engineering. *Green Chem.* **2013**, *15*, 1456–1472.

(12) Jiménez-González, C.; Poechlauer, P.; Broxterman, Q. B.; Yang, B.-S.; Am Ende, D.; Baird, J.; Bertsch, C.; Hannah, R. E.; Dell'Orco, P.; Noorman, H. *et al.* Key Green Engineering Research Areas for Sustainable Manufacturing: A Perspective from Pharmaceutical and Fine Chemicals Manufacturers. *Org. Process Res. Dev.* **2011**, *15*, 900–911.

(13) Wiles, C.; Watts, P. Continuous process technology: a tool for sustainable production. *Green Chem.* **2014**, *16*, 55–62.

(14) Ley, S. V. On Being Green: Can Flow Chemistry Help? *Chem. Rec.* **2012**, *12*, 378–390.

(15) Plumb, K. Continuous Processing in the Pharmaceutical Industry. *Chem. Eng. Res. Des.* **2005**, *83*, 730–738.

(16) BfArM - Pressemitteilung 5/18 - Valsartan: chargenbezogener Rückruf valsartanhaltiger Arzneimittel, deren Wirkstoff von dem chinesischen Hersteller Zhejiang Huahai Pharmaceutical produziert wurde. https://www.bfarm.de/SharedDocs/Pressemitteilungen/DE/2018/pm5-2018.html (accessed October 14, 2019).

(17) ONLINE, S.; Hamburg; Germany. Valsartan-Skandal: Hunderttausende betroffene Patienten, viele offene Fragen - SPIEGEL ONLINE - Gesundheit. https://www.spiegel.de/gesundheit/diagnose/valsartan-skandal-viele-fragen-um-verunreinigte-blutdrucksenker-a-1220544.html (accessed October 14, 2019).

(18) Bühlmayer, P.; Ostermayer, F.; Schmidlin, T. Acyl compounds. Eur. Patent 0 443 983 A1, Feb 12, 1991.

(19) Hiebler, K.; Soritz, S.; Gavric, K.; Birrer, S.; Maier, M. C.; Grabner, B.; Gruber-Woelfler, H. Multistep synthesis of a valsartan precursor in continuous flow. *J. Flow Chem.* **2019**, *116*.

(20) Ksander, G. Biaryl substituted 4-amino-butyric acid amides. U.S. Patent 5,217,996, Jun 8, 1993.

(21) Hook, D.; Ruch, T.; Riss, B.; Wietfeld, B.; Sedelmeier, G.; Napp, M.; Bänziger, M.; Hawker, S.; Ciszewski, L.; Waykole, L. M. New process. WO 2008/083967 A2, Jul 17, 2008.

(22) Hook, D.; Zhou, J.; Li, Y. Process for the preparation of intermediates for the manufacture of NEP inhibitors. WO 2012/025501 A1, Mar 1, 2012.

(23) Hook, D.; Riss, B.; Zhou, J.; Li, Y.; Bappert, E. New process for the preaparation of intermediates useful for the manufacture NEP inhibitors. WO 2012/025502 A1, Mar 1, 2012.

(24) Vellanki, S. R. P.; Sahu, A.; Shimpi, N. A.; Prathi, S. K.; Ampolu, L. R. Novel process for the preparation of sacubitril and its intermediates. WO 2016/135751 A1, Sep 1, 2016.

(25) Lau, S.-H.; Bourne, S. L.; Martin, B.; Schenkel, B.; Penn, G.; Ley, S. V. Synthesis of a Precursor to Sacubitril Using Enabling Technologies. *Org. Lett.* **2015**, *17*, 5436–5439.

(26) Wang, Y.; Chen, F.-E.; Shi, Y.; Tian, W.-S. Multigram scale, chiron-based synthesis of sacubitril. *Tetrahedron Lett.* **2016**, *57*, 5928–5930.

(27) Martin, B.; Mandrelli, F.; Venturoni, F. Process and intermediates for the preparation of NEP inhibitors. US 2018/0022690 A1, Jan 25, 2018.

(28) Wu, X.-F.; Anbarasan, P.; Neumann, H.; Beller, M. From noble metal to Nobel Prize: palladium-catalyzed coupling reactions as key methods in organic synthesis. *Angew. Chem. Int. Ed.* **2010**, *49*, 9047–9050.

(29) Yin, L.; Liebscher, J. Carbon-Carbon Coupling Reactions Catalyzed by Heterogeneous Palladium Catalysts. *Chem. Rev.* **2007**, *107*, 133–173.

(30) Hagen, J. *Chemiereaktoren: Auslegung und Simulation*; Wiley-VCH: Weinheim, Germany, 2004.

(31) Müller-Erlwein, E. *Chemische Reaktionstechnik*, 3rd ed.; Chemie in der Praxis; Springer Spektrum: Wiesbaden, Germany, 2015.

(32) Schmidt, L. D. *The engineering of chemical reactions*; Topics in chemical engineering; Oxford University Press: New York, NY, 1998.

(33) Gruber-Woelfler, H.; Radaschitz, P. F.; Feenstra, P. W.; Haas, W.; Khinast, J. G. Synthesis, catalytic activity, and leaching studies of a heterogeneous Pd-catalyst including an immobilized bis(oxazoline) ligand. *J. Catal.* **2012**, *286*, 30–40.

(34) Hiebler, K.; Lichtenegger, G. J.; Maier, M. C.; Park, E. S.; Gonzales-Groom, R.; Binks, B. P.; Gruber-Woelfler, H. Heterogeneous Pd catalysts as emulsifiers in Pickering emulsions for integrated multistep synthesis in flow chemistry. *Beilstein J. Org. Chem.* **2018**, *14*, 648–658.

(35) Lichtenegger, G. J.; Maier, M.; Hackl, M.; Khinast, J. G.; Gössler, W.; Griesser, T.; Kumar, V. S. P.; Gruber-Woelfler, H.; Deshpande, P. A. Suzuki-Miyaura coupling reactions using novel metal oxide supported ionic palladium catalysts. *J. Mol. Catal. A: Chem.* **2017**, *426*, 39–51.

(36) Lichtenegger, G. J.; Maier, M.; Khinast, J. G.; Gruber-Wölfler, H. Continuous Suzuki—Miyaura reactions with Novel Ce—Sn—Pd Oxides and Integrated Crystallization as Continuous Downstream Protocol. *J. Flow Chem.* **2016**, *6*, 244–251.

(37) Mancia, G.; Fagard, R.; Narkiewicz, K.; Redon, J.; Zanchetti, A.; Böhm, M.; Christiaens, T.; Cifkova, R.; Backer, G. de; Dominiczak, A. *et al.* 2013 ESH/ESC guidelines for the management of arterial hypertension: the Task Force for the Management of Arterial Hypertension of the European Society of Hypertension (ESH) and of the European Society of Cardiology (ESC). *Eur. Heart J.* **2013**, *34*, 2159–2219.

(38) Kemp, C. D.; Conte, J. V. The pathophysiology of heart failure. *Cardiovasc. Pathol.* **2012**, *21*, 365–371.

(39) Hunt, S. A.; Abraham, W. T.; Chin, M. H.; Feldman, A. M.; Francis, G. S.; Ganiats, T. G.; Jessup, M.; Konstam, M. A.; Mancini, D. M.; Michl, K. *et al.* 2009 Focused Update Incorporated Into the ACC/AHA 2005 Guidelines for the Diagnosis and Management of Heart Failure in Adults. *J. Am. Coll. Cardiol.* **2009**, *53*, e1-e90.

(40) Andersen, M. B.; Simonsen, U.; Wehland, M.; Pietsch, J.; Grimm, D. LCZ696 (Valsartan/Sacubitril) - A Possible New Treatment for Hypertension and Heart Failure. *Basic & clinical pharmacology & toxicology* **2016**, *118*, 14–22.

(41) Pandarus, V.; Gingras, G.; Béland, F.; Ciriminna, R.; Pagliaro, M. Process Intensification of the Suzuki–Miyaura Reaction over Sol–Gel Entrapped Catalyst Silia Cat DPP-Pd Under Conditions of Continuous Flow. *Org. Process Res. Dev.* **2014**, *18*, 1550–1555.

(42) Nagaki, A.; Hirose, K.; Tonomura, O.; Taniguchi, S.; Taga, T.; Hasebe, S.; Ishizuka, N.; Yoshida, J.-i. Design of a Numbering-up System of Monolithic Microreactors and Its Application to Synthesis of a Key Intermediate of Valsartan. *Org. Process Res. Dev.* **2016**, *20*, 687–691.

(43) Ksander, G. M.; Ghai, R. D.; deJesus, R.; Diefenbacher, C.; Yuan, A.; Berry, C.; Sakane, Y.; Trapani, A. Dicarboxylic Acid Dipeptide Neutral Endopeptidase Inhibitors. *J. Med. Chem.* **1995**, *38*, 1689–1700.

(44) Felder, R. M.; Rousseau, R. W. *Elementary principles of chemical processes*, 3rd ed.; Wiley: New York, NY, 2000.

(45) Levenspiel, O. *Chemical reaction engineering*, 3rd ed.; Wiley: Hoboken, NJ, 1999.

(46) Callis, J. B.; Illman, D. L.; Kowalski, B. R. Process Analytical. *Anal. Chem.* **1987**, *59*, 624A–637A.

(47) Minnich, C.; Hardy, S.; Krämer, S. Stopping the Babylonian Confusion: An Updated Nomenclature for Process Analyzers in PAT Applications. *Chem. Ing. Tech.* **2016**, *88*, 694–697.

(48) Roberge, D. M.; Ducry, L.; Bieler, N.; Cretton, P.; Zimmermann, B. Microreactor Technology: A Revolution for the Fine Chemical and Pharmaceutical Industries? *Chem. Eng. Technol.* **2005**, *28*, 318–323.

(49) Gruber-Woelfler, H.; Schnitzer, H.; Narodoslawsky, M.; Khinast, J. G. IPPE-TU Graz: green engineering inside and beyond the borders of process technology. *Green Process. Synth,* **2015**, *4*, 51–55.

(50) Lichtenegger, G. J.; Tursic, V.; Kitzler, H.; Obermaier, K.; Khinast, J. G.; Gruber-Wölfler, H. The Plug & Play Reactor: A Highly Flexible Device for Heterogeneous Reactions in Continuous Flow. *Chem. Ing. Tech.* **2016**, *88*, 1518–1523.

(51) Hagen, J. *Industrial Catalysis: A Practical Approach*, 3rd ed.; Wiley-VCH: Weinheim, Germany, 2015.

(52) Chorkendorff, I.; Niemantsverdriet, J. W. *Concepts of modern catalysis and kinetics*; Wiley-VCH: Weinheim, Germany, 2005.

(53) Mortimer, C. E.; Müller, U.; Beck, J. *Chemie: Das Basiswissen der Chemie*, 12th ed.; Thieme: Stuttgart, Germany, 2015.

(54) Farrauto, R. J.; Dorazio, L.; Bartholomew, C. H. *Introduction to catalysis and industrial catalytic processes*; Wiley: Hoboken, NJ, 2016.

(55) Steinborn, D. *Grundlagen der metallorganischen Komplexkatalyse*; Teubner: Wiesbaden, Germany, 2007.

(56) Rothenberg, G. *Catalysis: Concepts and Green Applications*; Wiley-VCH: Weinheim, Germany, 2008.

(57) McMorn, P.; Hutchings, G. J. Heterogeneous enantioselective catalysts: strategies for the immobilisation of homogeneous catalysts. *Chem. Soc. Rev.* **2004**, *33*, 108–122.

(58) Bates, R. *Organic synthesis using transition metals*, 2nd ed.; Wiley: Chichester, U.K., 2012.

(59) Clayden, J.; Greeves, N.; Warren, S. G. *Organic chemistry*, 2nd ed.; Oxford University Press: Oxford, U.K., 2012.

(60) Miyaura, N.; Suzuki, A. Stereoselective Synthesis of Arylated (E)-Alkenes by the Reaction of Alk-1-enylboranes with Aryl Halides in the Presence of Palladium Catalyst. *J. Chem. Soc., Chem. Commun.* **1979**, 866–867.

(61) Suzuki, A. Recent advances in the cross-coupling reactions of organoboron derivatives with organic electrophiles **1999**, *576*, 147–168.

(62) Hall, D. G. *Boronic Acids: Preparation and Applications in Organic Synthesis, Medicine and Materials*; Wiley-VCH: Weinheim, Germany, 2011.

(63) *Synthetic methods in drug discovery;* Blakemore, D.; Doyle, P.; Fobian, Y., Eds.; RSC drug discovery series no. 52-53; Royal Society of Chemistry: Cambridge, U.K., 2016.

(64) Kotha, S.; Lahiri, K.; Kashinath, D. Recent applications of the Suzuki-Miyaura cross-coupling reaction in organic synthesis. *Tetrahedron* **2002**, *58*, 9633–9695.

(65) Magano, J.; Dunetz, J. R. Large-Scale Applications of Transition Metal-Catalyzed Couplings for the Synthesis of Pharmaceuticals. *Chem. Rev.* **2011**, *111*, 2177–2250.

(66) Miyaura, N.; Suzuki, A. Palladium-Catalyzed Cross-Coupling Reactions of Organoboron Compounds. *Chem. Rev.* **1995**, *95*, 2457–2483.

(67) Nicolaou, K. C.; Bulger, P. G.; Sarlah, D. Palladium-Catalyzed Cross-Coupling Reactions in Total Synthesis. *Angew. Chem. Int. Ed.* **2005**, *44*, 4442–4489.

(68) Miyaura, N. Cross-coupling reaction of organoboron compounds via base-assisted transmetalation to palladium(II) complexes **2002**, *653*, 54–57.

(69) Suzuki, A. Cross-coupling reactions via organoboranes. *J. Organomet. Chem.* **2002**, *653*, 83–90.

(70) Noël, T.; Buchwald, S. L. Cross-coupling in flow. *Chem. Soc. Rev.* **2011**, *40*, 5010–5029.

(71) Cantillo, D.; Kappe, C. O. Immobilized Transition Metals as Catalysts for Cross-Couplings in Continuous Flow-A Critical Assessment of the Reaction Mechanism and Metal Leaching. *ChemCatChem* **2014**, *6*, 3286–3305.

(72) Garrett, C. E.; Prasad, K. The Art of Meeting Palladium Specifications in Active Pharmaceutical Ingredients Produced by Pd-Catalyzed Reactions. *Adv. Synth. Catal.* **2004**, *346*, 889–900.

(73) Baidya, T.; Gupta, A.; Deshpandey, P. A.; Madras, G.; Hegde, M. S. High Oxygen Storage Capacity and High Rates of CO Oxidation and NO Reduction Catalytic Properties of Ce 1− x Sn x O 2 and Ce 0.78 Sn 0.2 Pd 0.02 O 2-δ. *J. Phys. Chem. C* **2009**, *113*, 4059–4068.

(74) Patil, K. C. *Chemistry of Nanocrystalline Oxide Materials: Combustion Synthesis, Properties and Applications*; World Scientific: Singapore, London, 2008.

(75) Mallik, S. K.; Li, D. Y.; Cui, M.; Song, H.-O.; Park, H.; Kim, H. S. Synthesis and evaluation of peptidyl α,β-unsaturated carbonyl derivatives as anti-malarial calpain inhibitors. *Arch. Pharm. Res.* **2012**, *35*, 469–479.

(76) Wu, J.; Lawrence, N. J.; Sebti, S. M.; Lawrence, H. R. Indoline scaffold SHP-2 inhibitors and method of treating cancer. WO 2010/121212 A2, Oct 21, 2010.

(77) Ariga, K.; Nakanishi, T.; Hill, J. P.; Shirai, M.; Okuno, M.; Abe, T.; Kikuchi, J.-i. Tunable pK of Amino Acid Residues at the Air-Water Interface Gives an L-zyme (Langmuir Enzyme). *J. Am. Chem. Soc.* **2005**, *127*, 12074–12080.

(78) Kasai, S.; McGee, Jr., K. F. Derivatives of N-acyl-N'-phenylpiperazine useful (inter alia) for the prophylaxis or treatment of diabetes. WO 2010/119992 A1, Oct 21, 2010.

(79) Jorand-Lebrun, C.; Johnson, T. L.; Graedler, U.; Jiang, X.; Roche, D.; Lemoine, H.; Gilardone, M. Compounds for the inhibition of cyclophilins and uses thereof. WO 2017/173048 A1, Oct 5, 2017.

(80) Wei, Z.; Grottick, A. J.; Mills, D. M.; Smith, B. M. Methods and compounds useful in treating pruritus and methods for identifying such compounds. WO 2013/151982 A1, Oct 10, 2013.

(81) Gao, P.; Sistla, A.; Shenoy, N. Pharmaceutical formulations comprising indolinone derivatives. WO 03/045307 A2, Jun 5, 2003.

(82) Basel, Y.; Hassner, A. Di-tert-butyl Dicarbonate and 4-(Dimethylamino)pyridine Revisited. Their Reactions with Amines and Alcohols. *The Journal of Organic Chemistry* **2000**, *65*, 6368–6380.

(83) Tang, X.; Tang, G.; Wang, H.; Luo, L.; Yang, D. A convenient and highly efficient synthesis of one kind of peptide nucleic acid monomer. *Bull. Chem. Soc. Ethiop.* **2012**, *26*, 415–420.

(84) Mollica, A.; Feliciani, F.; Stefanucci, A.; Costante, R.; Lucente, G.; Pinnen, F.; Notaristefano, D.; Spisani, S. Synthesis and biological evaluation of new active For-Met-Leu-Phe-OMe analogues containing para-substituted Phe residues. *J. Pept. Sci.* **2012**, *18*, 418–426.

(85) Mori, M.; Deodato, D.; Kasula, M.; Ferraris, D. M.; Sanna, A.; Logu, A. de; Rizzi, M.; Botta, M. Design, synthesis, SAR and biological investigation of 3-(carboxymethyl)rhodanine and aminothiazole inhibitors of Mycobacterium tuberculosis Zmp1. *Bioorg. Med. Chem. Lett.* **2018**, *28*, 637–641.

(86) Liu, J.; Kimmel, K.; Dao, K.; Liu, Y.; Qi, M. Identification and Elimination of an Unexpected Catalyst Poison in Suzuki Coupling. *Org. Process Res. Dev.* **2018**, *22*, 111–116.

(87) Blaszczak, L. C.; Mathes, B. M.; Pulley, S. R.; Robertson, M. A.; Sheehan, S. M.; Shi, Q.; Watson, B. M.; Wiley, M. R. Pyridine derivatives as dipeptedyl peptidase inhibitors. WO 2007/015767 A1, Feb 8, 2007.

(88) Sun, T.; Zhang, W.; Zong, C.; Wang, P.; Li, Y. Total synthesis and stereochemical reassignment of tasiamide B. *J. Pept. Sci.* **2010**, *16*, 364–374.

(89) Widegren, M. B.; Clarke, M. L. Manganese Catalyzed Hydrogenation of Enantiomerically Pure Esters. *Org. Lett.* **2018**, *20*, 2654–2658.

(90) Wuts, P. G. M.; Greene, T. W. *Greene's protective groups in organic synthesis*, 4th ed.; Wiley-Interscience: Hoboken, NJ, 2007.

(91) Pereira, V. L. P.; Moura, A. L. d. S.; Vieira, D. P. P.; Carvalho, L. L. de; Torres, E. R. B.; Costa, J. d. S. A versatile and efficient approach for the synthesis of chiral 1,3-nitroamines and 1,3-diamines via conjugate addition to new (S,E)-γ-aminated nitroalkenes derived from L-α-amino acids. *Beilstein J. Org. Chem.* **2013**, *9*, 832–837.

(92) Ahmed, S. T.; Parmeggiani, F.; Weise, N. J.; Flitsch, S. L.; Turner, N. J. Chemoenzymatic Synthesis of Optically Pure L- and D-Biarylalanines through Biocatalytic Asymmetric Amination and Palladium-Catalyzed Arylation. *ACS Catal.* **2015**, *5*, 5410–5413.

(93) Seo, C. S. G.; Morris, R. H. Catalytic Homogeneous Asymmetric Hydrogenation: Successes and Opportunities. *Organometallics* **2019**, *38*, 47–65.

(94) Meemken, F.; Baiker, A. Recent Progress in Heterogeneous Asymmetric Hydrogenation of C═O and C═C Bonds on Supported Noble Metal Catalysts. *Chem. Rev.* **2017**, *117*, 11522–11569.

(95) Brown, J. W.; Keung, W.; Li, Z.; Tyhonas, J. Renin Inhibitors. WO 2010/111634 A2, Sep 30, 2010.

(96) Roach, A. G.; Maillol, C. E. A.; Wilson, F. X.; Wynne, G. M.; Raufer, J.; Vile, J.; Thomas, N.; Storer, R.; Middleton, P.; Moor, O. de. Dual calpain-ros inhibitors. UK Pat. Appl. GB 2467562 A, Aug 11, 2010.

(97) Fulmer, G. R.; Miller, A. J. M.; Sherden, N. H.; Gottlieb, H. E.; Nudelman, A.; Stoltz, B. M.; Bercaw, J. E.; Goldberg, K. I. NMR Chemical Shifts of Trace Impurities: Common Laboratory Solvents, Organics, and Gases in Deuterated Solvents Relevant to the Organometallic Chemist. *Organometallics* **2010**, *29*, 2176–2179.

(98) Chai, Y.; Ullrich, A.; Kazmaier, U.; Müller, R. Bioactive Pre-tubulysins and Use thereof. WO 2010/034724 A1, Apr 1, 2010.

(99) Coppola, G. M.; Iwaki, Y.; Karki, R. G.; Kawanami, T.; Ksander, G. M.; Mogi, M. Substituted Aminopropionic Derivatives as Neprilysin Inhibitors. WO 2010/136493 A1, Dec 2, 2010.

7 Appendix

7.1 High Performance Liquid Chromatography (HPLC)

7.1.1 HPLC Methods

For HPLC measurements, MeOH and H_2O:H_3PO_4 = 300:1 (v:v) (H_3PO_4 buffer) were used as mobile phases and a temperature of 25 °C and a flow rate of 1 mL/min were applied.

The applied isocratic elution methods are summarized in Table 7.1, the methods for gradient elution in Table 7.2.

Table 7.1: HPLC method for isocratic elution

Method	**MeOH [% v/v]**	**H_3PO_4 buffer [% v/v]**	**Run time [min]**
A	75	25	5

Table 7.2: HPLC methods for gradient elution

Method	**Time [min]**	**MeOH [% v/v]**	**H_3PO_4 buffer [% v/v]**
B	0	70	30
	10	90	10
	12	70	30
	15	70	30
C	0	60	40
	10	80	20
	12	60	40
	15	60	40

7.1.2 Quantification of Analytes with HPLC

In order to examine reaction progress of the Suzuki cross-coupling reaction in the optimization and flow experiments, calibrations of compound **5** as well as the internal standard anisole were necessary. As solvent, iPrOH:H_2O = 7:3 (v:v) mixed with MeOH:H_3PO_4 buffer = 75:25 in a ratio of 1+10 was utilized, which corresponds to the sample solvents.

For the calibration of **5**, a stock solution of compound **5** (2.75 mM) was prepared in the above-mentioned solvent and dissolved by ultrasonic radiation. Samples with concentrations in a range of 0.150 – 2.75 mM as well as a blank were prepared and analyzed by HPLC (method A) (Figure 7.1).

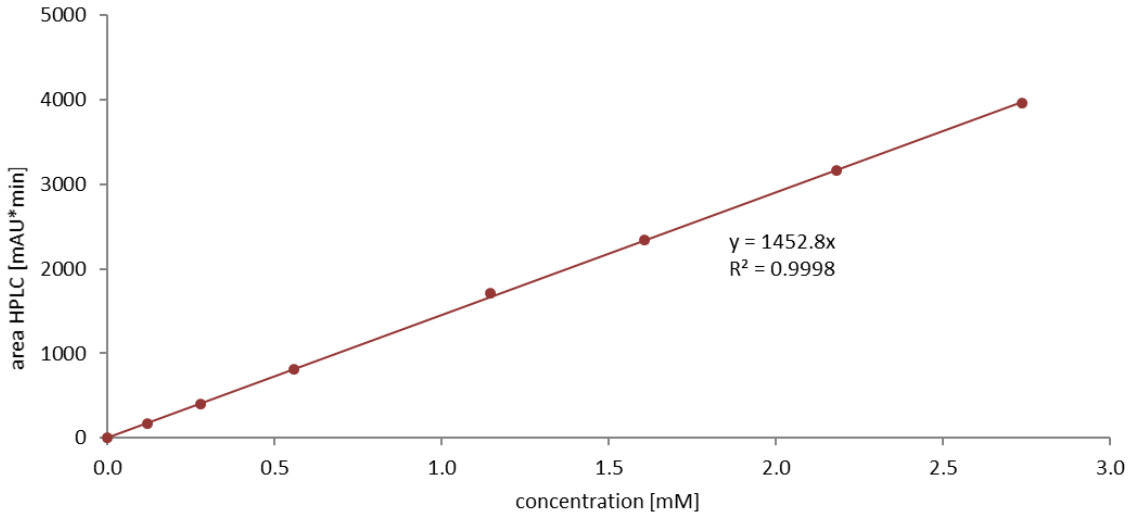

Figure 7.1: Calibration curve of compound **5** at 237 nm

The calibration of anisole was performed similarly, using a 10 mM stock solution of anisole in the respective solvent. Samples with concentrations in a range of 1.00 – 10.0 mM as well as a blank were prepared and analyzed by HPLC (method A) (Figure 7.2).

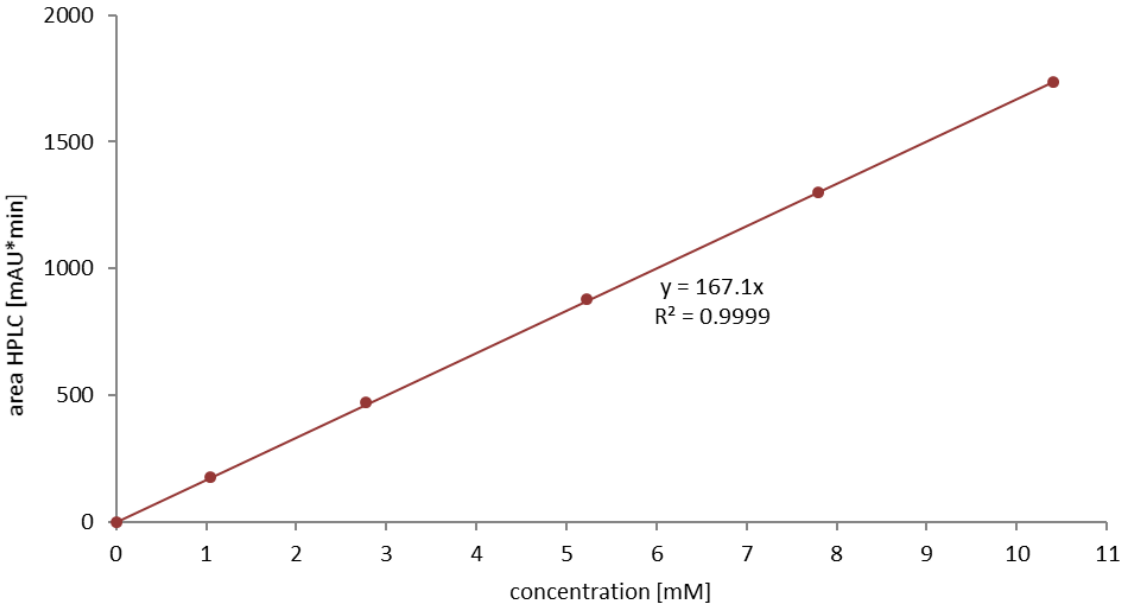

Figure 7.2: Calibration curve of anisole at 270 nm

7.2 Nuclear Magnetic Resonance (NMR) Spectra

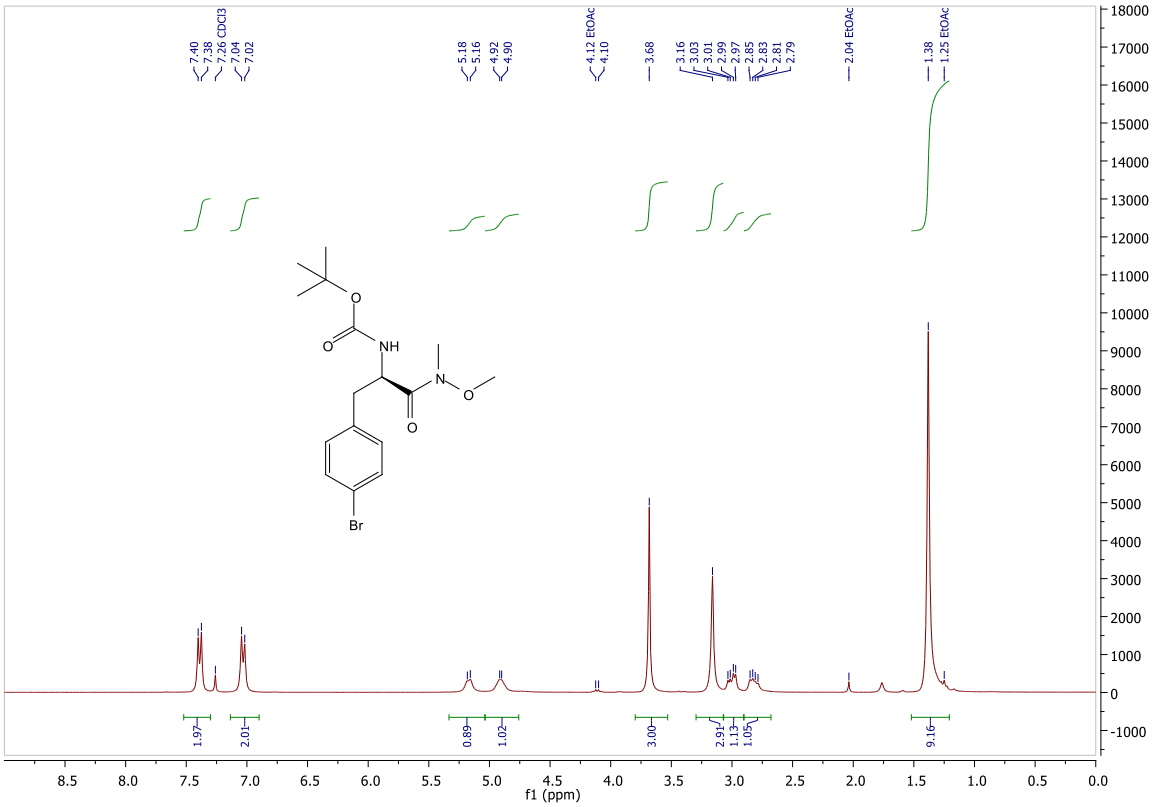

Figure 7.3: ^{1}H NMR spectrum of compound **2b** in $CDCl_3$

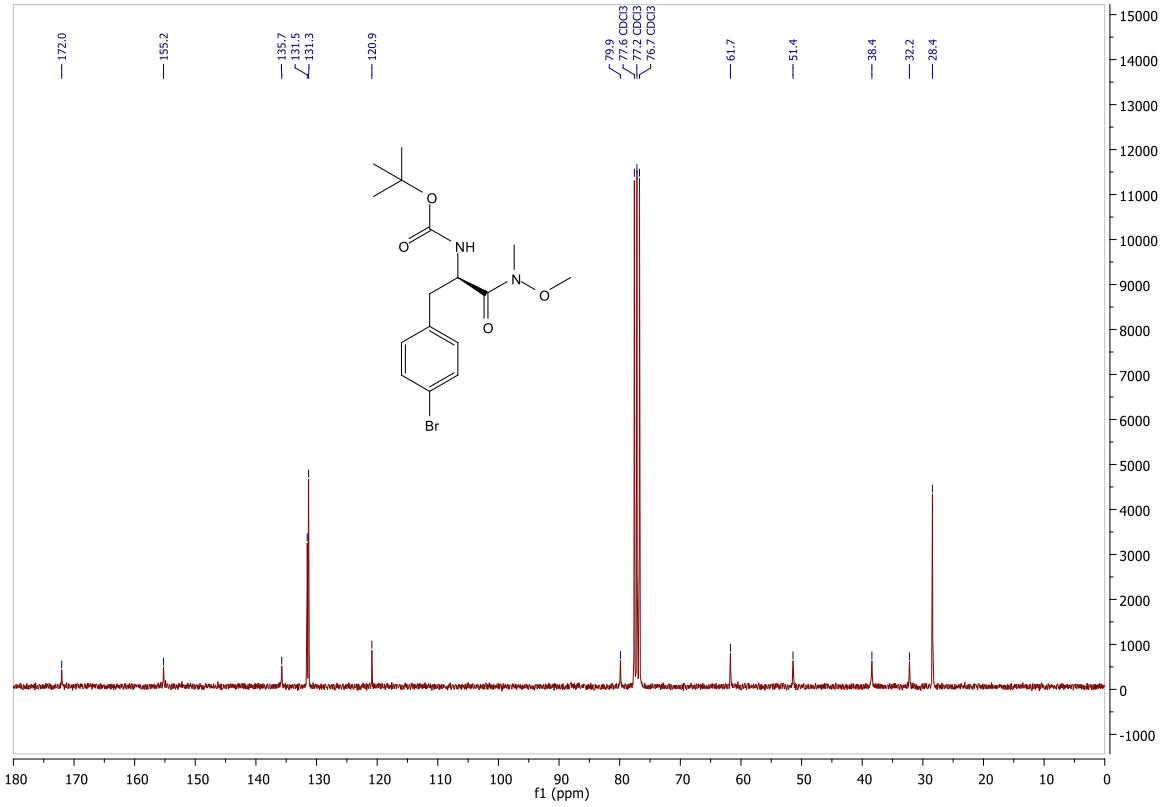

Figure 7.4: ^{13}C NMR spectrum of compound **2b** in $CDCl_3$

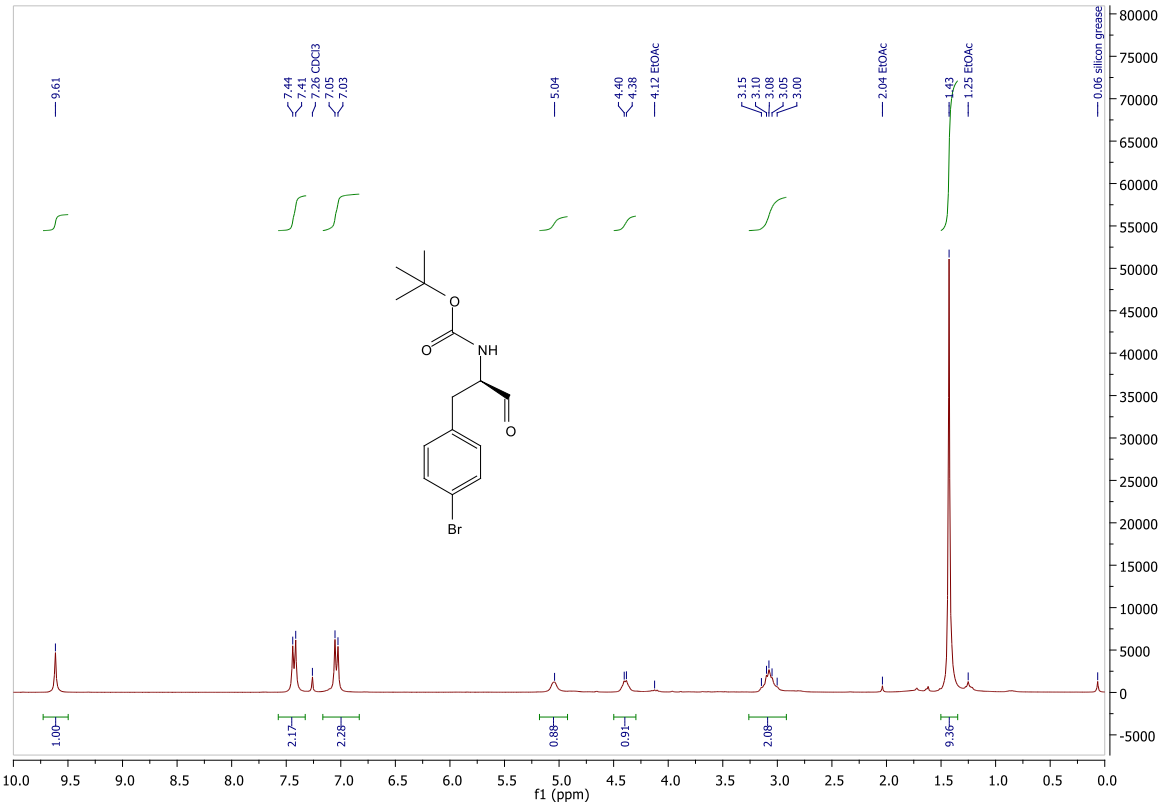

Figure 7.5: ^{1}H NMR spectrum of compound **3b** in $CDCl_3$

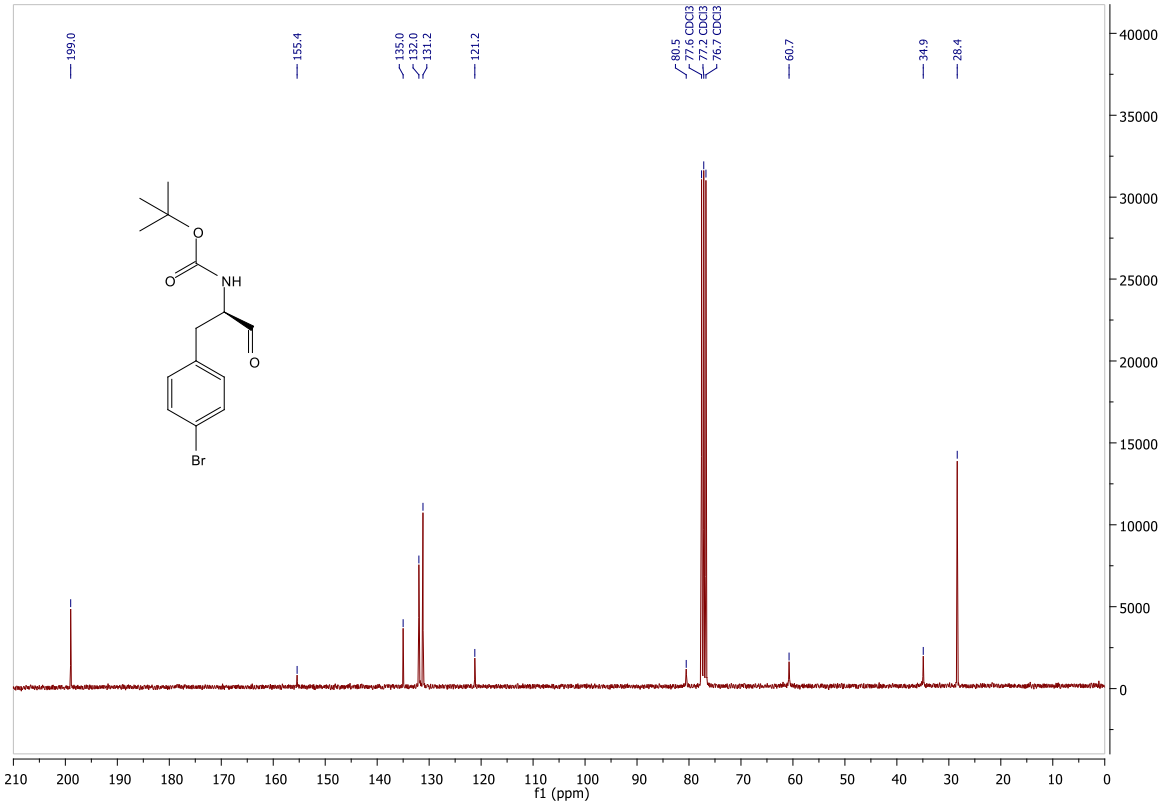

Figure 7.6: ^{13}C NMR spectrum of compound **3b** in $CDCl_3$

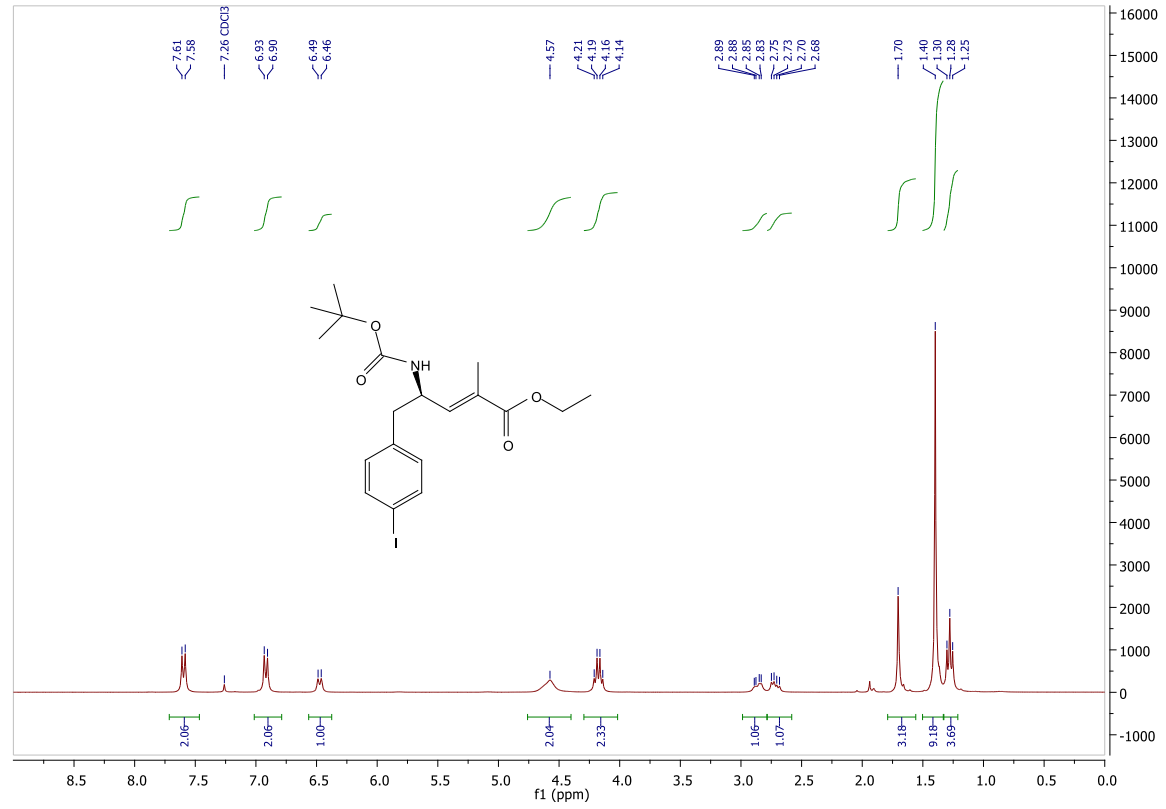

Figure 7.7: ^{1}H NMR spectrum of compound **4a** in $CDCl_3$

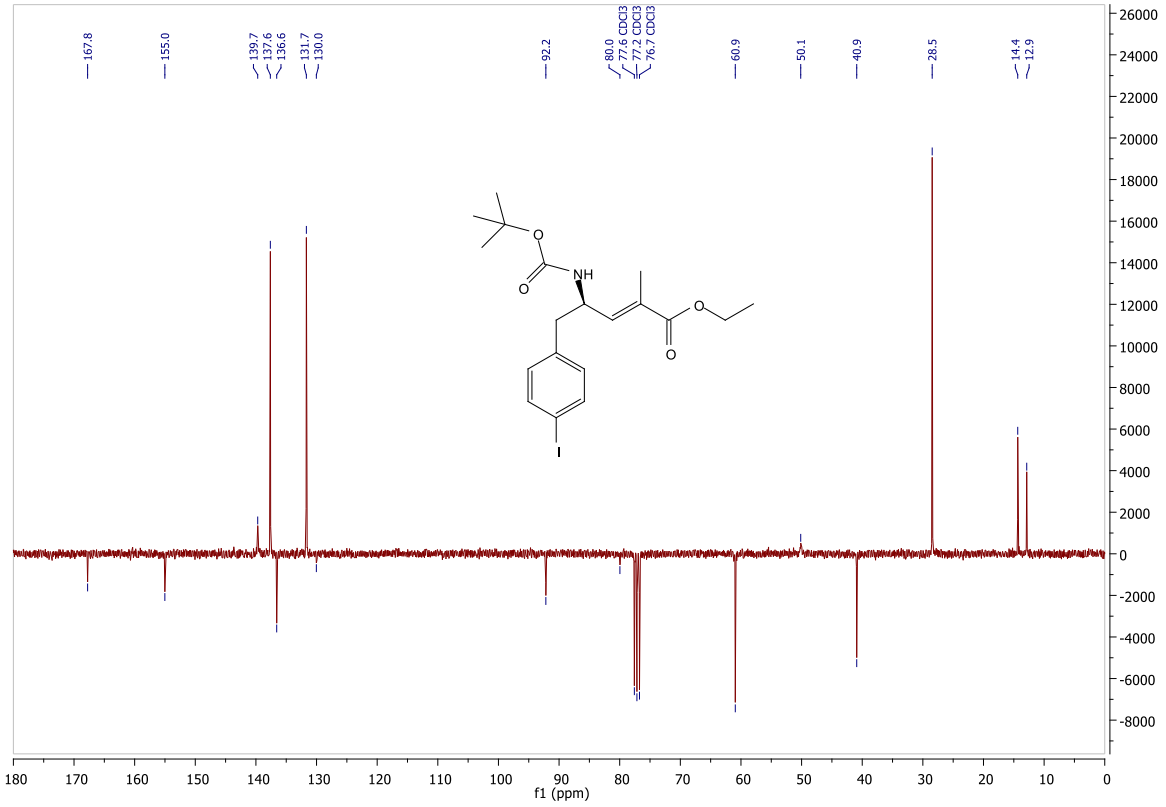

Figure 7.8: ^{13}C NMR (APT) spectrum of compound **4a** in $CDCl_3$

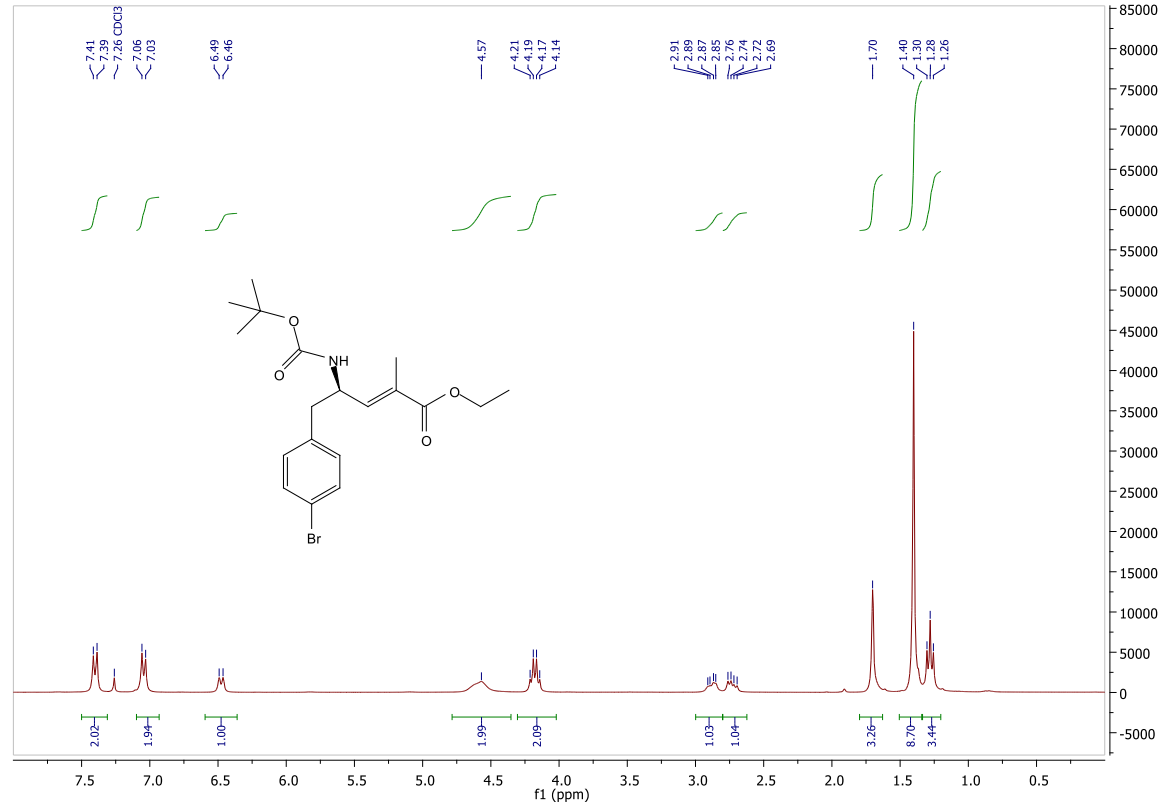

Figure 7.9: ^{1}H NMR spectrum of compound **4b** in $CDCl_3$

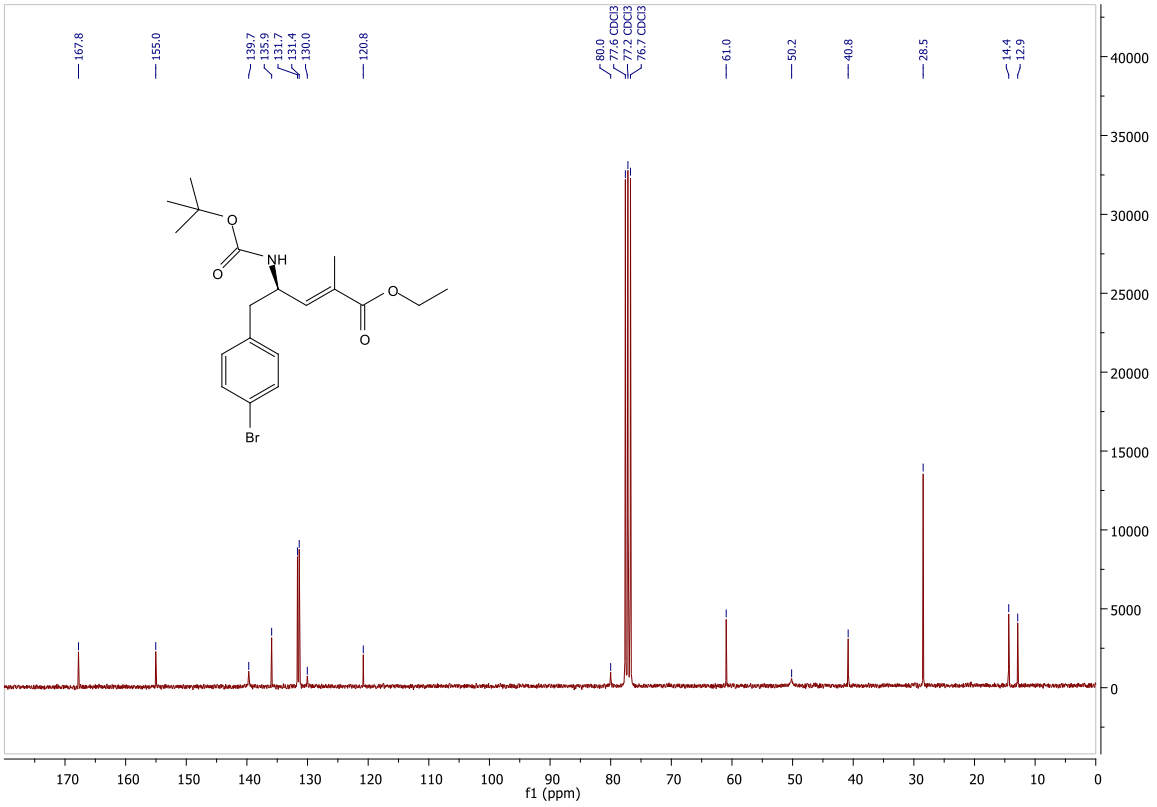

Figure 7.10: ^{13}C NMR spectrum of compound **4b** in $CDCl_3$

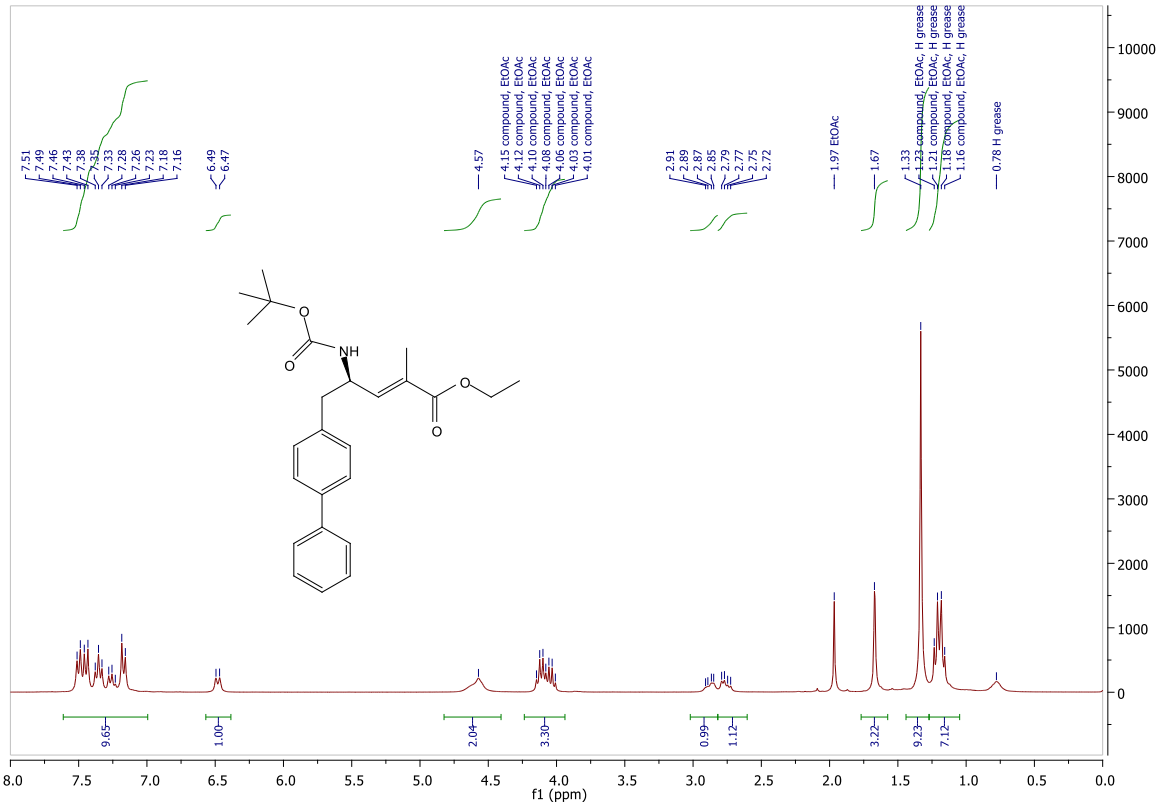

Figure 7.11: ^{1}H NMR spectrum of compound **5** in $CDCl_3$

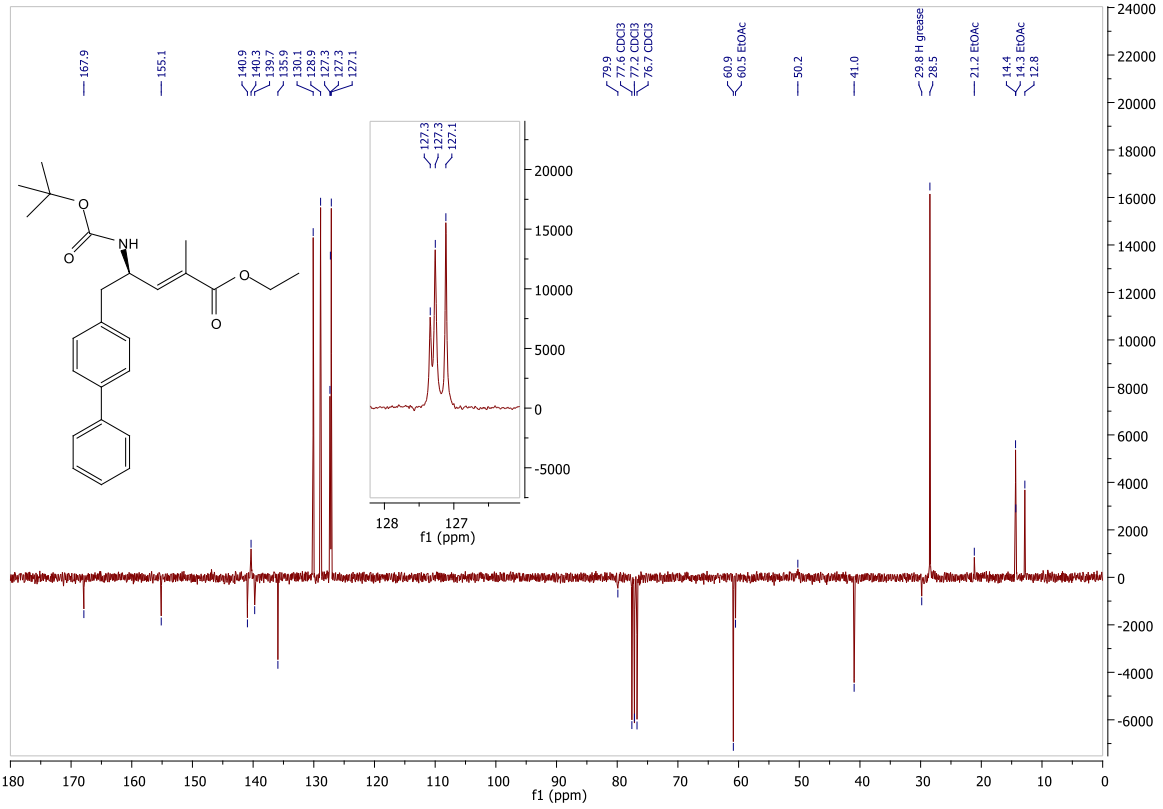

Figure 7.12: ^{13}C NMR (APT) spectrum of compound **5** in $CDCl_3$

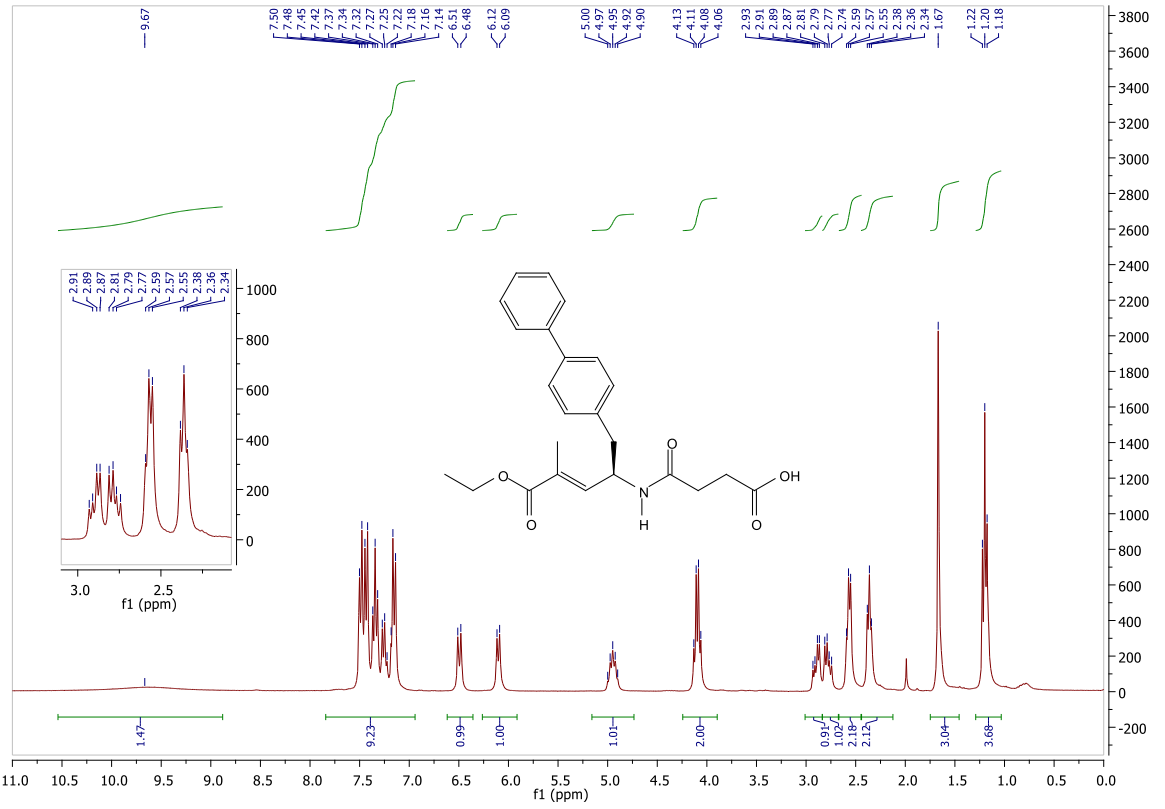

Figure 7.13: ^{1}H NMR spectrum of compound **7** in $CDCl_3$

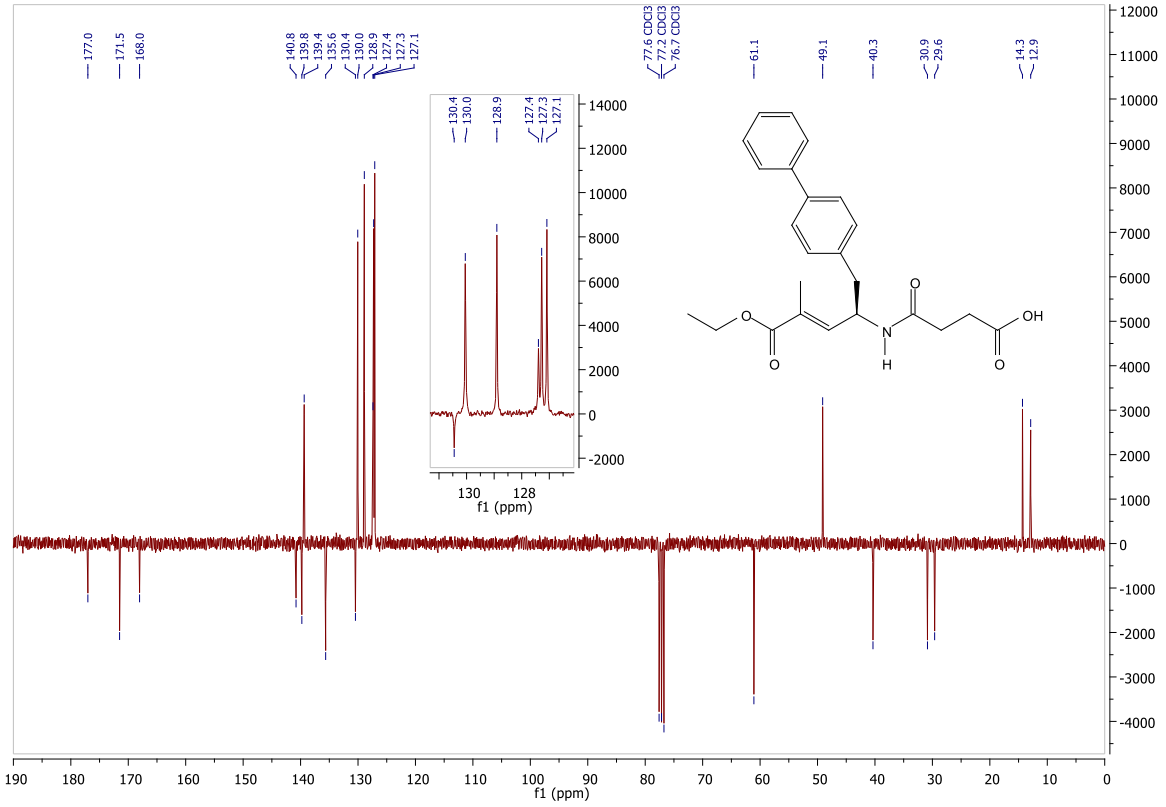

Figure 7.14: ^{13}C NMR (APT) spectrum of compound **7** in $CDCl_3$

7.3 Abbreviations

Table 7.3: List of abbreviations

Abbreviation	Meaning
4-DMAP	4-dimethylaminopyridine
Ac	acetyl
APT	attached proton test
aq.	aqueous
AU	absorbance unit
Bn	benzyl
Boc	*tert*-butyloxycarbonyl
BOX	bis(oxazoline)
BR	batch reactor
bs	broad singlet
C_{ar}	aromatic carbon
cat.	catalyst
C_q	quaternary carbon
CSTR	continuous stirred tank reactor
d	doublet
DCM	dichloromethane

dd	doublet of doublets
DMF	dimethylformamide
dt	doublet of triplets
EDC HCl	1-ethyl-3-(3-dimethylaminopropyl)carbodiimide hydrochloride
Et	ethyl
HPLC	high performance liquid chromatography
iPrOH	isopropanol
IR	infrared
ISt	internal standard
J	coupling constant
L x I.D.	length x inner diameter
m	multiplet
Me	methyl
MPSG	mercaptopropyl-functionalized silica gel
MS	mass spectrometry
NMR	nuclear magnetic resonance
OTf	triflate
Oxyma Pure	ethyl(hydroxyimino)cyanoacetate
PE	petroleum ether
PFR	plug flow reactor
Ph	phenyl
q	quartet
R_f	retention factor
RT	room temperature
s	singlet
S	selectivity
sat.	saturated
t	triplet
TFA	trifluoroacetic acid
THF	tetrahydrofuran
TLC	thin layer chromatography
UV	ultraviolet
δ	chemical shift
δ	vacancies in the oxide crystal lattice

7.4 List of Figures

7.5 List of Schemes

7.6 List of Tables

7.7 List of Equations